INVESTIGATION AND RECONSTRUCTIONS OF THE HYDROCLIMATIC VARIABILITY OF THE SOURIS RIVER BASIN

A Thesis

Submitted to the Faculty of Graduate Studies and Research

In Partial Fulfillment of the Requirements

For the Degree of

Master of Science

In

Geography

University of Regina

By

Jessica Rae Vanstone

Regina, Saskatcehwan

February, 2012

UNIVERSITY OF REGINA

FACULTY OF GRADUATE STUDIES AND RESEARCH

SUPERVISORY AND EXAMINING COMMITTEE

Jessica Rae Vanstone, candidate for the degree of Master of Science in Geography**,** has presented a thesis titled, ***Investigation and Reconstructions of the Hydroclimatic Variability of the Souris River Basin,*** in an oral examination held on January 18, 2012. The following committee members have found the thesis acceptable in form and content, and that the candidate demonstrated satisfactory knowledge of the subject material.

External Examiner:	Dr. Chris Spence, Environment Canada
Supervisor:	Dr. David Sauchyn, Department of Geography
Committee Member:	*Dr. Joseph Piwowar, Department of Geography
Committee Member:	Dr. Kyle Hodder, Department of Geography
Chair of Defense:	Dr. Thomas Bredohl, Faculty of Arts

*Not present at defense

ABSTRACT

A growing dependence on surface water resources in the Prairie Provinces has resulted in an increasing vulnerability to hydrological drought. A serious risk from recent and projected climate warming in the Canadian Prairies is a shift in the amount and timing of streamflow. The Souris River Basin has, over the years, been plagued with problems associated with either inadequate water supplies and flooding, both of which affect the social and economic well being of the residents of the Souris River Basin. Managing for the greater range of hydrologic variability evident in proxy records versus gauged, hydrometric records can prepare water managers for adaptation to climate change. Fourteen (2 previously collected and 12 new) moisture sensitive tree-ring sites were chosen and 37 chronologies (annual, earlywood, and latewood) were developed and used to create robust multi-proxy reconstructions of annual water year (October – September) and summer (June – August) streamflow for four gauges within the Souris River Basin. Multiple linear regressions were able to account for ~54-76% and ~38-67% of the instrumental variance for water-year and summer flows, respectively, extending the historical record as far back as 1726, for a total of 280 years. Hydrological extremes were quantified and classified as abnormally wet years being in the 75th percentile, while discharge in the lowest 25th percentile were considered as drought years, with the most severe episodes indicated by flows in the lowest 10th percentile. Water year flows indicate that the most severe low flow events took place in the late 1810s, mid 1830s, 1860s, late 1890s to early 1900s, and again in the mid 1950s. Streamflow reconstructions for the Souris Basin capture the low flow events occurring during the late 1880s through

the 1890s (the ‘Great Die-Up’); as well as another event known as one of the most severe and long lasting reconstructed droughts from 1841 through 1865, the drought of the late 1790s through the early 1800s, and the occurrence of ‘El Año del Hambre’ – the year of hunger, during the late 1780s , as well as during the 12 year period from the 1750s to early 1760s. Spectral analyses provide evidence that streamflow variability in the Souris River Basin is driven by a combination of interannual (~2-6 year), interdecadal (~7-11 year), and multidecadal (~20-30 year) ocean-atmosphere oscillations, such as indices of ENSO, solar sunspot cycles, and PDO, respectively. Correlation analyses, cross-wavelet transforms and wavelet transform coherence identify significant periods of high common power and coherence of high, interdecadal, and low frequency oscillation relationships of streamflow with ENSO, solar sunspot cycles, and PDO indices, respectively. When these sea-surface temperatures and atmospheric oscillations are coupled, and in-phase with each other, it may lead to more prolonged and possibly greater in magnitude extremes than when climate anomalies are out of phase, resulting in a relatively modest influence of streamflow variability.

ACKNOWLEDGEMENTS

Financial support for this research was provided by the National Sciences and Engineering Research Council of Canada, the Faculty of Graduate Studies and Research, and also from the Prairie Adaptation Research Collaborative.

I am grateful to many people for their continuous and invaluable help and support throughout this project, and I wish to especially thank my supervisor Dr. Dave Sauchyn for his support, guidance and opportunities to travel for fieldwork and attend many conferences from which I have gained professional knowledge and experience to further my career. I would like to thank and acknowledge the Prairie Adaptation Research Collaborative (PARC) and my colleagues there for providing a pleasant and inspiring place to work while expanding my academic career.

Without the advice and support of Carol Graham of the Manitoba Agro Woodlot Program, Dr. Marc Rivard of the Manitoba Watershed Authority, Dr. Joe Zeleznik at North Dakota State University, Kathy Duttenhefner from North Dakota Parks and Recreation Department, and private landowners throughout Saskatchewan and Manitoba, this research and site locations would not have been possible. Thanks to all my present and past colleagues and friends, Cesar Perez-Valdivia, Jeannine-Marie St. Jacques, Mariya Krestvanskaya, Svetlana Esenkulova, Suzan Lapp, Jonathan Barichavich, Jill Deschamps, Golden Gooding, Nataliia Prytula, Ted Morris, and Jeremy Pittman, for their help, support, and muscles when coring the tough oak trees in the field.

Very special thanks go to my colleague and best friend Cesar Perez-Valdivia, for whom without, I never would have learned or accomplished as much I have throughout this chapter in my career and for that I thank you.

Finally I wish to thank my family and friends who have provided me with continual encouragement, support, patience and love, enabling me to complete my graduate work. Without you I would be lost.

TABLE OF CONTENTS

LIST OF FIGURES

LIST OF TABLES

LIST OF APPENDICES

1. INTRODUCTION

A growing dependence on surface water resources in the Prairie Provinces has resulted in an increasing vulnerability to hydrological drought (Schindler and Donahue 2006; Wheaton *et al.* 2008). Over time, water demand and vulnerability to hydrological drought will likely increase in the Prairie Provinces due to population growth, increasing intensification of agriculture, and the predicted global warming of 1.4 to 5.8^{o}C between 1900 and 2100. All of these factors contribute to the need to understand the vulnerability of the Prairie region to climate change and for developing adaptation strategies. The most serious risk from recent and projected climate warming in western Canada is a shift in the amount and timing of streamflow (Sauchyn and Kulshreshtha 2008). The snow-dominated basins of mid-latitudes to high latitudes are losing the advantage of a cold winter; snow and ice are the most reliable, predictable and abundant sources of spring and summer runoff (Axelson *et al.* 2009). Due to low and variable rainfall within the Prairies, there is high dependence on streamflow for consumptive and non-consumptive water uses (McKay *et al.* 1989).

The Souris River basin has, over the years, been plagued with problems associated with either inadequate water supplies (*i.e.* droughts and low flow events) and flooding, both of which affect the social and economic well being of the residents of the Souris River Basin. The Souris River, therefore, has been the subject of numerous studies and investigations over the years by both Federal and Provincial Government departments responsible for water resources and associated problems (Manitoba Water Commission 1984). Flooding and low flows affecting the water supply and water quality can counteract economic development. The social and economic welfare of the people of

the Souris River Basin depends to a considerable degree on the way in which its limited water and related resources are managed to serve such uses as agriculture, recreation, waste assimilation, domestic, municipal and industrial water supply (SRB Study Board 1978).

Managing for the greater range of hydrologic variability evident in proxy and projected, versus gauged, hydrometric records can prepare water managers for adaptation to climate change (Axelson *et al.* 2009). Centuries long tree-ring reconstructions of streamflow capture hydroclimatic variability at annual to multidecadal scales (Stockton and Jacoby 1976; Meko *et al.* 1991; Woodhouse 2001; Case and MacDonald 2003; Gedalof *et al.* 2004). Absolutely dated tree-ring chronologies are an important archive for evaluating both past and current natural climate/hydroclimate variability occurring over centuries and millennia, as well as changes over recent decades and at annual and sub-annual temporal resolutions.

1.1 Research objective and hypotheses:

This study will examine the hydroclimatic variability in the Souris River Basin using dendroclimatic reconstructions of streamflow for the Souris River and its major contributing tributaries. Relationships between tree-rings, and historical climate and streamflow records will be investigated in order to capture the full range of hydroclimatic variability (*i.e.* prolonged periods of drought), as well as atmospheric and sea-surface temperature forcings thought to be possible drivers of annual and sub-annual fluctuations in streamflow within the Souris Basin.

Previous investigations of the dendrochronological potential of *Quercus macrocarpa* provide evidence to support the notion that bur oak are suitable proxies of

precipitation and streamflow for nearby instrumental stations (St. George and Nielsen 2000; St. George et al. 1999, 2001, 2008; Vanstone and Sauchyn 2010). Vanstone (2007) and Vanstone and Sauchyn (2010) created the first bur-oak tree-ring chronologies for southeastern Saskatchewan, and were ultimately successful in accurately capturing the historical occurrence of single and multi-year droughts that had occurred in eastern portions of the Canadian Prairies; a step towards filling the void in the 'Prairie-gap' in the Canadian dendrochronological-network.

The objective of my study is to develop a systematic and comprehensive understanding of the capacity of various moisture sensitive *Q. macrocarpa* tree-ring chronologies, from the Canadian Prairies and northern Great Plains region, to create robust reconstructions of historical streamflow for the Souris River Basin. The significance of my proposed research is in the use of innovative high-resolution dendrochronological analyses to gain longer perspectives on streamflow variability and extreme events (*i.e.* droughts), than provided by instrumental records. Investigations will include stations along the Souris River, Long Creek, and Pipestone Creek (two major contributing tributaries for the Souris River) within southeastern Saskatchewan, southwestern Manitoba and northern North Dakota aiming to provide spatial and temporal results of hydrological drought frequency, severity and synchrony within the entire Souris River Basin.

A further step will be the study of not only *annual* ring-width chronologies, but also seasonal growth responses of *Q. macrocarpa* to test the hypothesis that early- and latewood chronologies can serve as multi-proxies of streamflow providing more reliable

information at annual and sub-annual (seasonal) time scales than flow reconstructions derived from chronologies of annual ring width alone.

Further objectives will be to quantify and identify hydrological extremes (*i.e.* single and multi-year droughts) in each of the reconstructions, and to determine and extract dominant oscillation modes of variability using spectral analyses, while trying to contribute these dominant modes as possible drivers for drought.

1.2 Background:

1.1.1 Synoptic controls on drought in the Prairies:

"While drought may be easily attributed to regional pressure and wind systems, physical understanding must include larger-scale atmospheric teleconnections and interactions between the atmosphere and abnormalities at its lower boundary, such as variation in sea surface temperatures, snow and ice cover, and the character of soil and its moisture content" (Namais (1983) in Khandenkar 2004, 13). Earlier studies of Dey and Chakravarty (1976) identified the presence of a mid-tropospheric ridge centered over the Prairie Provinces leading to extended dry spells and precipitation deficits during the summer seasons, which can be linked to certain configurations of Pacific Sea Surface Temperature (SST) patterns.

The El Niño-Southern Oscillation (ENSO) is a prominent example of teleconnections in our climate system that has raised popular and scientific awareness of broad scale climatic processes. ENSO is a cyclical but irregular 3-7 year SST oscillation in the tropical Pacific Ocean, consisting of a warm (El Niño) phase, during which SSTs in the tropical eastern Pacific are anomalously warm, and a cool (La Niña) phase associated with cool SSTs in the eastern Pacific (Case 2000; Rasmusson and Carpenter

1982). Prairie precipitation is less affected by ENSO than temperature; however, winter precipitation during El Niño is significantly lower than normal and is significantly higher during La Niña events (Shabbar *et al.* 1997). The escalating interest in teleconnections has lead scientists to look for other long-term oscillations in the climate system that may lead to climate predictions and a deeper understanding of the linked marine-terrestrial system

Some SST anomaly patterns recur on a regular basis. The Pacific Decadal Oscillation (PDO; Mantua *et al.* 1997; Minobe 1997; MacDonald and Case 2005) and the North Atlantic Oscillation (NOA; Barnston and Livezey 1987) are two of the more important SST phenomena that affect climate in the Northern Hemisphere besides ENSO (Speer 2010).

The Pacific Decadal Oscillation (PDO) is a large scale pattern of SST variability characterized by a gradient between anomalously cool SSTs in the east-central North Pacific and anomalously warm SSTs off the central west coast of North America (Case 2000; Mantua *et al.* 1997; Minobe 1997). North Pacific SSTs affect precipitation amounts on the Prairies through links with 500 mb height anomalies in the mid-troposphere. During a positive phase of the PDO, this teleconnection occurs more frequently, resulting in long-term persistence of the negative precipitation anomaly (Knox and Lawford 1990). The PDO has positive (warm) and negative (cool) phases that appear to persist for two-three decades. Positive PDO (warm) phases occurred between 1925-46 and 1977-1998. These periods have been associated with warm winter and spring time temperatures in northwest North America, and dry conditions in the west to central North America (Fagre *et al.* 2003). Negative (cool) PDO phases occurred

between 1900-1924 and 1947-1976, bringing with them cool winter and spring temperatures over western North America, as well as wet conditions in the Pacific Northwest, northern Rockies and central Prairies.

The North Atlantic Oscillation (NAO) is a large-scale atmospheric circulation between the Icelandic Low and Azores High (Cook *et. al.* 1998). The NAO is an important large-scale oscillation, first identified by Sir Gilbert Walker in his pioneering studies (in the early 1900s) on the correlation between the Indian monsoon and worldwide weather elements (Khandekar 2004). It has been since recognized as being a key source of seasonal to decadal-state climate variability in the North Atlantic sector (Van Loon and Rogers 1978; Cook 1998). The NAO is measured by the height of the 500 mb isobar with a positive phase representing below-normal heights in the high latitudes of the North Atlantic and above-normal heights over the central North Atlantic (Speer 2010). Winter is most impacted by the NAO, however Rogers (1990) shows that the NAO accounts for the largest amount of interannual variability in monthly North Atlantic sea-level pressure data in all but four months of the year and persists well into the summer months. The NAO is now recognized as having a definite impact on temperature and precipitation patterns over eastern Canada, and is believed to extend occasionally into central Canada and the eastern Prairies (Khandekar 2004). Spectral analyses have shown that the NAO as having significant periodicities around 7.3-8.0 years (Rogers 1984; D'Arrigo *et al.* 1993; Hurrell 1995) associated with a seesaw of warm and cold winter temperature severity between Europe and Greenland (Van Loon and Rogers 1978).

The hypothesis that solar variation causes fluctuations in climate has existed for some time; described early by A.E. Douglass' investigation of the affect on the growth of trees (1919, 1928, 1936). Several studies since then (Currie 1990; 1991) have been able to link solar activity to drought occurrence on the US Prairies and the Great Plains in general, with some of most severe droughts (1917, 1937) being associated to sunspot cycles of 11 or 22 years (Khandekar 2004). For example, Currie and O'Brien (1990) suggested that the cyclical variation of dry and wet years on the Plains can be explained using epochs of maximum and minimum solar tidal forcing of the atmospheric luni-solar cycle. However, Namias (1983) concluded that as there is no actual 'physical' mechanism for a possible link between sunspot cycles and a specific atmospheric flow pattern leading to a drought or a wet season, causing some to remain skeptical of the relationship (LaMarche and Fritts 1972). Recent climate modeling of global warming has included the influence of varying solar flux to simulate the rapid warming of the surface of the earth during the years 1910-1940 (Meehl *et al.* 2003; Khandekar 2004). Several other recent studies (Lean *et al.* 1995; Lean and Rind 1998) have now identified changing solar radiation as an important mechanism of climate change. It is possible that some of the extreme droughts of the dust bowl years were triggered or made worse by solar flux variation (Khandekar 2004).

The empirical probability of recurrence of “severe drought is of interest to long range planning for agriculture and water resources, but gauged rainfall cannot record long-term drought history in the Great Plains [and Prairie Provinces] back beyond the late 1800s” (Stockton and Meko 1983, 17); therefore the usefulness of proxy records (*i.e.* tree-rings) are a prime method for extending regional drought history. Broad-scale tree-

ring networks can be more generally applied in synoptic climatology - the study of climate from the perspective of atmospheric circulation (Speer 2010). Circulation patterns can be inferred from reconstructed patterns of precipitation, temperature, streamflow, and atmospheric pressure (Fritts *et al.* 1971; Blasing and Fritts 1976; Fritts 1976; Fritts and Shao 1992; Hirschboeck *et al.* 1996; Barber *et al.* 2004; Girardin *et al.* 2006). Beyond simple reconstructions of temperature and precipitation, researchers are exploring correlations with other variables and strengthening our understanding of the connectivity of the global circulation system (teleconnections). However, Cook *et al.* (1997) point out that the scarcity of proxy climate data from the northern high plains of the U.S. and southern Canada hinders a better understanding of the synoptic characteristics of North American drought; thereby suggesting the need for studies within the Prairies as a means of better understanding the large-scale controls on drought.

1.1.2 The need for dendroclimatic investigation:

Current scientific concern to establish the nature and the rate of climatic changes, considered to be exacerbated by human activities, should serve to reinforce determination to understand similar details of the 'natural' (*i.e.* non-anthropogenic) variability of climate (Storch and Navarra 1999). Studying past climatic change puts current trends in perspective, reveals the mechanisms that govern the Earth's climate systems, provides data to test predictive models and evaluates the impact of climatic change on biological and geographical systems and processes (St. George *et al.* 2001). Irrespective of the causes and intensity of change, ecosystems are often naturally able to recover, and often prove useful as 'markers or recorders' for key environmental events, such as droughts or massive floods (Bazzaz, 1996). Therefore, the use of these 'natural markers' for

reconstructing past climates on all timescales is clearly important if we hope to understand the mechanisms that control climate today. However, the scope and the rapidity of the changes foreseen in many scenarios of an 'enhanced-greenhouse' world, highlight the particular relevance of palaeoclimatic studies that focus on recent centuries and millennia (Eddy, 1992). Thus "'natural' records of past climate variability ('proxy' climate data), that are annually resolved and that capture decadal-to-century timescale variability, represent an essential basis for comparison with relatively short modern climate records, which are rarely longer than a hundred years" (Storch and Navarra 1990, 78).

Proxy reconstructions of climatic variability have two major advantages for studies of environmental change; they place the modern instrumental or human observed record into a longer term context of natural variation, and identify themes or places of past changes which may provide analogues for future changes (St. George *et al.* 1999). Although palaeoclimatic and dendroclimatic research has made significant advances toward understanding how the Earth's climate has changed, long, high-resolution records of climatic change are still relatively few at global and national scales, and large gaps still exist in the current Canadian palaeoclimatic network. Although proven useful, there are many spatial biases when collecting these proxy records as the changes in average global conditions are not experienced in all regions uniformly (St. George *et al.* 2001). As global change results in changes at the regional or local levels, there is therefore a critical need to understand climate history at these scales.

1.3 Study area:

1.3.1 Geography and climate

Ecologically, the Souris Basin is located within the Prairies/Great Plains Region, more specifically, within the Aspen Parkland/Northern Glaciated Plains Region (Figure 1.1; U.S. Environmental Protection Agency 2010). This ecological region is distinguished particularly by its relatively little topographic relief, grasslands and a scarcity of forests, with a subhumid to semiarid climate. Undisturbed, the Aspen Parkland ecoregion is a mix of aspen groves and fescue grasslands, and represents the zone of transition between open grasslands and continuous forest. Agricultural use has drastically altered this ecoregion, with 80 percent of the landscape now cropland (Saskatchewan Watershed Authority 2005).

The Souris River Basin covers an area of approximately 60 400 square kilometres in southeast Saskatchewan, north-central North Dakota, and southwest Manitoba (Figure 1.2). The Souris River is approximately 700 kilometres in length, and originates in the Province of Saskatchewan, passing through the state of North Dakota, then veering north and re-crossing the international boundary into Manitoba, before joining the Assiniboine River near Brandon, Manitoba. The river valley is flat and shallow, and its semi-arid prairie has been extensively cultivated. The Souris River Basin is an international transboundary basin, subject to the Boundary Water Treaty of 1909, under the terms of which the International Joint Commission was established to regulate the use of the Souris River on either side of the International Boundary. Surface waters are heavily regulated throughout the basin as the International Souris River Board, appointed control in the 1940s, has a role in managing the waters of the Souris River Basin through its

mandates for flow apportionment and flood control, by adhering to threshold levels/values set forth by the International Joint Commission administering the Boundary Waters Treaty (Manitoba Water Commission 1984; International Joint Commission 2011). As such, major reservoirs have been constructed in both the U.S. and Canadian portions of the basin, including Boundary, Rafferty and Alameda Reservoirs in Saskatchewan, and Lake Darling in North Dakota (International Joint Commission 2011).

Soils within the basin are commonly deep, and throughout most of the region were originally highly fertile. Today, soils of agricultural potential through the area face problems of reduced nutrient potential, increasing salinity and susceptibility to wind and water erosion. The climate is both dry and semi-arid, and continental, characterized in the north by short, hot summers and long, cold winters. High winds are an important climatic factor in this ecological region. It is also subject to periodic, intense droughts and frosts. On average, annual precipitation received throughout the area is low, ~250 - 500 mm, with higher amounts occurring in the east. Mean annual temperature for the area is approximately 3°C, with mean summer temperatures around 17°C and mean winter temperatures around -13°C.

Cold winters lock up snowfall until the spring melt, which then provides most of the stream flow. The flat landscape leaves much of the water sitting in sloughs and ponds, where hot, dry summers quickly evaporate this water as well as that within reservoirs, plants and soil. With these conditions, not much water makes its way into the Souris River, especially since the annual potential evaporation rate is triple the average precipitation (International Souris River Board 2009).

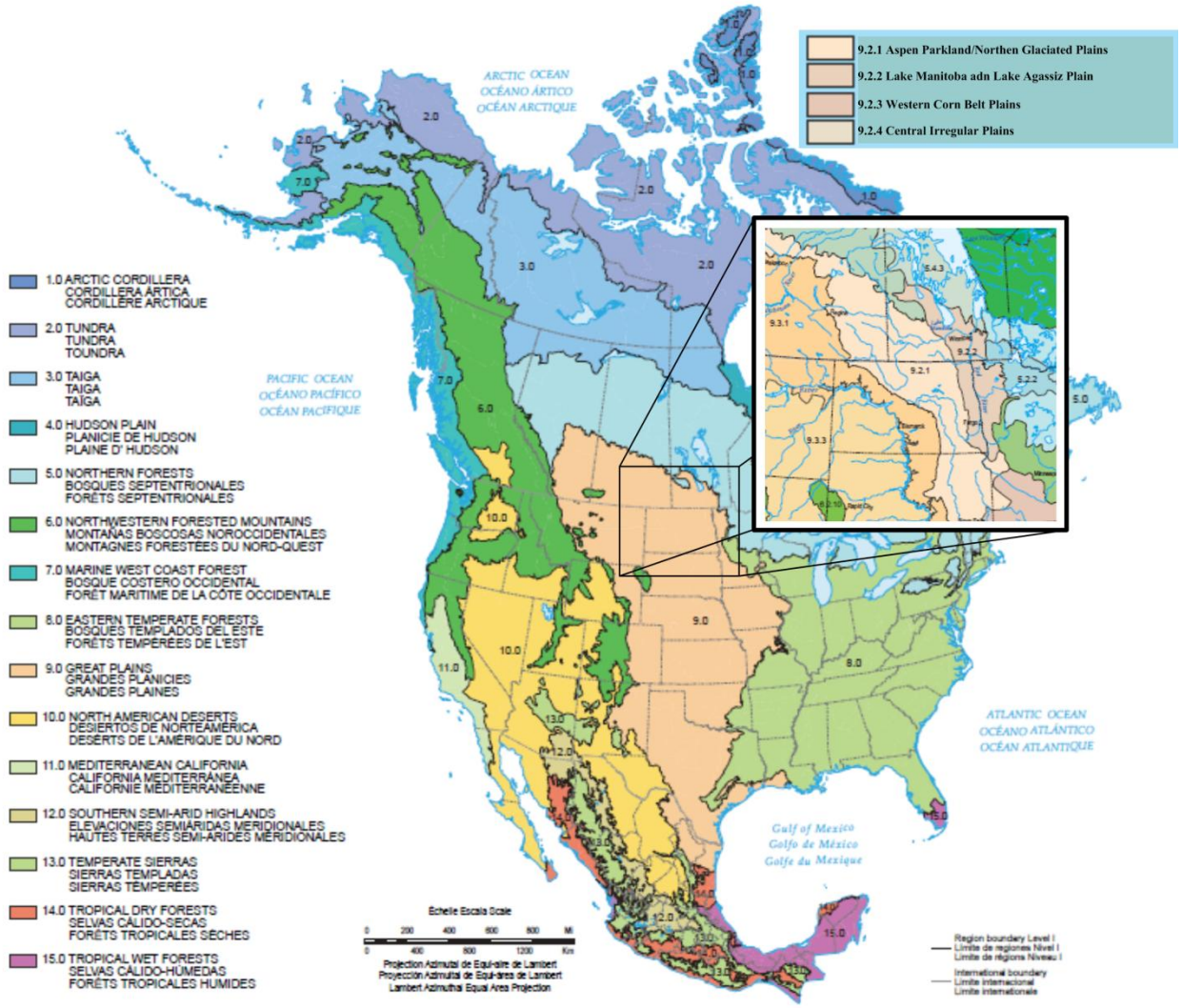

Figure 1.1 Ecoregions of North America. Source: U.S. Environmental Protection Agency 2010.

1.4 Species selection:

Quercus macrocarpa (Bur Oak) which is widely distributed throughout the Eastern United States and the Great Plains is a drought-tolerant and slow-growing species and among the longest lived deciduous trees of the northern Plains region (Drunasky and Struve, 2005; Johnson, 1990; Nixon, 2006). The genus Quercus is one of the most important clades of woody angiosperms in the northern hemisphere in terms of species diversity, ecological dominance, and economic value. Oaks also enter, and are important, along the margins of various other vegetation types, such as coniferous forests, prairies,

tropical grasslands, desert and semi-desert scrublands, dry (deciduous) tropical forest, and in some evergreen tropical forests (Nixon, 2006). Within the Souris Basin, oak forests play significant roles on the landscape, as they act as significant ecological reserves for wildlife, such as within the Souris River Bend Wildlife Management Area. The oak also provide a rich food source in the form of acorns for wildlife in addition to protection and shelter during migration along the major Souris River water course.

Quercus macrocarpa is a ring-porous angiosperm (described as wood with an abrupt change in vessel size across the ring; Metcalfe and Chalk 1950), with a deep root system and fire-resistant bark. Its tolerance to a wide range of soil and moisture conditions enables bur oak to act as a pioneer species along the southeastern edge of the Prairies (Lawson *et al.,* 1980). The patterns within the annual layers of *Quercus* tree-rings suggest that precipitation influences the size and density of vessels within the ring, either by acting as a limiting factor for growth or through fine tuning of the wood structure (probably characteristics relating to water conduction) to environmental conditions (Woodcock, 1989).

The transition from earlywood to latewood in many species is gradual not sharp; however, a distinct intra-annual boundary permits width measurements of earlywood and latewood in *Quercus* species (Phipps 1982). Spring growth, or earlywood, including large vessels which appear circular in cross section, is used for vertical conduction of water. The vessel-bearing part of the ring porous species is more properly referred to as the pore zone, and the cambial derivatives that enlarge and differentiate into vessels are cut off from the cambium, not during the current spring, but at the end of the previous growing

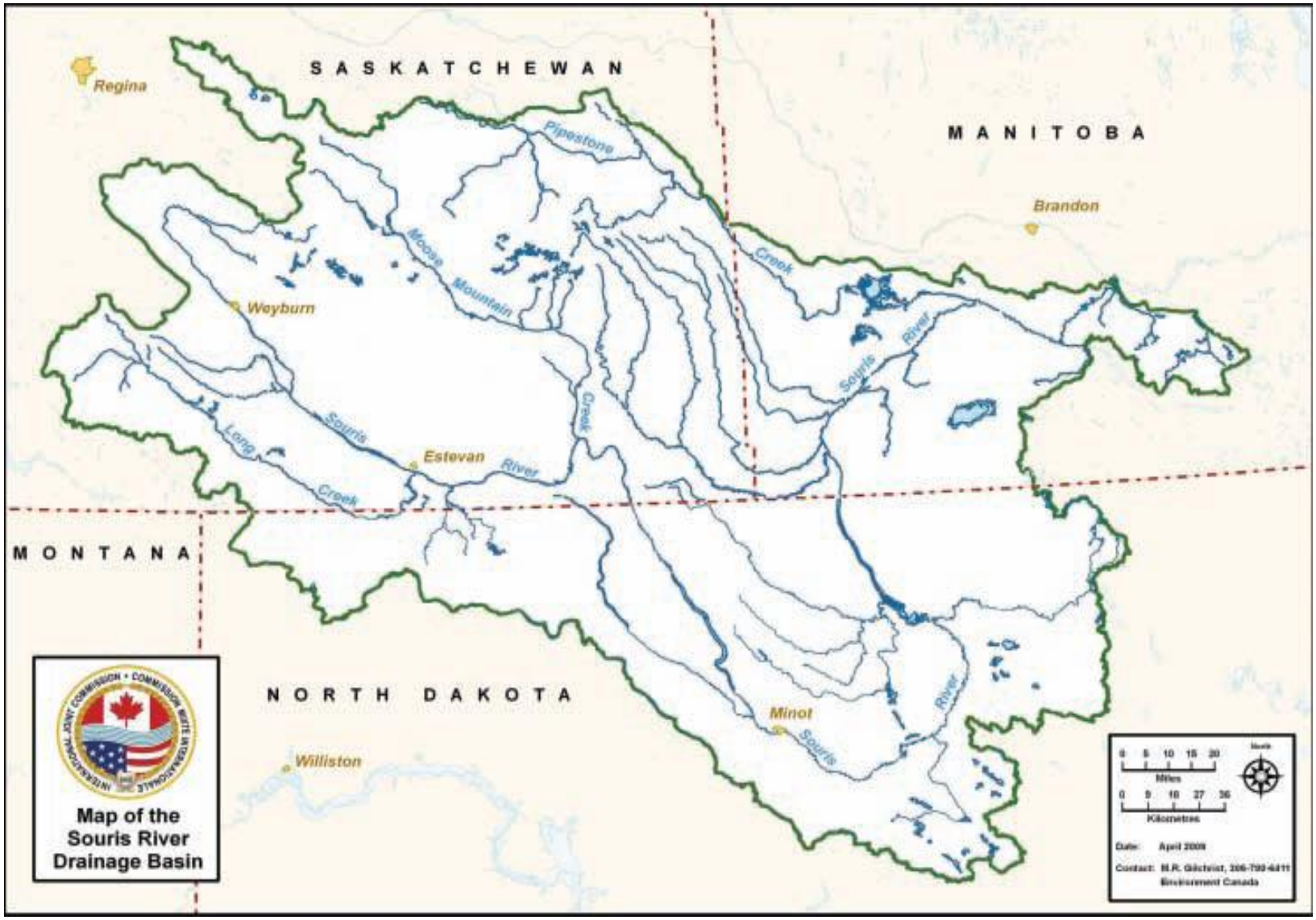

Figure 1.2 Map of the Souris River Drainage Basin. Source: International Souris River Board of the International Joint Commission.

season (Phipps 1967). Thus the number of vessels may be a condition of the latter part of the previous growing season, and the pore zone width (*i.e.* earlywood width) is a function of conditions of the current spring. The latewood part of the annual ring, formed during the summer or later growing season, contains smaller vessels or none at all. Large vessels are formed during the early part of the growing season to conduct large amounts of water to the leaves, while the smaller latewood vessels reflect a reduction in water demand and availability later in the year (St. George and Nielsen, 2001; Woodcock, 1989). In general, *Quercus* species have the ability to sustain stomatal conductance at low soil and leaf water potentials and have an inherently low capacity for water loss that contributes to their success in dry locations (Drunasky and Struve, 2005). Diameter and density of the vessels have been related to vulnerability to water stress, with smaller, denser, vessels associated with decreased vulnerability, such as during a drought (Carlquist, 1975).

2. THEORETICAL FOUNDATION

2.1 Dendrochronology:

2.1.1 Philosophical approach:

Conducting scientific research is a creative experience that requires the theoretical framework not only to bring order and method to the act of inquiry, but also to advance science. The theoretical framework that informs dendrochronology is a positivist scientific approach, using deductive and inductive-probabilistic reasoning (Axelson 2007). There is strong emphasis on quantitative analysis with a sound mechanistic and statistical basis (Hughes 2002), where inferential statistics are employed to analyse the relationship between the environment and tree-rings (Fritts 1976; Cook and Kairiukstis 1990).

"Every science accumulates a body of knowledge from which generalizations can be made. These generalizations, based upon repeated observations and experience, may be described as principles or concepts which embody the fundamental truths of science" (Fritts 1976, 14). Because of the many possible applications of its use, dendrochronology is a scientific method at the crossroads of many scientific disciplines, as it borrows ideas from such fields as wood anatomy, isotope analysis, and chemistry, and serves such disciplines as archaeology, climatology, hydrology, and forest ecology (Dobbertin and Grissino Mayer 2004). Regardless of the area of research where tree-ring analyses are implemented, a number of principles inform dendrochronology and are a point from which scientific generalizations can be made.

2.1.2 Principles of dendrochronology:

Uniformitarianism, a concept originally proposed by James Hutton in 1785, implies that earth processes occurring in the present were the same processes that had operated in the past, and would be the processes that operate in the future. "Applied to dendrochronology, the uniformitarian principle implies that the physical and biological processes which link today's environment with today's variations in tree growth must have been in operation in the past. Likewise, the types of weather variations and climatic patterns observed today also must have occurred in the past. Therefore, one can establish the relationship between variations of tree growth and variations in present day climate and infer from past rings the nature of past climate" (Fritts 1976, 15).

Based on the uniformitarian principle, weather and climatic patterns that occur today must have been observed in the past, which further implies that the same kinds of limiting conditions (*i.e.* precipitation, temperature, etc.) affected the same kinds of processes in the same ways in the past as in the present, only the frequencies, intensities and localities of the limiting conditions affecting growth may have changed; thus leading to the *principle of limiting factors*. During 'non-stressful' growth years (*i.e.* precipitation and temperature are adequate for optimal growth), growth will be limited by yet another factor such as sunlight, soil nutrients, or species competition for example. This is known as the *principle of aggregate tree growth*, which states that any individual tree-growth series can be 'decomposed' into an aggregate of environmental factors, both human and natural, that can affect the patterns of tree growth over time. "Where limiting factors result in tree-ring width variability, the next two concepts address the necessity of evaluating the environment where trees are growing" (Axelson 2007, 13).

"Each species, depending upon hereditary factors which determine its phenotype, may grow and reproduce over a certain range of habitats. This range is known as a species' *ecological amplitude*" (Fritts 1976, 16). This is an important principle because individual trees that are most useful to dendrochronology are often found at sites where they are under stress; commonly near the margins of their natural range, latitudinally, longitudinally, and elevationally (Bradley 1985). In such situations, variations in climate conditions, such as precipitation or temperature, will greatly influence annual growth increments. Following from ecological amplitude, the concept of *site selection* highlights the necessity to collect samples that are similarly affected by a set of growth limiting factors, resulting in the non-random nature of sampling in dendrochronology (Fritts 1976). "Thus in studies of ring widths and drought, it is important to rely upon trees growing in the driest sites, for those are the individuals in which ring width is most likely to have been limited by drought" (Fritts 1976, 19).

Because tree-rings enable absolute dating, *crossdating* is the most important principle of dendrochronology. Its application provides a type of 'experimental' control because it assures the proper placement in time of each growth layer (Fritts 1976). This principle is applied by 'pattern recognition/matching' of ring-widths among all the samples at a given site. These sequences may not be repeated exactly from tree to tree, as a result of microclimate variations experienced by individual trees within a stand. Similar environmental conditions that ultimately limit tree growth will be common to all trees in a stand, thus producing synchronous variation in ring-width structure, making *crossdating* possible. Ring-width variation from year to year, and the degree to which this variation is present, is referred to as *sensitivity*. "Such fluctuations in ring width can

be estimated qualitatively by visual inspection of the rings; or it can be calculated from measurements of width and expressed as a statistic called mean sensitivity, which is a measure of the relative differences in width between adjacent rings" (Fritts 1976, 19). In order to maximize the environmental signal being investigated (inherently exploiting the sensitivity), and minimize the amount of 'noise'(environmental factors not of interest, *i.e.* air pollution), the *principle of replication* is instated, by sampling more than one increment/sample per tree, and more than one tree per site (Grissino-Mayer 2006).

2.1.3 Debates and limitations of dendrochronology:

The greatest strength of dendrochronology is the capability to date tree-rings to the calendar year in which they were produced, with a very high degree of confidence. A recognized weakness is a lack of understanding how climate influences tree rings, especially of the relationship between large trees and their environment.

> "Some physiologists have argued that because we do not completely understand the mechanisms that occur from the assimilation of abiotic elements from the environment to the formation of the tree-ring, we should not be conducting dendrochronological studies. However, countless analyses of the correlation between tree growth and environment variables have demonstrated consistent predictable results demonstrating that despite our lack of understanding of the exact mechanisms, we know that tree growth does reflect environmental variables. Over 100 years of productive research in dendrochronology supports its validity and importance in environmental reconstruction" (Speer 2008, 7-8).

Related to the principle of site selection and ecological amplitude, the development of well-dated tree-ring chronologies for the reconstruction of environmental variables is restricted by the location of sensitive tree-ring series (Fritts 1976). Like those of the Canadian Prairies, long-lived tree stands are often sparse and scattered and even when they are present, dendrochronologists must choose specific sites that are likely to record and maximize the environmental variable that they wish to study. For example,

tree-ring studies of drought conditions would involve sampling trees growing on south-facing slopes, areas of maximum radiation exposure and slope, in areas known to be water limited (Fritts 1976). These constraints geographically limit dendrochronology to areas where the trees produce datable annual rings and where local paired climate or ecological data exist for calibration of the trees' response (Speer 2008). Climate reconstructions based on tree-ring variables rarely capture a high percentage of the variance of the chosen instrumental variable, which could be due to the scarcity and continuity of climate stations and records, respectively. Because trees were not 'designed' as climate recorders, there should be no surprise "that they are imperfect recorders of climate, as are all natural archives" (Martinelli 2004, 102). Although these imperfections may exist, when evaluated with meteorological data (at mico- (station) and macro- (gridded) levels), tree-ring records are quite comparable (Fritts et al. 1971; Briffa et al. 1986; Fritts 1991; Cook et al. 1994, 1999; Zhang et al. 2004).

Practically, it should be clear that every process or phenomenon, by definition, must occur across a certain area (space) and last for a certain period or duration (time). It is well documented that the characteristic scales of many physical and ecological phenomena are related in space versus time, such that the ratio between spatial and temporal scales tend to be relatively invariant over a range of scales, thus certain entities will be affected similarly by processes/phenomena occurring over a range of spatial and temporal scales. The underlying principle of dendrochronology, *uniformitarianism* – processes occurring today are the same processes that occurred in the past (*i.e.* climate affecting tree-ring growth), suggests much in the same. Climate seems to be one of the main controlling factors of most tree growth processes across all spatial and temporal

scales; therefore, dendrochronologists are interested in past climate so that variations and trends of modern climate can be put into perspective. In order to actually 'link' variations in tree-ring width with variations in climate, and to chose sites representative of this variability, it is necessary for the dendrochronologist to understand and be aware of the spatial and temporal domains the climatic component of interest actually covers.

Reflection of scale differences is combined with recognition that there is unlikely to be a single, best representation of reality across all scales. An appropriate representation at one scale, derived from a specific method, will not form an appropriate representation at another scale (Inkpen 2005). As the scale of study changes, the nature of the phenomenon changes and the means to represent it in an appropriate manner alters. Effective scale detection requires that the scale of the analysis be of equal extent or duration with the intrinsic scale of the phenomenon under study; however because the latter is usually unknown *a priori*, multiple observation sets at different scales usually are necessary (Allen *et al.* 1984; Wu 1999).

Dendroclimatic micro-scale fluctuations, (*i.e.* precipitation events at a discrete location), are generally sampled for at distinct locations, where a few (two or more) sites within relative proximity (less than 100 km apart) are chosen to theoretically represent the aerial extent the phenomenon(a) would likely cover. Meso- to macroclimatic scale studies (*i.e.* atmospheric circulation patterns) customarily require an increase in number of sampling sites, as well as a broader spatial extent (distances greater than 100 km apart) for sampling in order to adequately cover the large spatial area influenced by such phenomena. Only when the scales of observation and analysis are properly chosen may the characteristic scale of the phenomenon of interest be detected correctly; and only

when the scales of experiments and models are appropriate, may the results of experiments and models be relevant.

As scale changes, in any geographical investigation, new patterns and processes may emerge, and controlling factors may shift even for the same phenomena. Broad-scale observations may not have enough details necessary to understand fine-scale dynamics, whereas on the other hand, observations made at fine scales may miss important patterns and processes operating on broader scales. Dendroclimatological investigations have made attempts at minimizing the adverse effects of scaling and reducing the probability of making false inferences, via the implementation of detrending methods, statistical techniques, and the use of spectral analysis.

Detrending is the statistical or mathematical operation of removing trends from the tree-ring time-series, and is often applied to remove a feature or features (*i.e.* non-climatic influences or 'noise' – competition, anthropogenic effects) thought to distort or obscure the growth relationship of interest, retaining as much variance as possible at the long wavelengths or low frequencies. Such variance represents the gradual fluctuations in growth over periods of decades and longer.

The use of statistics and model verification is an important part of any dendrochronological investigation, and great care must be taken to apply the many well-developed and tested methods for reconstructions of any nature. Uncertainty is inherent in any type of reconstruction; however, methods like multiple linear regressions yield an estimate of the reconstruction uncertainty in terms of the error variance, which reflects the goodness of fit of the model, and is critical to the interpretation of the reconstructed statistics (Meko and Woodhouse 2011). Additional uncertainty is due to the time-varying

makeup of predictors used to create reconstructions, such that some series may pre-date the calibration period, (*i.e.* tree-ring time series from remnant wood or archaeological samples). However, quality control methods, such as the expressed population signal (EPS) and principal component analysis, are available, and allow for chronologies to be extended back in time via the inclusion of older series, while retaining a common signal even though the sample size may diminish throughout this period.

Analysis of the spatial and temporal variability of tree-ring signals determines whether the signals recorded in the tree-ring chronologies at local scales prove useful as proxies at macroclimatic scales. Singular spectrum analysis (SSA; Vautard and Ghil 1989), and wavelet analysis (Torrence and Compo 1998) are used to examine the cyclicity of synoptic-scale signals detected in regional growth responses of the tree-ring time series, thereby detecting influences related to regional climatic/environmental variability, while minimizing contributions from local, non-climatic noise (St. George *et al.* 2008).

Uncertainty in any reconstruction can never be completely eliminated, however, it may be greatly diminished by incorporating information from tree-ring variables other than ring width index in the reconstruction model (Meko and Woodhouse 2011). Variables might include wood density, (Briffa *et al.* 1988), early and/or latewood widths (Vanstone and Sauchyn 2010) stable isotope ratios in tree rings (Leavitt and Wright 2002), or the anatomical features of cambial cells (Vaganov 1990; Vaganov *et al.* 2006). Even with the inclusion of these extra variables, a perfect reconstruction will not be reached, but the improvements in accuracy may enhance the usefulness of the reconstruction for water resource management (Meko and Woodhouse 2011).

Understanding natural historical hydroclimatic variability, beyond the length of instrumental records can be obtained from centuries long tree-ring reconstructions, which aid in the identification of major drivers or forcings that influence climate on local and regional scales. "These large-scale controls are likely to continue to operate in the future, and a baseline knowledge of the role of oceanic/atmospheric conditions in long-term regional hydroclimatic variability is necessary to understand how the climate system operates now and how it will under warmer conditions. The challenge will be to blend the knowledge gleaned from the past with projections for climate under climate change scenarios to get a better indication of the range of hydroclimatic conditions and events to expect in the future" (Meko and Woodhouse 2011, 256).

2.2 Hydrologic factors:

Hydrology is concerned primarily with the continental phase of the water cycle, the flow of surface water, and the relationship between water and living organisms (Hendricks 1962). Variability in streamflow reflects the seasonal and inter-annual variability in the amount and timing of runoff as influenced by climate factors such as precipitation and temperature, and by non-climatic factors such as soil and vegetation conditions (Ward and Robinson 2000). Expressing runoff as depth equivalent over the drainage area allows comparisons between basins of different sizes and to the precipitation and evaporation. Low amounts of runoff (International Souris River Board 2009) makes the Souris River and its tributaries very sensitive to precipitation and runoff conditions, where flow can change from a trickle to a torrent in a few days, illustrating the extreme variability that can occur from day to day and from year to year (Saskatchewan Watershed Authority 2005).

The main hydrologic inputs affecting the natural streamflow within the Souris Basin are snowmelt and rainfall. Unlike the river basins to the west, the Souris Basin receives no hydrological input from snowmelt or glacial meltwater from the Rocky Mountains. Groundwater does not play a major role in the flow of the Souris or its tributaries (International Souris River Board 2009). When precipitation, either snowmelt or rain, reaches the ground surface, it may seep into sand, soak into dry loam, puddle on the wet ground, or run off of ice-covered surfaces. Surface runoff gathers in low spots, and begins to flow across fields and down ditches into creeks, eventually reaching the Souris River. The exceptions are non-contributing areas, such as sloughs and the land sloping into them, that do not drain into streams. Approximately two thirds of the Souris basin is considered to be non-contributing, however, during times of extremely wet conditions, non-contributing areas can fill and then contribute flow. As the Souris River is quite flat, 0.3 m/km, increased flows and floods can take many days before moving the entire length of the river (International Souris River Board 2009).

2.3 Tree growth and streamflow:

Reconstructions of past streamflow events is of great interest to water resources engineers, policy makers, government agencies and the like, since water resources planning and design require the best possible estimates of extreme flow conditions (Bonin and Burn 2005). The most common problem faced by water managers is the lack of extensive instrumental data, which usually are no longer than 50 to 100 years. Paleoclimatic data have played a major role in convincing hydrologists and decision makers that the narrow window of climatic variation given in the instrumental records does not accurately capture all modes of variability important in planning for adaptation

to climate/environmental fluctuations (Meko and Woodhouse 2011). A distinguishing feature/contribution of dendroclimatic research is the lengthening/extension of instrumental hydrologic records, (such as precipitation and streamflow), on which major water planning decisions are made, as the use of tree-ring chronologies has proven very valuable in the analysis of long-term hydroclimatic phenomena (Stockton and Meko 1975; Fritts 1976; Michaelsen *et al* 1987; Briffa *et al.* 1990; Loaiciga *et al.* 1992).

Dendrohydrology, a subfield of dendrochronology, is concerned with the past, long-term, hydrologic phenomena based on tree-ring reconstructions (Schweingruber 1996). Dendrohydrology requires a thorough understanding of the interaction between tree stands and watershed hydrologic conditions such as the balance of precipitation, runoff, groundwater, evapotranspiration, and other hydrologic fluxes, and the ecological conditions and their effect on the biologic responses of trees (Loaiciga *et al.* 1993). The response of trees is 'recorded' primarily in the widths of annual tree rings, (although other measurable indicators of biologic responses, such as early- and latewood widths, and latewood density, are also useful in dendrohydrologic analysis), and reflects the environmental conditions experienced during each year of growth (Fritts 1976; Cleaveland *et al.* 1993; Bonin and Burn 2005; Fonti and García-González 2008; Campbell *et al.* 2007, 2011.).

The hydrologic regime of a stream represents the integrated basin response to climatic inputs, primarily precipitation and runoff (Meko and Graybill 1995; Zhang 2001; Rood *et al.* 2005). Much in the same, it is well documented that tree growth is particularly sensitive to moisture availability, a growth limiting factor that can be accurately discerned from properly selected tree-ring data (Loaiciga *et al.* 1993).

Although tree-ring data are point samples they correlate over distances of 100s of kilometers reflecting a regional (basin) hydroclimatic signal (Loaiciga *et al.* 1993). Dendrochronology can therefore be linked to streamflow through the common responses of tree-growth and streamflow to variations in net precipitation and runoff (Stockton and Jacoby 1976). The statistical relationship between time series of tree-ring indices and streamflow has been exploited for multi-century reconstructions of flow for river basins in many parts of the world (Akkemik *et al.* 2004; Gou *et al.* 2007; D'Arrigo *et al.* 2009; Liu *et al.* 2010; Meko *et al.* 2010). In North America, dendrohydrological studies began in the 1930s, exploring the relationships between tree growth and streamflow, and the possible uses of tree-ring records for extending gauge records (Hardman and Reil 1936; Hawley 1937; Keen 1937). "Hardman and Reil's (1936) work concerning the flow of the Truckee River, California - Nevada, was the first to examine these relationships in view of possible applications to water resource management, particularly in the agricultural regions of the Truckee River basin" (Meko and Woodhouse 2011, p 233). Since then, dendrohydrological studies expanded throughout much of the United States and along the Pacific Coast. In 1970, Stockton's work was the first to take advantage of the implementation of new quantitative methods made possible by the development of high-speed computers, including multivariate statistical analysis (Fritts *et al.* 1971) and standardization protocols (Stokes and Smiley 1968; Fritts 1976) for the reconstruction of climate and tree growth/runoff analysis, demonstrating the great value of extending records of streamflow for water resource planning and management in a long term context (Meko and Woodhouse 2011). A further review of the methodology and

applications of streamflow reconstructions from tree rings is provided by Loaiciga *et al.* (1993) and Meko and Woodhouse (2011).

2.4 Previous studies:

2.4.1 Suitability of Oak:

The earliest study of the dendroclimatic potential of *Q. macrocarpa* was carried out in North Dakota during the 1940s when Will concluded that "the alternate periods of rainfall or drought as reflected in the tree rings of the master oak are reasonably valid for a very considerable area" (1946, p.19). Since then, investigations of bur oak and its response to climate variability, have proven useful, due to its clear annual character, long life, and easily distinguishable outer wood, which aids in the accuracy of dating.

As stated previously, bur oak is a ring porous species consisting of very distinguishable vessel elements defining earlywood and latewood growth. Earlywood growth in oak consists of large vessels formed during the season of shoot growth, usually during March to May (Baillie 1982) before the establishment of any great photosynthetic leaf area, and therefore relies on food stores laid down in the previous year (Varley and Gradwell 1962). After initial photosynthesis and expansion of leaf area, hormonal activity dictates changes in the quality of the xylem and the latewood becomes increasingly fibrous and vessel sizes decrease substantially (Baillie 1982). In general, the large earlywood vessels are comparatively uniform in size and occur in bands usually one or two vessels wide, exhibiting very little variation from year to year, in comparison with variations of latewood width. The fact that earlywood is present every year, while latewood can be completely absent, indicates that the former is a much more certain process, and suggests that latewood is therefore dependent on the amount of

photosynthetic food supply for the tree, which in turn is dependent on factors such as foliage canopy, temperature, moisture availability, and sunlight (Baillie 1982). Because of this, we can infer that the stored information (*i.e.* climate variability) available through the use of tree-rings of oak, is contained almost entirely in the width of the latewood.

Woodcock (1989) found similar results when investigating the anatomical features in bur oak, stating that ring width is closely related to the physical characteristics of the latewood and exhibits generally nonsignificant relationships with earlywood variables. Analyses revealed that the amount of earlywood produced annually appeared to be largely independent of climatic conditions, as was shown by dry years of narrow rings composed completely of earlywood vessels (Phipps 1967; Woodcock 1989).

Since Will's initial dendrochronological investigation in 1946, *Quercus* species on the US and Canadian Great Plains have been successfully used to reconstruct drought histories in the Corn Belt and southeastern region (Will 1946; Lawson *et al.* 1980; Woodcock 1989, Sieg *et al.* 1996). In addition, dendroclimatic investigations of *Q. macrocarpa* in Nebraska and the Dakotas have indicated the longevity and moisture sensitivity of this species and its potential for drought reconstruction (Lawson *et al.* 1980; Woodcock 1989; Sieg *et al.* 1996). Although most trees used for dendrochronological analysis have false (two rings per year) or missing rings, these types of anomalies are "unknown in oak" (Baillie 1982, 53), thus cross-dating practices are very reliable in producing accurate chronologies. Lowson (1966) suggested that age estimates in oak, based on ring-counts, are subject to only a small amount of uncertainty, and it is extremely rare to find an oak which has missed a year's growth or which shows two distinct rings in a single year. Dating accuracy again can be related to the porosity of

oak's wood, and the distinct visibility of the production of earlywood from year to year. Baillie (1982) claims that the production of earlywood is governed by a photoperiodic/temperature change to trigger cambial activity, which will take place each year with 100% certainty, therefore the formation of earlywood is as equally certain.

In Nebraska Lawson *et al.* (1980) found a high correlation between standardized chronologies and regional climate, suggesting the feasibility of regional climatic reconstructions based on bur oak cores. Sieg *et al.* (1996) also found that the dendroclimatic potential of bur oak was excellent, and that the wide spatial distribution of bur oak and the high correlation of chronologies with precipitation were promising for climatological and ecological studies for sub-regional scales within the northern Great Plains. In 1999, Cook *et al.* used oak as part of a vast network of chronologies in the eastern United States to reconstruct broad-scale spatial patterns of drought across the coterminous U.S.

Oaks located within a warm and xeric climate quite often experience more physiological stress and put forth a more varied climatic response (White *et al.* 2011). As such, oaks within the Prairie region that often experience marked climatic variability throughout the growing season, should therefore reflect these fluctuations within their growth rings. Many studies have acknowledged the potential of the oak's sub-annual growth parameters' (*i.e.* earlywood and latewood) sensitivity to variable moisture conditions, and have been successful in investigations of and reconstructing climatic variability and streamflow, and some century- to millennia-long tree-ring chronologies are already available (St. George *et al.* 1999; Case 2000; St. George and Nielsen 2000;

St. George *et al.* 2002; García-González and Eckstein 2003; García-González and Fonti 2008).

2.4.2 Multi-proxy approaches:

Tree rings embody information about past climate, as the physical and chemical properties of wood reflect environmental influences (Campbell *et al.* 2007; García-González and Fonti 2006). The feature of xylem anatomy used most frequently as a proxy of past climate conditions, and for the construction of continuous time series, is annual ring width (García-González and Fonti 2006; Campelo *et al.* 2010). This variable, which can be determined easily and largely nondestructively, incorporates growth responses to environmental conditions during the whole growing season, and therefore tends to be inappropriate for reconstructing climatic conditions at temporal resolutions shorter than on annual scales. For higher temporal resolution, analysis of the wood at the cellular level is more suitable. Intra-annual tree-ring features comprise sequences of cells formed at different points in the growing season whose metrics (*i.e.* size, shape or wall thickness) respond to external conditions occurring during cell formation (Fonti and García-González 2008). Since the factors that influence cell development are not necessarily the same as the factors determining radial growth (*i.e.* the total amount and types of cells produced during the growing seasons), it is expected that additional information can be gained from anatomical tree-ring features, for other parts of the year, or for other climatic factors where annual ring width is not an appropriate proxy (Campbell *et al.* 2007; Domec and Gartner 2002; Fonti and García-González 2008).

There are two distinct zones of growth within a tree-ring - earlywood and latewood. Early- and latewood describe wood of differing densities typically formed

early and late in the growing season of a tree (Meko and Baisan 2001). Earlywood is the first-formed portion of the growth ring, characterised by large cells with thin walls, and lower density wood, and can account for 40-80% of a ring's annual growth increment (Domec and Gartner 2002; Meko and Baisan 2001). Latewood is the later-formed portion, characterised by smaller cells with thick walls, and higher density wood (Hoadley 1990). In some conifer tree species, the transition between earlywood and latewood is readily recognizable as a sharp change from lighter to darker wood (Kozlowski and Pallardy 1997). In ring porous angiosperms, such as the *Quercus* species, a distinct decrease in vessel size occurs at the transition from early- to latewood. The size and density differences are imparted by differences in rates and durations of cell processes. Patterns within the annual/intra-annual layers of tree-rings suggest that climate influences the size and density of cells within the ring, either by acting as a limiting factor for growth or through fine tuning of the wood structure to environmental (water) conditions (Woodcock 1989), therefore changes in early-/latewood growth patterns reflect, in part, the control of wood properties by water availability (Domec and Gartner 2002).

Intra-ring variation is mainly due to differences between cell structure and formation between earlywood and latewood (Koubaa *et* al 2002). The identification of such anatomical structures in wood is based on cell characteristics, such as maximum density, cell wall thickness, vessel diameter, vessel area, etc., which are affected by environmental factors during the process of wood formation (Eckstein 2004; Fonti *et al.* 2009b). When one or more of these parameters covaries consistently with a single environmental factor, it may be used as a proxy for that factor (Kirdyanov *et al.* 2007).

Although the potential for parameters of wood anatomy as proxies of past climate has been long recognized, extracting relative intra-annual information from tree rings has been hindered historically by analytical procedures that were too time-consuming and costly for many tree-ring laboratories (Campbell *et al.* 2007). Within the last few decades, recent advances in computer technology and microscopic and digital imaging analysis have made measurements of potential intra-annual proxies across sequences of tree rings much easier (García-González and Fonti 2006).

The utility of intra-ring features as potential proxies for dendroecological studies depends on their capacity to provide distinct signals or to increase the signal strength of traditional tree-ring variables (Campelo *et al.* 2010). Several investigations proved that intra-annual ring width parameters contain ecological information, although their signals vary among species, climatic regions, site conditions and anatomical features (Fonti *et al.* 2007). In North America, Woodcock (1987, 1989) was the first to assess the relationship between climate variables and vessel features in tree rings of bur oak, *Quercus macrocarpa* Michx., where it was concluded that latewood vessel diameter could be successfully used to reconstruct past precipitation. García-González and Eckstein (2003) found that mean vessel area in the earlywood of the ring porous *Quercus robur* L. was strongly correlated to early spring precipitation. Fonti and García-González (2004) reported that mean vessel lumen area in the European sweet chestnut, *Castanea sativa* Mill., could also be used as a climate proxy (Tardif and Conciatori 2006). In other investigations using the *Quercus* species, earlywood vessel size registered temperature in a dry inner-Alpine valley (Eilmann *et al.* 2006), and periods of flooding along riverbanks (Astrade and Begin 1997; St. George and Nielsen 2000).

Many studies have investigated the climatic signal of vessel time series as alternate proxies of past climate. As monthly temperature and precipitation during growing and dormancy periods vary considerably from year to year, it is better to study the relationships between climate and the constituents of the annual tree-ring, earlywood and latewood separately (Miina 2000). Previous work in northern Europe summarized by Miina (2000) demonstrated that pine earlywood is independent of growing season temperature, however the amount of pine latewood, as well as spruce earlywood and latewood are very much dependent on temperature fluctuations during the growing season. In northern Norway, Bergan (1987) found latewood width of spruce to correlate positively with variations in temperature of the late growing season. Density analysis revealed wide variations in year to year maximum latewood density of spruce and pine in Scandinavia related to annual fluctuations in summer temperatures (Briffa *et al.* 1988; Schweingruber *et al.* 1988; Briffa *et al.* 1990). Positive relationships between latewood width and growing season precipitation have been reported in correlation studies for various tree species growing in widely differing climate regimes (Meko and Baisan 2001). As well, numerous studies have shown that in general, higher wood density, as a consequence of a greater proportion of latewood, is triggered by drought stress (Domec and Gartner 2002; Zobel and Van Buijtenen 1989). In growing seasons with lower precipitation than normal or excessively low temperatures, tree growth is diminished and the proportion of latewood is higher (Domec and Gartner 2002). Conversely, when growing conditions are ideal, tree growth is enhanced and the proportion of latewood reduced (Kennedy 1961). It is clear from the literature that parameters of intra-annual ring widths, such as early- and latewood growth hold potential for studying hydrologic

variability on annual and sub-annual time scales, however, the application of such data to palaeoclimatology has been limited by relatively few chronologies that have been developed and analyzed (Meko and Baisan 2001).

3. DATA SETS

3.1 Site selection:

In conventional dendroclimatological studies, where ring-width variations are the source of climatic information, trees are sampled where growth is limited by an environmental factor (*i.e.* temperature, moisture); commonly, this involves selection of trees which are growing close to their extreme ecological range (Bradley 1985). In Canada, the extreme northwestern edge of the ecological distribution of *Q. macrocarpa* is located within southeastern Saskatchewan and southwestern Manitoba (Figure 3.1). According to the principle of ecological amplitude, samples obtained within this region will be most favourable for dendrochronology, as specimens potentially possess the strongest and most sensitive growth responses to varying climatic signals.

Figure 3.1 Native range of *Quercus macrocarpa*. Source: Burns and Honkala 1990.

For this study, I wanted to create a robust network of tree-ring chronologies within and around the Souris River Basin to investigate climatic signals affecting streamflow within the basin; and also to ultimately fill the dendrochronological 'gap' in much of the central Prairies (Figure 3.2), that previous studies (Watson and Luckman 2004, 2005; Girardin *et al.* 2006a; St. George *et al.* 2009) have failed to include, as their investigations and study areas were limited to the proximities of the Prairie region.

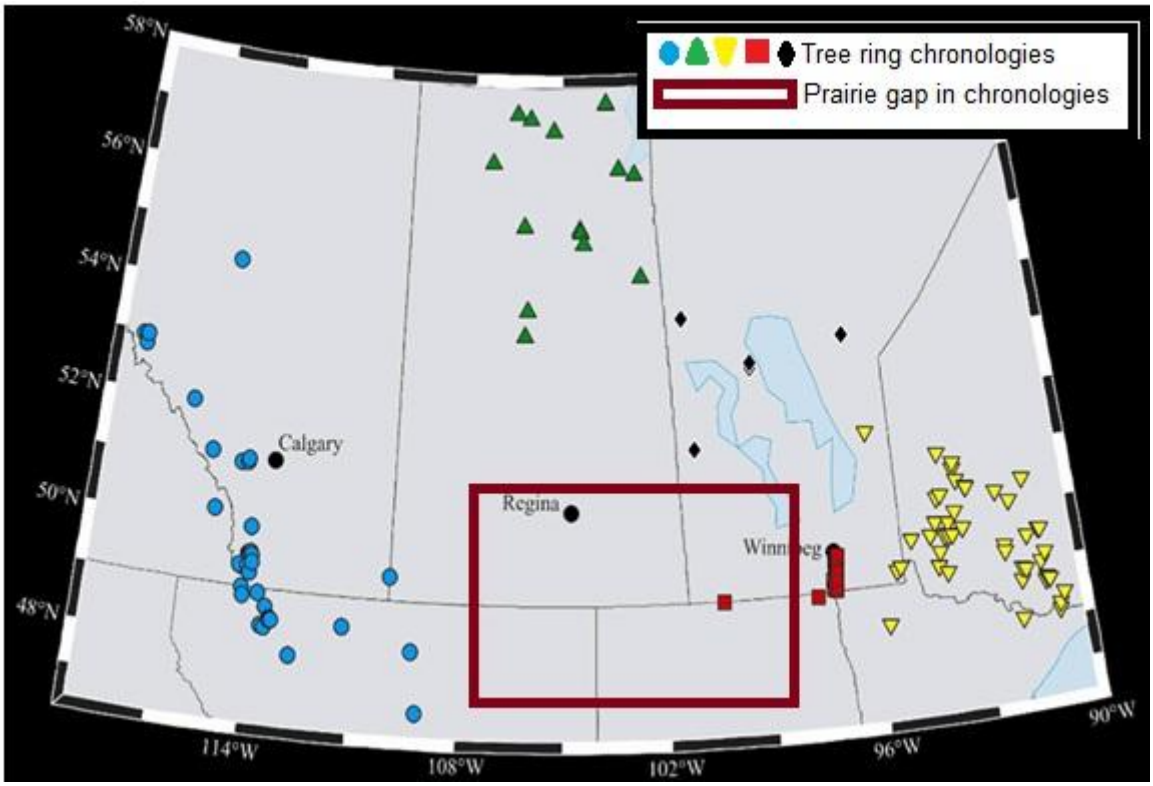

Figure 3.2 Prairie tree-ring network. Source: St. George *et al.* 2009.

In dry climates, precipitation is the dominant environmental growth-limiting factor for annual ring-width variation, therefore *Q. macrocarpa* sampling sites were chosen based primarily on areas/slopes where precipitation has a maximum influence on tree-ring growth. At all sites, samples were collected from trees growing on south facing slopes where moisture is most limiting (Fritts 1976), in stands comprised of dead and living trees, and evidence of limited disturbance. As one of the objectives of this

research was to extend the streamflow records as far into the past as possible, in addition to the physical characteristics of the sites themselves, sites that hosted old growth trees were of primary consideration.

In total, 14 (a combination of two previously collected, Devon Farm and Hillside (Vanstone 2007), and 12 new) moisture sensitive tree-ring chronologies were produced (Table 3.1). Full site names and characteristics of each sampling location are given in Table 3.1, however, for the remainder of the work, site codes will be referred to, when discussing the chronologies. Five sites were collected from southeastern Saskatchewan, four from southwestern Manitoba, and five from northern North Dakota (Figure 3.3).

Table 3.1 Sample site information.

Site name	Code	Province/State	Latitude	Longitude	Elevation (m.a.s.l.)
Devon Farm	DEV	Saskatchewan	50° 28' 12"	101° 49' 12"	440
Fafards	FAF	Saskatchewan	50° 31' 12"	101° 37' 12"	503
Hillside	HIL	Saskatchewan	50° 31' 48"	101° 57' 36"	450
Junction	JCT	Saskatchewan	50° 31' 48"	101° 52' 48"	528
Wildlife Lands	WLL	Saskatchewan	50° 30' 0"	101° 43' 12"	522
Bessant	BES	Manitoba	49° 31' 16"	99° 49' 1"	421
Newcomb's Hollow	NCH	Manitoba	49° 8' 2"	100° 24' 0"	544
Shady Lane Farms	SLF	Manitoba	50° 7' 55"	101° 0' 40"	449
Van der Velde	VDV	Manitoba	49° 55' 59"	100° 20' 9"	408
Camp Grafton	CGT	North Dakota	48° 3' 32"	98° 55' 8"	454
Cross Ranch	CRR	North Dakota	47° 11' 2"	100° 59' 38"	514
Graham's Island	GRI	North Dakota	48° 2' 53"	99° 3' 25"	447
Kildeer	KIL	North Dakota	47° 33' 36"	102° 45' 32"	740
Lake Metigoshe	LMG	North Dakota	48° 59' 28"	100° 20' 20"	658

Locating sites of potentially the longest-lived, moisture sensitive, bur oak trees within and in close proximity to the Souris Basin area, was accomplished via correspondence with park managers, private landowners, and environmental consultants, and by consulting digital vegetation maps, and visual species recognition while driving

the many valley and back roads through Saskatchewan, Manitoba and North Dakota. As this area is an agricultural region, bur oak stands are confined to valleys and uplands, where the distribution of the trees is limited to sites where the land has not (cannot) been cultivated.

Of the sites located in Saskatchewan, three, (DEV, JCT and WLL), are sectors of government land owned by the Bear Creek Wildlife Lands, while FAF and HIL are located on private land, within the Qu'Appelle Valley. Cores and discs of deadwood were collected from all sites, from both living and dead trees (respectively), that had either died naturally or were recently felled by the land owners. All locations were dominated by *Q. macrocarpa*, with trembling aspen and balsam poplar scattered throughout, with a relatively dense shrub-brush understory below.

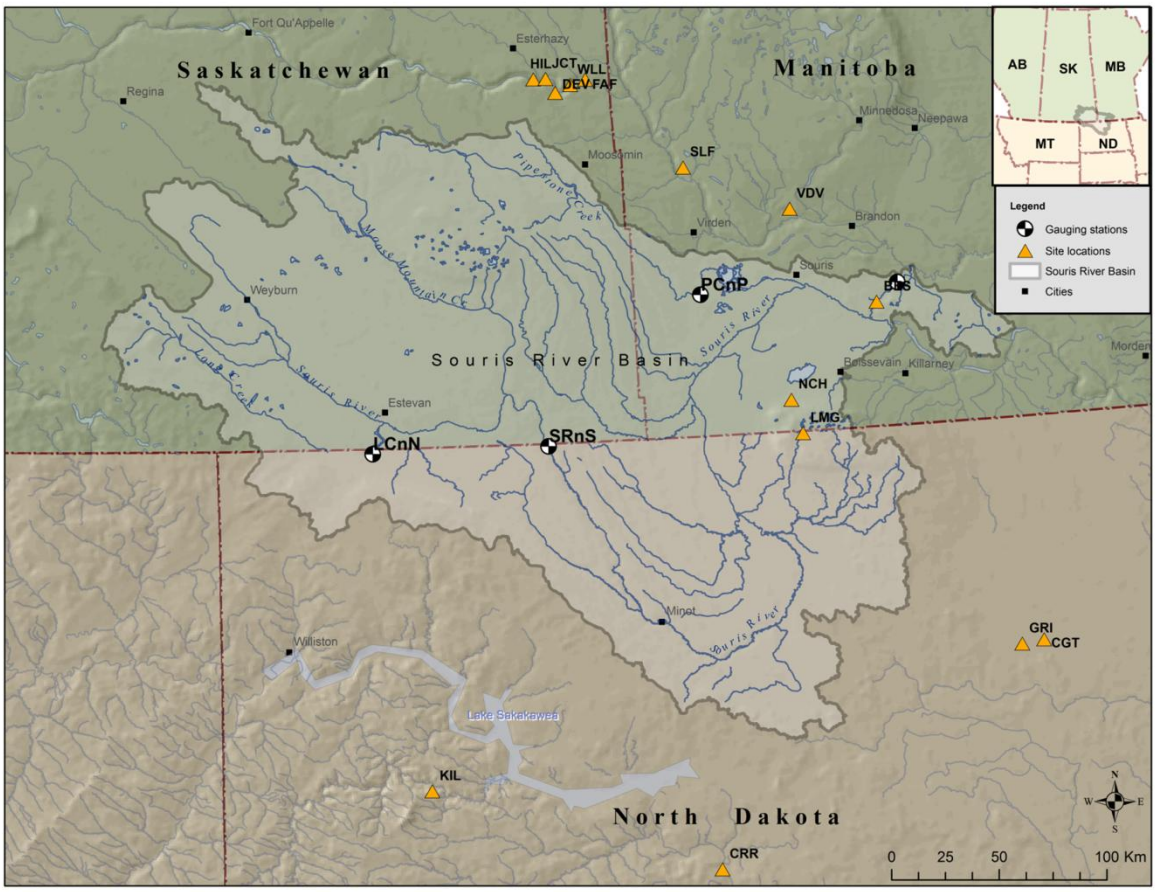

Figure 3.3 Sampling site locations in the Souris River Basin.

Three of the four sites in Manitoba were privately owned, and chosen for sampling based on previous land surveys by the Manitoba Agro Woodlot Program (BES, 2002; NCH, 2005; VDV, 2007). The fourth and most northern site in Manitoba, SLF, was recommended by Mr. Marc Rivard, with the Upper Assiniboine River Conservation District. As before, all locations were selected based on the criteria set forth above, to exploit the concepts of limiting factors and site specificity. At all locations, bur oak was the dominant species, and occasionally grew in association with green ash, Manitoba maple and white birch, where soil moisture content was higher. The understory supported several shrub and native mixed grass species. The terrain where sampling sites are located, is characterized by considerable slopes and valleys, with wetlands occupying the lower areas and grasslands on the upper ridges.

Oak sampling locations in North Dakota were chosen based on correspondence with Dr. Joe Zeleznik, Forester with North Dakota State University in the Plant Sciences Department, who provided prime locations of old-growth oak stands. At all sites, bur oak were less common on the floodplains and at lower riparian area elevations, but were well represented on some of the oldest terraces and were common in many ravines and valley hills. Typically each of the five sites were dominated by bur oak stands and mixed grass prairie, however there were a few other species interspersed amongst the oak. The most northern site, LMG, was predominantly oak, and transitioned to an aspen-oak woodland with a dense underbrush. Moving southeast to GRI, bur oak was again the dominant species at higher elevations, and was scattered with green ash, American elm and boxelder closer to the base of the site location. The vegetation of Camp Grafton, (CGT), located at the ARNG Major Training Centre of the North Dakota Army National Guard

in Devils Lake, is composed of almost solely a bur oak community, with a minimal dispersal of young elms, and relatively very little underbrush. Cross Ranch (CRR) was dominated by oak at higher elevations, along the hills surrounding the floodplain area, but oak was less common at lower elevations, where it was mixed with a cottonwood-willow community. Lastly, KIL was located along the boundary of the badlands in southwestern North Dakota. This area was comprised of a mix of species, predominantly oak at the highest elevations, and an increasing mix of elm, birch, aspen and a very thick underbrush as elevation decreased.

3.2 Chronology development:

3.2.1 Sample collection and preparation:

Q. macrocarpa samples were collected in two forms: cores and cross-sectional discs. Core samples were obtained using a Swedish increment borer, which removes a thin cylindrical section of wood from the stem of the tree. As trees grow by adding wood radially about the pith, preferred cores ideally pass directly through the centre of the tree, capturing the pith within the core. Where ring patterns are likely to be distorted, most commonly near branches and on the up- or downhill sides of leaning trunks were avoided. All cores were taken well below the first set of branches and on the sides of the main stem facing across the hill. This is done to avoid compression wood, which grows thicker in the impacted area of the tree to compensate for leaning and ultimately results in non-circum uniformity, which can confound cross-dating errors (Schweingruber 1992). Trees were chosen in a non-random fashion explicitly sampling chose individuals believed to be the oldest, with minimal disturbance and or visible physical damage. Two

cores were sampled from each tree at least 90° radially apart from one another, leaving the tree unharmed. Dead trees were sampled with a chainsaw collecting either a full disc, if the tree had already fallen or had been felled, or a wedge, if the dead tree was still standing. To develop reliable chronologies 20-30 trees are sampled within a site; however if the trees are highly sensitive to a growth limiting factor then a reliable chronology may be constructed using as few as 5-7 trees (Schweingruber *et al.* 1990).

Once collected, cores were stored in labeled plastic straws for protection until transported to the lab for processing. Standard procedures, described by Stokes and Smiley (1968) and Fritts (1976), were followed in preparing cores and cross-sections for analyses. Cores were dried and glued on to wooden mounts and oriented such that cells are vertically aligned. Orienting the cores correctly is of utmost importance because when the cells are horizontally aligned, the ring boundaries are nearly impossible to detect even after vigorous amounts of sanding and intense magnification (Stokes and Smiley 1968).

3.2.2 Processing and chronology development:

After proper drying time had been allotted for the mounted cores, each sample, cores and discs, was then surfaced using a succession of progressively finer sandpaper, ranging from 120-400 grit. In order to provide clearest distinction of annual and sub-annual rings, the samples were subjected to a final manual sanding using 600 and 1200 grit sandpaper, to create a highly polished surface. Following surfacing, samples were scanned using an Epson® Expression 10000 flatbed scanner, at resolutions between 800 and 1200 dpi. Higher resolution images were used for distinguishing narrow rings in periods of suppressed growth if the coarser resolution was deemed inefficient for this

purpose. Dating, measuring, and visual crossdating of annual rings were carried out using the program WinDendro™ Density (version 2009b). Early- and latewood width measurements were aided by the distinct size differentiation of early- and latewood vessels in bur oak samples. Early- and latewood measurements were based on a defined boundary of 40% of the minimum to maximum relative pixel density in the reflectance values, where the onset of latewood growth has more dense and compacted vessels being darker in nature. Some early- latewood boundaries were adjusted manually to correct for errors in the automatic detection process. COFECHA, a quality-control computer program, (Holmes 1983), was used to verify crossdating and provide statistics that describe the strength of intercorrelation between tree-ring samples at each site. COFECHA uses segmented time series correlation techniques to assess the quality of crossdating and measurement accuracy, by providing a statistical match between segments of each core and the master chronology that is made of the measurements that are entered into the program (Grissino-Mayer 2001; Speer 2010). COFECHA analyzes the dated measurements and detects and flags 'outlier' rings, rings that may be locally absent or false and would therefore contribute to poor dating of a tree-ring chronology (Grissino-Mayer 2001).

3.2.3 Creating index chronologies:

The information contained in annual tree rings is a valuable resource for studying environmental change, however, the extraction of the desired signal from the unwanted noise can be difficult and uncertain. It is from this basis that the problem of signal extraction in tree-ring research is related to the disaggregation of the observed ring

widths into a number of signals that represent the sum of the environmental influences on tree growth (Cook and Briffa 1990; Cook 1990) given by the following equation:

$$R_t = A_t + C_t + \delta D1_t + \delta D2_t + E_t \quad (3.1)$$

where:

R_t = the observed ring-width series;
A_t = the age-size related trend in ring width;
C_t = the climatically related environmental signal;
$D1_t$ = the disturbance pulse caused by a local endogenous disturbance;
$D2_t$ = the disturbance pulse caused by a standwide exogenous disturbance; and
E_t = the largely unexplained year-to-year variability not related to the other signals.

The common climatic component, C_t, is the signal of interest, since A_t, $D1_t$, and $D2_t$ can be described collectively as the estimated growth trend, (a function of the pure age trend A_t, and the stochastic impingers of pure age trend, $\delta D1_t$ and $\delta D2_t$) - non-climatic variance or noise. The process of selective removal of unwanted variance in raw measurement series, prior to averaging to form mean chronologies, is known as 'standardization' (Briffa 1999).

ARSTAN, a computer software program developed by Cook (1985), was used to standardize the tree-ring widths (annual, early- and latewood) into a new series of stationary, relative tree-ring indices that have a defined mean of 1.0 and a relatively constant variance (Cook *et al.* 1990). Conservative detrending methods, using a combination of deterministic (negative exponential curve) and stochastic approaches (67% cubic smoothing spline - used when the negative exponential curve resulted in a negative slope), were applied to the tree-ring series to remove juvenile biological growth trends, and non-climatic variation associated with aging of the tree and ecological events such as suppression and release within the stand (Vanstone and Sauchyn 2010). Standard

(detrended index chronology), residual ('prewhitened' - autocorrelation is removed using autoregressive modeling), and arstan ('common' autocorrelation component modeled back into the residual series) (Fritts 1976; Cook 1985) chronologies were produced for each ringwidth series at each site. Because residual chronologies have no significant serial autocorrelation, as a result of pre-whitening performed in ARSTAN, they will be used for the entirety of the analyses, as they present the best predictors for accurately modelling streamflow, (also determined to have no significant serial autocorrelation, described later) within the Souris River Basin.

3.2.4 Site statistics:

Table 3.2 lists site statistics for all three residual proxy (annual, early-, and latewood) chronologies at each of the 14 sampling locations. Chronologies cover the period from 1725 to 2008, a period of 284 years. With the exception of the earlywood chronologies from JCT and LMG, all chronologies exceed the critical ($p < 0.05$) series intercorrelation of 0.321. Based on series intercorrelations it would appear that earlywood width chronologies may not be as responsive, or as consistent among trees at individual sites, as annual or latewood chronologies to climatic fluctuations influencing tree-ring growth. In almost all cases, annual and latewood chronologies' intercorrelations are well above 0.5, indicating a strong common stand-level signal recorded for each site. Similarly, all but four chronologies (EW at SLF, VDV, GRI, and LMG) exhibit a mean sensitivity exceeding 0.200, indicating that the measured year-to-year variability is acceptable/sensitive enough for climate reconstructions (Speer 2010). Site chronologies with higher sensitivity and intercorrelations have a greater likelihood of containing environmental information because common ring-width variability suggests that growth

is responding to external factors, likely, inter-annual variability in hydroclimate. While earlywood indices may not be as useful, chronology statistics and correlations among the three chronology parameters (RW, EW, and LW; Figures 3.4 – 3.6) suggest that latewood widths are more closely related to annual ringwidth indices in their sensitivity and ability to record their frequency and magnitude of climatic fluctuations affecting tree-ring growth (Vanstone and Sauchyn 2010).

Table 3.2 Chronology statistics. RW: annual; EW: earlywood; LW: latewood chronologies.

Code	Province State	Years	# Radii	# Trees	Type	Series Intercorrelation	Mean Sensitivity	Year EPS ≥ 0.85
DEV	SK	1854-2005	26	14	RW	0.582	0.291	1930
					EW	0.338	0.239	---
					LW	0.555	0.515	1930
FAF	SK	1886-2006	33	19	RW	0.573	0.220	1886
					EW	0.344	0.219	1940
					LW	0.565	0.407	1886
HIL	SK	1907-2004	14	7	RW	0.603	0.306	1907
					EW	0.369	0.222	1960
					LW	0.595	0.517	1907
JCT	SK	1813-2007	14	9	RW	0.539	0.239	1930
					EW	0.254	0.231	---
					LW	0.342	0.548	---
WLL	SK	1831-2006	50	27	RW	0.674	0.251	1831
					EW	0.442	0.219	1920
					LW	0.625	0.544	1831
BES	MB	1873-2008	30	16	RW	0.651	0.229	1873
					EW	0.362	0.207	1930
					LW	0.641	0.447	1873
NCH	MB	1808-2008	34	17	RW	0.619	0.240	1808
					EW	0.334	0.208	1920
					LW	0.609	0.468	1808
SLF	MB	1887-2007	20	10	RW	0.684	0.246	1887
					EW	0.356	0.195	---
					LW	0.683	0.465	1887
VDV	MB	1891-2008	30	15	RW	0.644	0.232	1891
					EW	0.350	0.183	---
					LW	0.678	0.455	1891
CGT	ND	1725-2008	25	13	RW	0.737	0.287	1725
					EW	0.379	0.230	1860
					LW	0.734	0.575	1725
CRR	ND	1769-2008	22	11	RW	0.659	0.245	1769
					EW	0.395	0.214	1940
					LW	0.625	0.473	1840
GRI	ND	1841-2008	20	10	RW	0.767	0.265	1841
					EW	0.434	0.196	1940
					LW	0.746	0.506	1841
KIL	ND	1899-2008	32	16	RW	0.694	0.267	1899
					EW	0.345	0.213	1899
					LW	0.697	0.508	1899
LMG	ND	1748-2008	8	4	RW	0.612	0.201	1748
					EW	0.261	0.190	---
					LW	0.611	0.411	1920

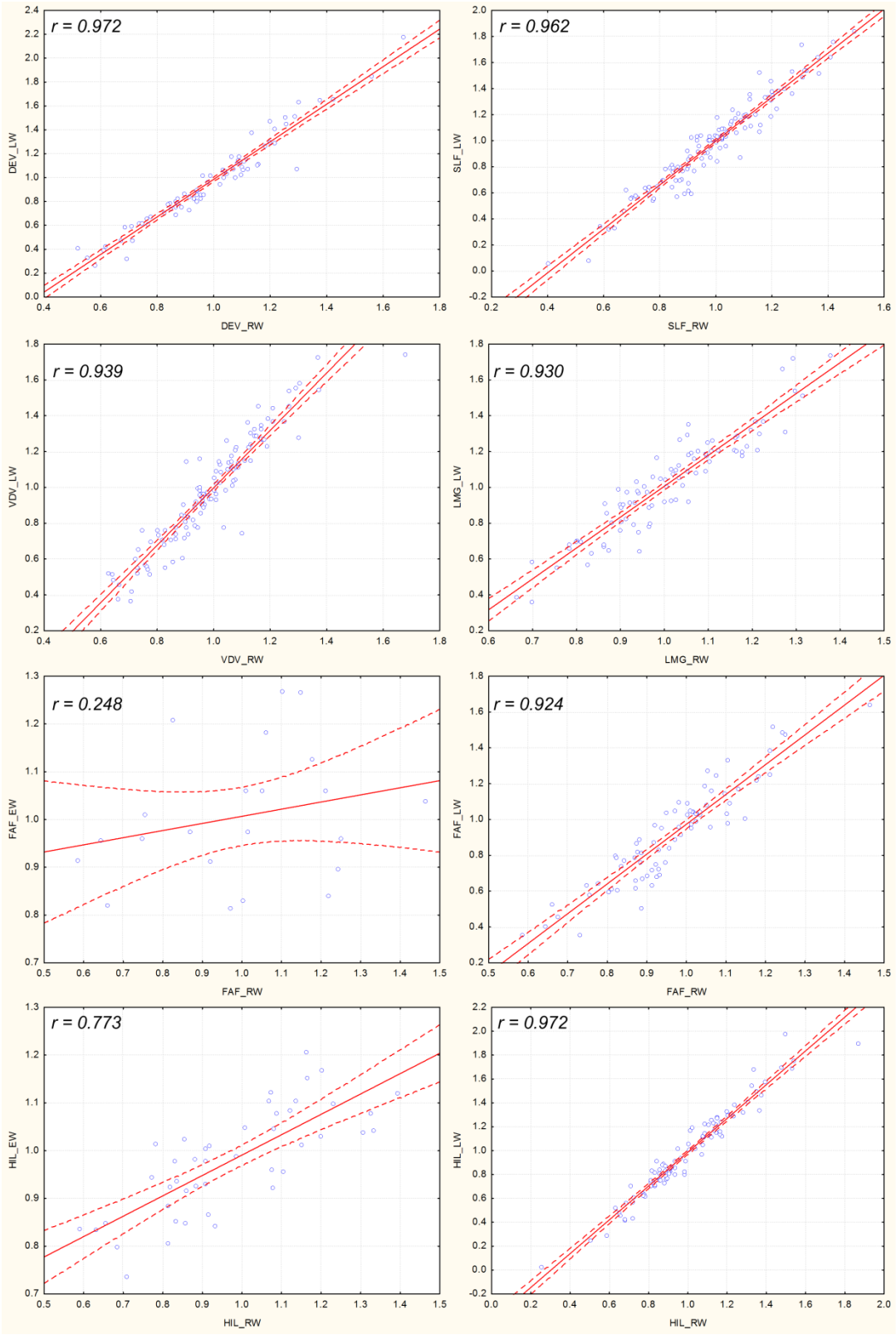

Figure 3.4 Correlations between annual ringwidth (RW), earlywood (EW) and (LW) chronologies. Correlations are significant at the $p<0.001$ level.

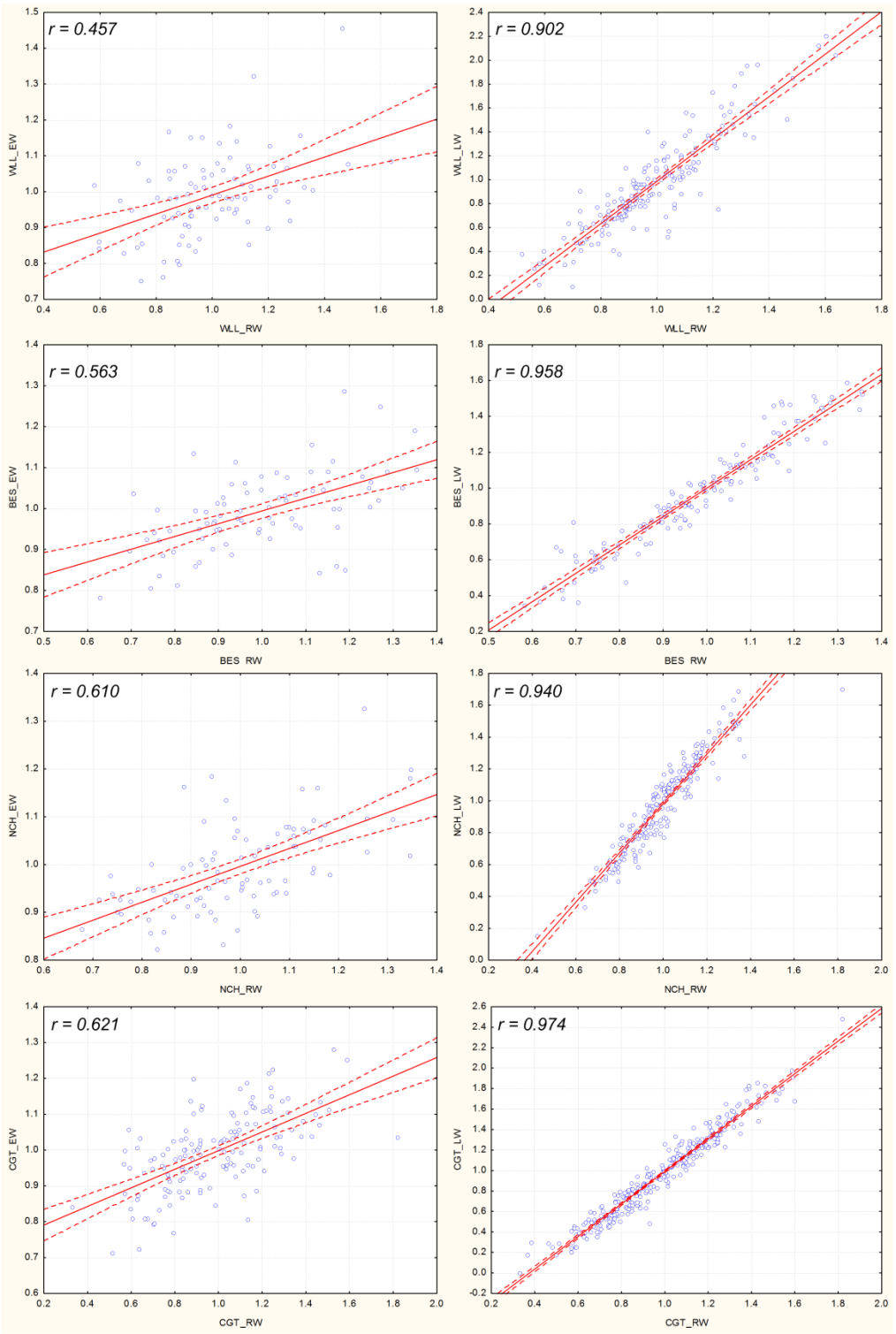

Figure 3.5 Correlations between annual ringwidth (RW), earlywood (EW) and (LW) chronologies. Correlations are significant at the $p<0.001$ level.

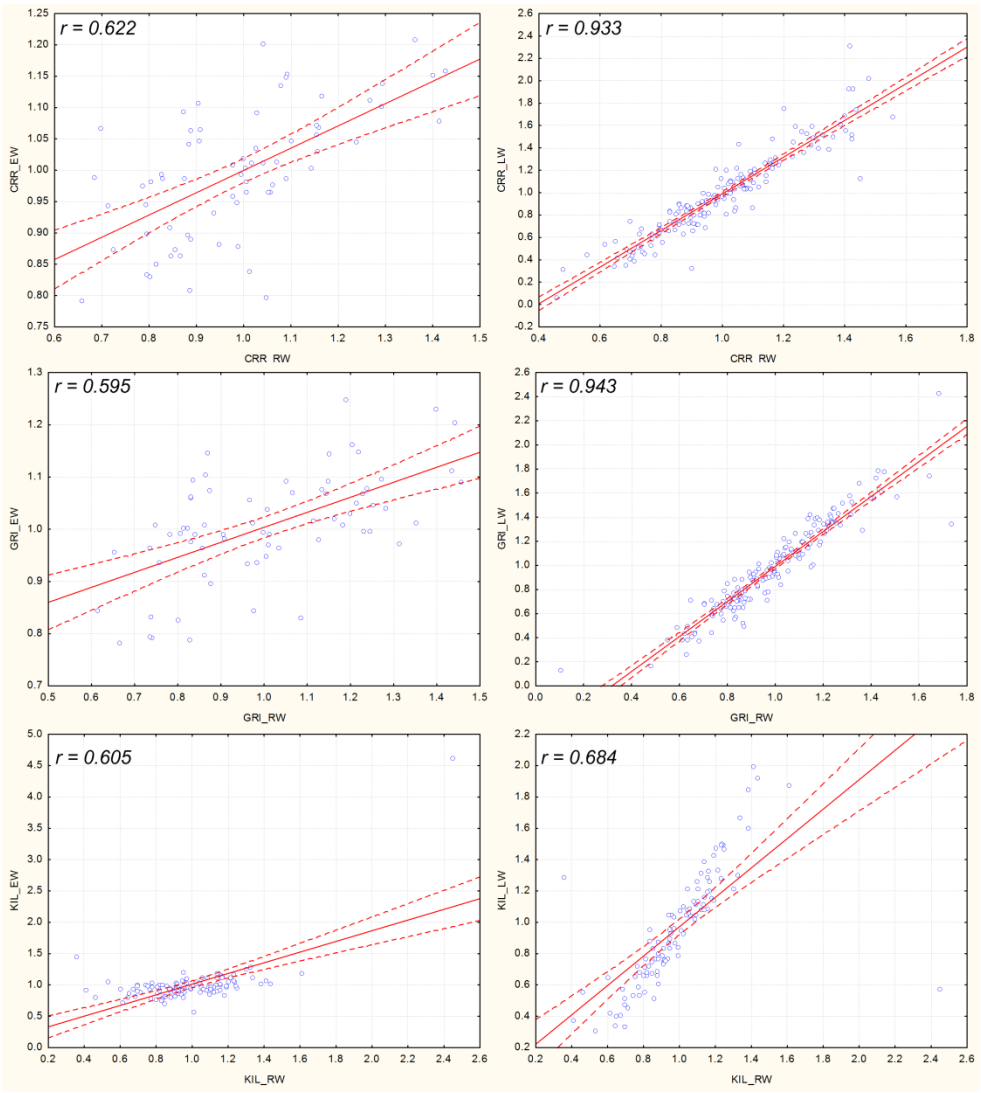

Figure 3.6 Correlations between annual ringwidth (RW), earlywood (EW) and (LW) chronologies. Correlations are significant at the $p<0.001$ level.

The expressed population signal (EPS; Briffa 1984; Wigley *et al.* 1984) was determined to assess the statistical quality and signal strength contained within a mean chronology (*i.e.* after standardization has been carried out), and the degree to which it represents the hypothetical perfect (noise-free) index (Briffa 1990). The EPS is a measure of the common variability in a chronology as a function of sample depth given by the following equation:

$$EPS_t = \frac{t * r_{bt}}{t * r_{bt} + (1 - r_{bt})} \quad (3.2)$$

where t is the average number of tree series using one core per tree and r_{bt} is the mean between-tree correlation (Briffa and Jones 1990). A threshold of 0.85 has been suggested (Wigley *et al.* 1984; Briffa and Jones 1990) to minimize inflation of variance due to decreasing sample size, where the chronology becomes dominated by the individual tree-level signal rather than a coherent stand-level signal (Speer 2010). Limiting the length of the index chronologies to the year where the EPS drops below the 0.85 critical threshold allows for a high degree of confidence to be held in each of the index chronologies for climatic investigations.

The applicability of each chronology for further regression analyses was tested using a user-written MATLAB function[1] that calculates the mean and standard deviation and by implementing the robust, non-parametric Lilliefors test for Normality (Table 3.3; 1967). As stated previously, ARSTAN's pre-whitens each series to create the residual chronologies, and therefore all site indices are free of significant serial autocorrelation. The standardization procedures are deemed effective from the very little deviation from a mean of 1.0 (Cook *et al.* 1990). The standard deviation from the mean compares well with the mean sensitivity for each chronology. The Lilliefors statistic (Lilliefors 1967) indicates that all indices are below critical threshold levels for rejecting the null hypothesis that each chronology comes from a normal distribution with unspecified mean and variance. Therefore the index data can be used as is, without need for transformation, for regression analyses (Conover 1980).

[1] Meko, D., 2005: GEOS 595 University of Arizona

Table 3.3 Statistical properties of index chronologies.

Site	Type	Mean	Standard deviation	Lilliefors statistic	$L_{critical}$	Normal
DEV	RW	0.988	0.226	0.049	0.102	yes
	LW	0.963	0.365	0.094	0.102	yes
FAF	RW	0.978	0.143	0.058	0.081	yes
	EW	0.999	0.108	0.089	0.108	yes
	LW	0.943	0.248	0.051	0.081	yes
HIL	RW	0.996	0.249	0.087	0.090	yes
	EW	0.980	0.110	0.075	0.131	yes
	LW	0.980	0.363	0.087	0.090	yes
JCT	RW	0.994	0.191	0.071	0.100	yes
WLL	RW	0.986	0.202	0.065	0.067	yes
	EW	0.990	0.115	0.084	0.095	yes
	LW	0.963	0.396	0.066	0.067	yes
BES	RW	0.974	0.180	0.054	0.077	yes
	EW	0.993	0.095	0.052	0.100	yes
	LW	0.959	0.297	0.053	0.077	yes
NCH	RW	0.994	0.174	0.048	0.063	yes
	EW	0.994	0.093	0.091	0.094	yes
	LW	0.973	0.286	0.046	0.063	yes
SLF	RW	0.979	0.193	0.048	0.081	yes
	LW	0.979	0.338	0.054	0.081	yes
VDV	RW	0.979	0.177	0.042	0.082	yes
	LW	0.980	0.302	0.054	0.082	yes
CGT	RW	0.982	0.257	0.053	0.054	yes
	EW	0.994	0.106	0.050	0.073	yes
	LW	0.963	0.420	0.052	0.053	yes
CRR	RW	0.999	0.239	0.056	0.058	yes
	EW	0.994	0.106	0.050	0.073	yes
	LW	0.980	0.374	0.055	0.069	yes
GRI	RW	0.994	0.241	0.059	0.069	yes
	EW	1.000	0.103	0.105	0.107	yes
	LW	0.983	0.372	0.068	0.069	yes
KIL	RW	0.983	0.263	0.074	0.085	yes
	EW	0.999	0.370	0.082	0.084	yes
	LW	0.956	0.361	0.073	0.085	yes
LMG	RW	0.999	0.193	0.054	0.056	yes
	LW	1.000	0.276	0.052	0.094	yes

3.3 Instrumental data:

3.3.1 Instrumental climate data:

Regional climate variables were derived from gridded climate data for the Prairie region, including and surrounding the Souris River Basin (45° to 60°N and 90° to 120°W). Monthly temperature data were extracted from the CRUTEM3+HadSST2 gridded (0.5°) dataset (Rayner *et al.* 2006), while monthly precipitation data were extracted from Mitchell and Jones' (2005) CRU TS3 – New World gridded (0.5°) dataset. These data were reduced to annual and seasonal (DJF, MAM, JJA, SON) means and totals for temperature and precipitation analyses, respectively.

3.3.2 Streamflow data:

In order to effectively model historical streamflow for the Souris River Basin, and to assess the patterns of variability both spatially and temporally, streamflow data for the Souris River, as well as its major tributaries, Long Creek and Pipestone Creek, were obtained from Environment Canada's National HYDAT water data archive (2010) and the United States Geological Survey (USGS) surface water database (2010). Ideal stations throughout the basin (Table 3.4) were selected based on their location, status (active or discontinued use), length and continuity of their records. To be deemed fit for investigation, stations had to be actively in use, with a minimum of 30 consecutive years of normally distributed data. Similar to preliminary investigations of tree-ring chronologies, a user-written MATLAB function[2] was used to calculate the mean, range, and standard deviation, and to test the hypothesis that each streamflow record comes from a random sample of normal distribution, by implementing the robust, non-parametric Lilliefors test for Normality (Table 3.5; 1967).

[2] Meko, D. 2005: GEOS 595 University of Arizona

Table 3.4 Properties of selected streamflow gauges.

Station	Province	Code	Length of record	# years	Seasonal / Continuous	Active / Discontinuous
Souris River near Sherwood	SK	SRnS	1931-2008	78	continuous	active
Souris River at Wawanesa	MB	SRnWa	1954-2008	55	continuous	active
Pipestone Creek near Pipestone	MB	PCnP	1957-1993	37	continuous	active
Long Creek n Noonan	ND	LCnN	1960-2008	49	continuous	active

Table 3.5 Statistical properties of selected streamflow gauges.

Site	Type[1]	Mean	Standard deviation	Range	N	Lilliefors statistic	$L_{critical}$	Normal	ACF[2] @ p < 0.05
LCnN	wy	1.100	1.305	5.698	49	0.124	0.126	yes	0
	JJA	0.702	1.128	4.903	49	0.123	0.126	yes	0
PCnP	wy	1.103	1.432	8.233	37	0.142	0.143	yes	0
	JJA	0.477	0.791	4.447	37	0.141	0.143	yes	0
SRnS	wy	3.444	4.375	25.061	78	0.098	0.100	yes	0
	JJA	2.214	3.329	20.588	78	0.097	0.100	yes	0
SRnWa	wy	13.846	17.049	87.180	55	0.115	0.119	yes	0
	JJA	17.605	25.352	105.959	55	0.117	0.119	yes	0

[1]: wy = water year flows (October - September); JJA = summer flows (June - August)
[2]:ACF = autocorrelation function; 0 = no significant firs-order autocorrelation

Tables 3.4 and 3.5 represent data for streamflow gauges selected throughout the Souris River Basin, from both headwater tributaries as well as locations downstream along the Souris River itself. Data were selected for four active, regulated gauges having at least 30 consecutive years of data from Saskatchewan (Souris River near Sherwood, SRnS), Manitoba (Souris River at Wawanesa, SRnWa, and Pipestone Creek near Pipestone, PCnP) and North Dakota (Long Creek near Noonan, LCnN; station abbreviations will be used here on out). Statistics for water year (October to September) and summer (June to August) flow at each station are given in Table 3.5. Average flow

(m^3/s) is given by the mean, while the standard deviation and range represent the amount of variability and dispersion from average flows at each of the stations. Lillifors' test statistics for all stations, annually (water year) and seasonally (summer - JJA) are below the critical threshold level, indicating that streamflow at all gauges come from a normal distribution. In addition to these basic statistics, autocorrelation functions (ACF) were calculated for all gauge records using a user-written MATLAB function[3]. All streamflow gauge records, at annual and seasonal timescales, were found free of any significant first order autocorrelation.

Very late into this study's investigation of streamflow variability within the Souris River basin, naturalized streamflow data covering the period 1912 to 1974, prepared by the Prairie Farm Rehabilitation Administration (PFRA; Martin and Godwin 1977), became available for use via correspondence with the Saskatchewan Watershed Authority. The development of natural flow at various locations in the Souris River Basin involved selecting available streamflow records, converting recorded flows to natural flows, and extending natural flows for the recorded period, 1925 to 1974, to the full study period. Historical water uses or adjustments (including: minor water use, irrigation, drainage, reservoir evaporation losses and storage changes, thermal power uses, wildlife and recreation, domestic, industrial, and municipal) were determined for the entire study period, 1912 to 1974 because the adjustments (modified by transfer factors) were added algebraically to recorded flows at hydrometric gauging stations having variable periods of record (Martin and Godwin 1977). The addition of adjustments to recorded flows produced natural flows at hydrometric gauging stations for

[3] Meko, D. 2005: GEOS 595 University of Arizona

the period of record, which were then extended to the study period by multiple regression techniques (Martin and Godwin 1977).

As stated previously, naturalized records became available very late into this investigation, and in order to determine the most appropriate records to use for the entirety of the analyses, the originally obtained regulated streamflow records were statistically compared to the 'newly' available naturalized records. Correlation analyses of the period of overlap between naturalized and regulated flows were investigated for both annual water year and seasonal records. Annual water year and seasonal flows were similar, and had no significant difference ($p < 0.001$) for the entire period of overlap, and showed no divergence in frequency and or magnitude of periods of high and low flow events. Therefore, it was felt that the use of the originally obtained regulated flows, for the stations in question, were adequate for the continuation and entirety of the analyses.

3.4 Exploratory analyses:

Dendrochronology has been linked to streamflow through the common responses of tree-growth and streamflow to variations in net precipitation, temperature, and runoff at time scales from seasons to centuries and longer (Stockton and Jacoby 1976; NRC 1998). Understanding the relationship that trees and river systems both integrate the effects of point source precipitation and temperature into a larger spatial unit representing regional hydroclimate (Axelson and Sauchyn 2007), thereby implies that tree-growth ultimately is a reflection of streamflow conditions. In order to accurately model streamflow variability within the Souris Basin, it is important to understand the linear relationship between streamflow, tree-ring growth, and factors, such as precipitation and temperature, that influence these variables.

3.4.1 Streamflow and climate:

Streamflow station data were examined for correlations with both precipitation (Mitchell and Jones 2005) and temperature (Rayner *et al.* 2006) for the Souris River Basin and surrounding Prairie Region area, via the use of the climate explorer tool developed by the Royal Netherlands Meteorological Institute available at http://climexp.knmi.nl/start.cgi?someone@somewhere. Correlations maps were created for each streamflow station based on annual and seasonal time scales, showing the significant area of influence that precipitation and temperature have on streamflow variability at different locations throughout the basin and surrounding area.

All four stations yielded similar results in that streamflow was positively correlated with regional precipitation and negatively correlated with temperature (Figure 3.7). Significant seasonal correlations for each station ($p < 0.05$) were found between streamflow and spring temperatures (MAM, $-0.5 < r < -0.2$), and summer precipitation (JJA, $0.2 < r < 0.5$). Since the Souris River is solely dependent on precipitation and immediate runoff and has no input of snow or glacial meltwater from the Rockies, increasingly warm temperatures early in the runoff season, impose high evaporation/potential evapotranspiration demands, resulting in decreased flows. Positive correlations with summer precipitation reflects the importance of summer rainfall on the Prairies (St. George *et al.* 2009), increasing streamflow in the Souris River Basin.

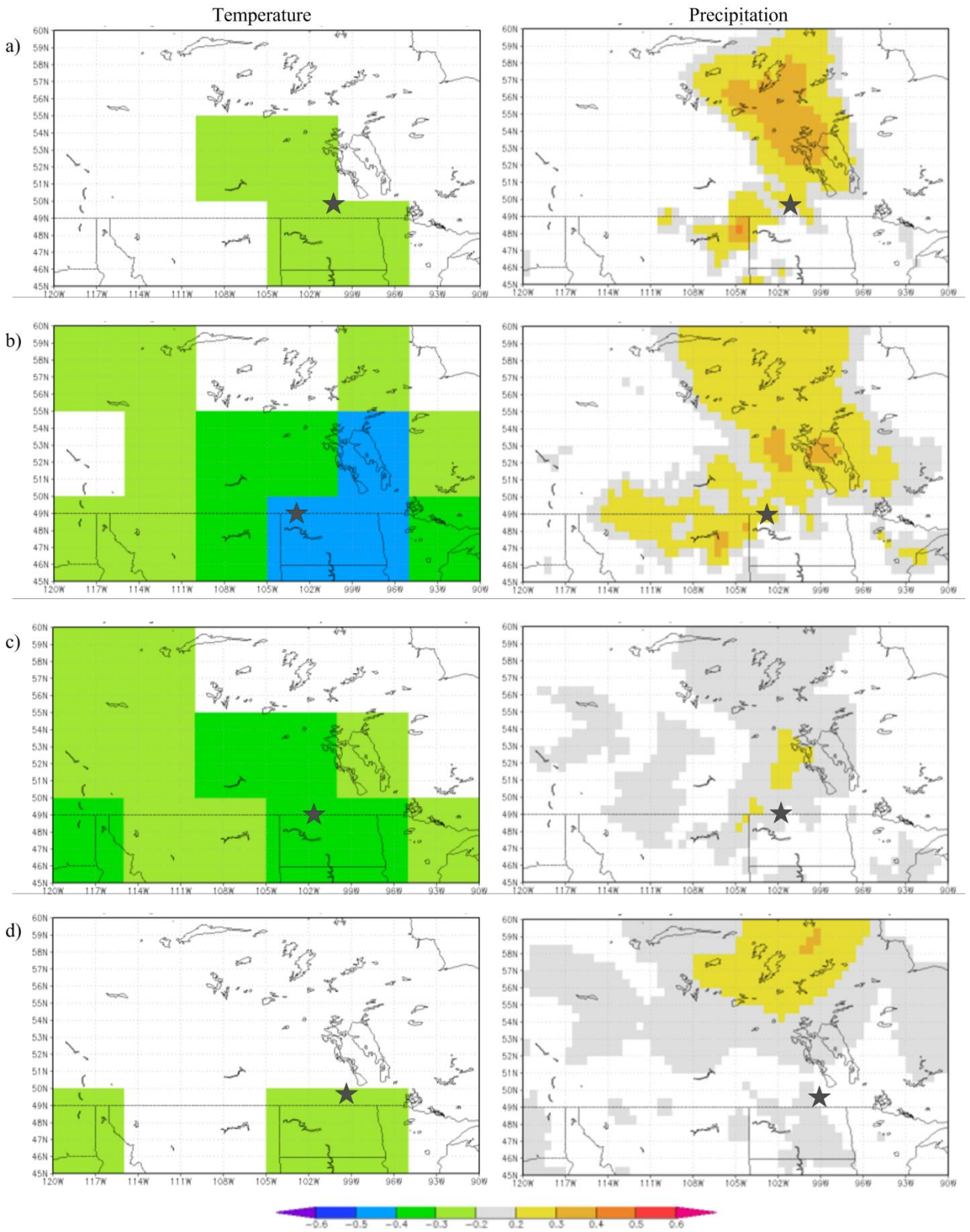

Figure 3.7 Correlation maps between streamflow gauges (stars: a)PCnP; b)LCnN; c)SrnS; d)SRnWa) and Mar-May temperature and Jun-Aug precipitation ($p<0.05$).

3.4.2 Tree-growth response to climate:

In order to investigate whether precipitation and temperature could also be considered predictors of tree growth, similar analyses were performed implementing the climate explorer tool to investigate the growth responses of annual, early- and latewood widths to regional climate variability within and surrounding the Souris River Basin. Similar to streamflow interactions, RW, EW, and LW ring-width indices were positively correlated with precipitation and negatively correlated with temperature (Figure 3.8), an indication that moisture stress is the major limitation to growth of the species at its western ecological range (Case 2000; St. George *et al.* 2009).

In general RW, EW, and LW indices have a weak negative correlation with May temperature ($-0.4 < r < -0.2$; $p < 0.05$). Negative growth responses again suggest that regionally higher spring temperatures impose high evapotranspiration demands, resulting in reduced annual ring growth (Vanstone and Sauchyn 2010). Earlywood chronologies had the most significant and widespread negative correlations to temperature, corresponding to the negative effect of temperature earlier in the year. During the cold (winter) months, ring porous species, such as bur oak, enter a quiescence phase restoring the ability to respond to growth-promoting conditions. During quiescence, before photosynthates are yet to be produced, the tree uses stored reserves from the previous growing season (Speer 2010), and changes at the ultrastructural level only occur within a tree (*i.e.* EW vessel formation; Farrar and Evert 1997). When conditions become favourable for LW growth later in the growing season, warming spring temperatures and increasing evapotranspiration correlate negatively with the production of EW growth (Vanstone and Sauchyn 2010).

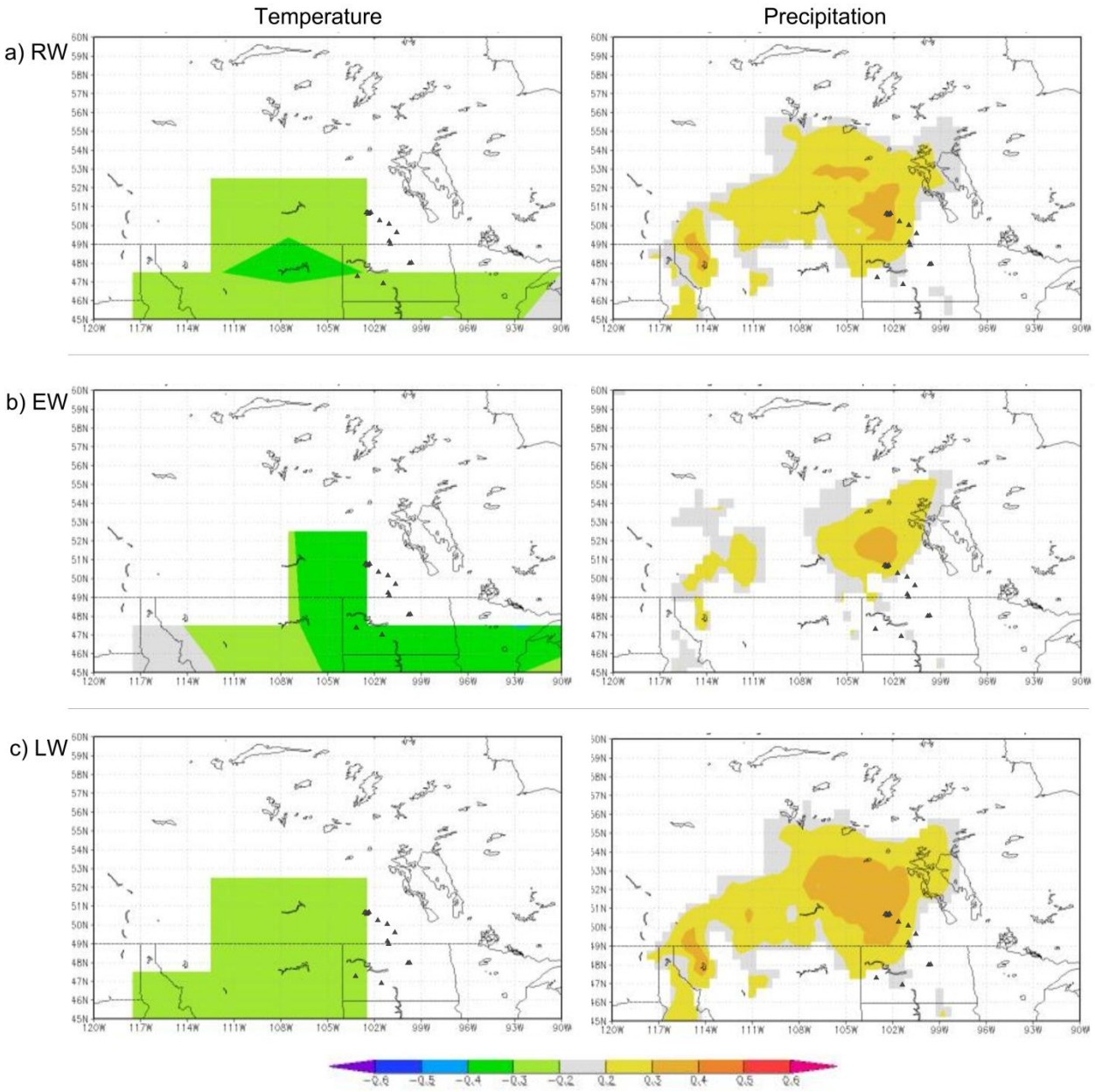

Figure 3.8 Correlation maps between RW, EW and LW ring-width indices May temperature and Jun-Aug precipitation ($p<0.05$). Triangles denote chronology locations.

Annual (RW), EW and LW growth indices are primarily correlated with summer (JJA) precipitation ($0.2 < r < 0.5$; $p < 0.05$). Correlation analyses show that regional RW and LW display a similar sensitivity to summer precipitation, while the moisture signal in EW is much weaker, supporting a closer relationship of RW to LW widths than to EW

widths (*i.e.* LW widths are more variable and therefore account for more of the variation in RW). Correlations between spring, autumn, winter, prior autumn and winter, and all ring-width series were not significant at a regional level (see Appendix). Although all chronologies were found to be significantly correlated with summer precipitation only, growth indices also correlate with annual (June to May) precipitation (Vanstone and Sauchyn 2010), "but this correspondence likely reflects the importance of summer rainfall on the Prairies rather than a real physical relationship between ring-width and total annual precipitation" (St. George *et al.* 2009). If an 'actual' significant annual correlation were to exist, growth indices would likely have some correlation with other seasons, most likely with prior winter precipitation, reflecting the importance of winter snowfall to soil moisture recharge and growth resumption in the spring (Robertson 1992; Case 2000).

The results of these analyses provide evidence that both tree-ring growth and streamflow, within the Souris River Basin, are controlled and therefore limited by precipitation and temperature, thereby satisfying the assumption that tree-ring growth and streamflow variability are significantly influenced by hydroclimatic variability.

3.4.3 Tree-rings and streamflow:

The 42 tree-ring width chronologies (RW, EW, and LW chronologies at each of the 14 sites), were examined for correlations with streamflow data to restrict the pool of predictors to those with a statistical relationship to hydrologic variability at annual (water year - October through September) and seasonal (DJF, MAM, JJA, SON) resolutions.

The highest correlations at each site for all three proxy chronologies (RW, EW, and LW; $p < 0.05$; Tables 3.6 – 3.9) were with annual (water year) streamflow.

Seasonally, chronologies exhibited significant correlations with spring, summer and previous summer flows, however highest interannual relationships were found with present summer (JJA) records.

In almost all cases, latewood chronologies demonstrated the most significant correlations with both annual and interannual streamflow records at all four stations. Significant but lower correlations were between the annual ring-width and streamflow data.

Where individual chronologies were used as predictors of streamflow, in subsequent analyses, the pool of predictors was limited to the most significant chronologies (RW, EW or LW) in terms of correlations with the predictand (streamflow gauge record), to reduce the chance of overfitting and creating an unrealistic model of historical streamflow.

Table 3.6 Correlation analyses for LCnN and tree-ring chronologies. Significant correlations ($p<0.05$) are highlighted in red.

RW	DEV	FAF	HIL	JCT	WLL	BES	NCH	SLF	VDV	CGT	CRR	GRI	KIL	LMG
water-year	0.333	0.007	0.307	0.193	0.170	0.161	0.370	0.290	0.357	0.242	0.205	0.245	0.238	0.204
JJA	0.255	0.120	0.150	0.236	0.074	0.386	0.267	0.152	0.296	-0.015	-0.034	-0.065	-0.002	0.001

EW	FAF	HIL	WLL	BES	NCH	CGT	CRR	GRI	KIL
water-year	0.024	0.339	0.104	0.092	0.156	0.141	0.330	0.228	0.227
JJA	0.123	0.219	0.117	0.275	0.189	-0.152	-0.144	0.038	0.059

LW	DEV	FAF	HIL	WLL	BES	NCH	SLF	VDV	CGT	CRR	GRI	KIL	LMG
water-year	0.396	0.088	0.306	0.284	0.181	0.438	0.294	0.384	0.247	0.083	0.224	0.334	0.152
JJA	0.292	0.128	0.096	0.133	0.367	0.269	0.135	0.262	0.006	-0.052	-0.051	0.009	-0.043

Table 3.7 Correlation analyses for PCnP and tree-ring chronologies. Significant correlations ($p<0.05$) are highlighted in red.

RW	DEV	FAF	HIL	JCT	WLL	BES	NCH	SLF	VDV	CGT	CRR	GRI	KIL	LMG
water-year	0.435	0.047	0.434	0.350	0.387	0.087	0.118	0.278	0.283	0.313	0.382	0.360	0.344	0.256
JJA	0.517	0.138	0.457	0.375	0.431	0.184	0.220	0.251	0.256	0.294	0.305	0.282	0.266	0.146

EW	FAF	HIL	WLL	BES	NCH	CGT	CRR	GRI	KIL
water-year	0.018	0.515	0.238	-0.086	-0.054	0.261	0.329	0.218	0.327
JJA	0.108	0.532	0.227	-0.029	0.049	0.185	0.141	0.120	0.231

LW	DEV	FAF	HIL	WLL	BES	NCH	SLF	VDV	CGT	CRR	GRI	KIL	LMG
water-year	0.483	0.101	0.445	0.553	0.143	0.221	0.315	0.315	0.316	0.327	0.335	0.377	0.321
JJA	0.577	0.158	0.460	0.590	0.212	0.288	0.279	0.276	0.295	0.283	0.262	0.295	0.209

Table 3.8 Correlation analyses for SRnS and tree-ring chronologies. Significant correlations ($p<0.05$) are highlighted in red.

RW	DEV	FAF	HIL	JCT	WLL	BES	NCH	SLF	VDV	CGT	CRR	GRI	KIL	LMG
water-year	0.352	0.033	0.312	0.149	0.178	0.137	0.242	0.245	0.343	0.276	0.196	0.303	0.218	0.166
JJA	0.450	0.089	0.402	0.330	0.297	0.300	0.327	0.261	0.453	0.089	0.017	0.102	0.049	-0.034

EW	FAF	HIL	WLL	BES	NCH	CGT	CRR	GRI	KIL
water-year	-0.021	0.349	0.154	-0.038	0.031	0.221	0.275	0.251	0.306
JJA	0.193	0.333	0.409	0.224	0.203	-0.018	0.023	0.039	0.155

LW	DEV	FAF	HIL	WLL	BES	NCH	SLF	VDV	CGT	CRR	GRI	KIL	LMG
water-year	0.392	0.088	0.343	0.274	0.187	0.335	0.270	0.380	0.274	0.128	0.271	0.293	0.135
JJA	0.469	0.050	0.389	0.296	0.290	0.328	0.236	0.437	0.108	0.005	0.089	0.095	-0.052

Table 3.9 Correlation analyses for SRnWa and tree-ring chronologies. Significant correlations ($p<0.05$) are highlighted in red.

RW	DEV	FAF	HIL	JCT	WLL	BES	NCH	SLF	VDV	CGT	CRR	GRI	KIL	LMG
water-year	0.428	0.174	0.468	0.322	0.414	0.236	0.304	0.382	0.350	0.248	0.261	0.251	0.203	0.201
JJA	0.352	0.090	0.470	0.299	0.383	0.309	0.307	0.392	0.271	0.254	0.181	0.217	0.119	0.183

EW	FAF	HIL	WLL	BES	NCH	CGT	CRR	GRI	KIL
water-year	0.022	0.420	0.183	-0.085	0.074	0.228	0.367	0.264	0.205
JJA	0.026	0.289	0.236	-0.001	0.120	0.262	0.287	0.311	0.144

LW	DEV	FAF	HIL	WLL	BES	NCH	SLF	VDV	CGT	CRR	GRI	KIL	LMG
water-year	0.493	0.248	0.503	0.566	0.301	0.393	0.393	0.387	0.252	0.190	0.231	0.232	0.204
JJA	0.399	0.158	0.523	0.522	0.382	0.384	0.371	0.289	0.229	0.117	0.173	0.150	0.125

4. TIME SERIES ANALYSES

4.1 Reconstructions:

The primary goal of dendroclimatology is the reconstruction of past climate (Fritts 1976). A typical approach to reconstructions has been to identify the climatic parameters corresponding to particular variations in ring width, eventually developing a statistical function to infer variations in climate from past variations in tree growth (Schulman 1956; Sirén 1963; Hughes *et al.* 1983). Dendroclimatic reconstructions are usually generated by a regression model in which the predictand is the climate/hydroclimate variable of interest (*i.e.* precipitation, temperature, streamflow, etc.), and the predictors are the site chronologies, in any form (RW, EW, LW or a combination of the aforementioned) (Meko 1997). Multiple linear regression (MLR) models have long been used in dendroclimatology for reconstructing climate/hydroclimatic variables from tree rings (e.g., Fritts 1976; Graumlich 1987; Cleaveland and Stahle 1989; Michaelsen 1989; Guiot 1990; Cleaveland and Duvick 1992; Loaiciga *et al.* 1993; and others) and will be used here to reconstruct historical streamflow for the Souris River Basin. Multiple linear regression models usually take the following form, expressing the value of a predictand variable as a linear function of one or more predictor variables and an error term:

$$Y_i = a + b_1X_{i,1} + b_2X_{i,2} + ... + b_kX_{i,k} + e_i \qquad (4.1)$$

where Y_i is the predictand (*i.e.* streamflow), a is the regression constant, $X_1...X_{ik}$ are the predictors (*i.e.* tree-ring chronologies), b_k the regression coefficients, and e_i is the error of

the regression (Ostrom 1990). MLR models are based on several assumptions, and if satisfied, the regression estimators are considered optimal, in the sense that they are unbiased, efficient, and consistent. Ostrom (1990) summarizes the assumptions as follows:

a) Linearity: a linear relationship exists between the predictand (*Y)* and the predictors (*X*);

b) Nonstochastic X: $E[e_i X_{i,k}] = 0$; (4.2)

c) Zero mean: $E[e_i] = 0$; (4.3)

d) Constant variance: $E[e_i^2] = \sigma^2$; (4.4)

e) Nonautoregression: $E[e_i e_{i-m}] = 0, \ (m \neq 0)$; (4.5)

f) Normality: error is normally distributed;

g) Non-multicollinearity: intercorrelation of variables is not too high, causing the variance of the regression to become inflated.

As stated previously, the relationship between the tree-ring chronologies (RW, EW, and LW indices) and streamflow (annual water year - October through September; and seasonal flow) were investigated via correlation analyses to determine which predictors had the highest correlations for each predictand, and also the temporal scale at which tree growth exhibits the best response (Fritts 1976; 1991). These results identified annual water year (October through September) and summer flow (JJA) as the optimal predictands. To reduce the chance of over-fitting, for each model, the pool of predictors was formed from the most significant chronologies in terms of correlations with each of the predictands (Sauchyn *et al. in press*).

Linear regression models were developed by a user-written MATLAB function[4] to estimate streamflow from a set of tree-ring (RW, EW, and LW) predictors through a forward step-wise procedure. Forward and negative lags of up to two years allowed the model to accommodate relationships between streamflow and tree growth response in the prior, current, and following growth year, for up to two years (Fritts 1976). Regression equations were calibrated on the period of instrumental record for annual water year and summer streamflow at each gauge, ranging from 37 to 78 years. Nested reconstructions were developed to accommodate the varying chronology lengths while exploiting the potential to accurately capture the long-term extreme events history of the region (Touchan *et al.* 2008). In this procedure, past streamflows were estimated from the stepwise regression model for the period covered by all the individual site chronologies. Statistical models were developed for progressively longer periods by successively removing the shortest chronologies from the pool of predictors, with their spans corresponding to significant changes with declining sample depth (Touchan *et al.* 2008). The individual reconstructions for each nest are joined into a single long reconstruction such that each time period is represented by the corresponding regression model with the maximum sample depth (Figure 4.1). This procedure allows for a maximum length reconstruction, although the earliest part of the record may have reduced robustness because of thin sample size (Figure 4.1) (Touchan *et al.* 2010).

[4] Meko, D. 2005: GEOS 595 University of Arizona.

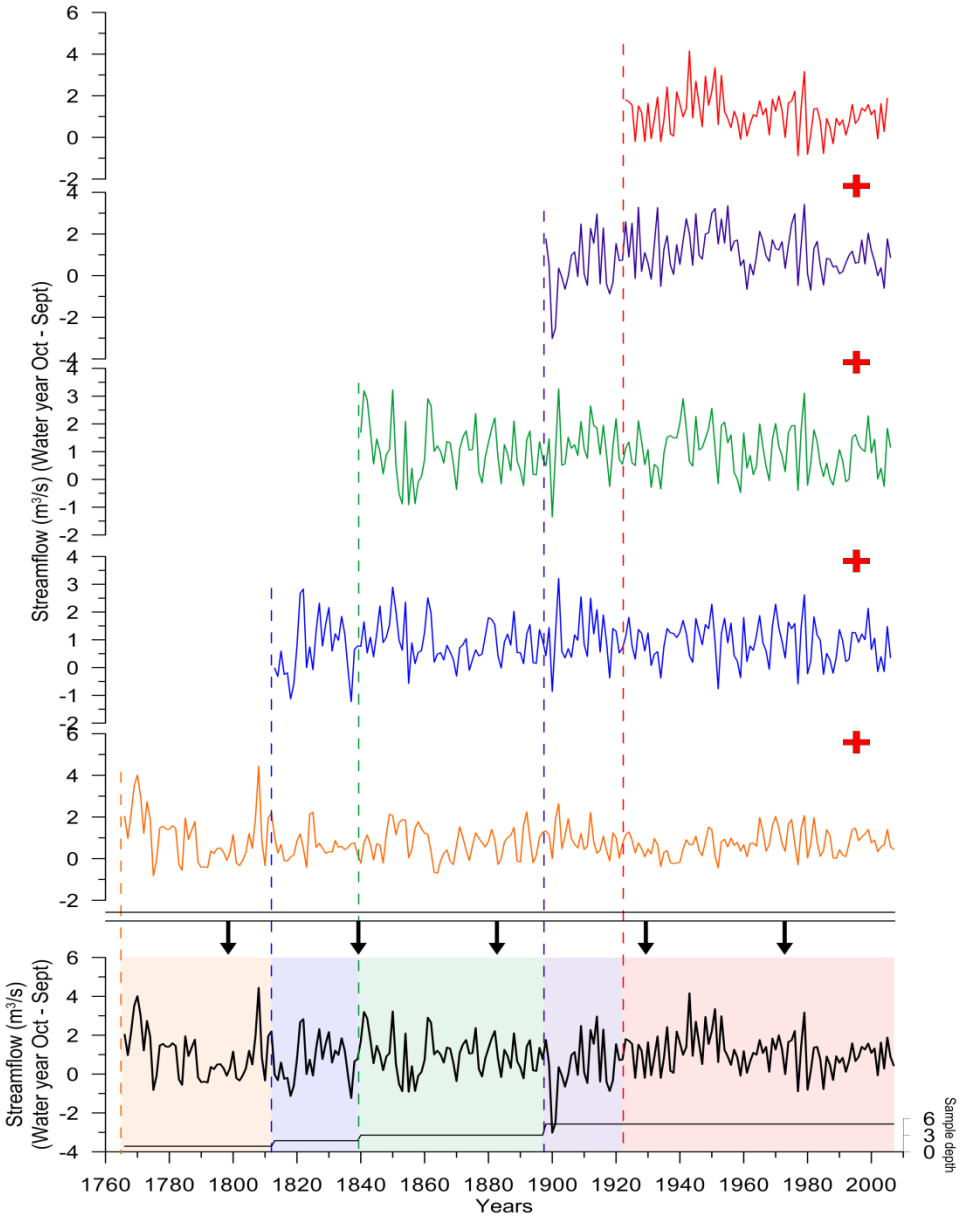

Figure 4.1 Nested reconstruction schematic.

4.1.1 Statistics and validation:

The MATLAB script guards against over-fitting the regression model by using the cross-validation as a guide for stopping the entry of additional predictors when creating the models (Wilks 1995). Cross-validation was carried out using the leave-*n*-out method, where a series of regression models are fit, each time deleting a different

observation from the calibration set and using the model to predict the predictand for the deleted observation. This validation method is particularly advantageous for relatively short predictand series, thus allowing the data to be tested to its maximum extent (Hughes *et al.* 1983). "By evaluating the performance of the model on data withheld from calibration at every step of the stepwise procedure, the level of complexity (number of predictors) above which the model is over-fit can be estimated. Graphs of change in calibration and validation accuracy statistics as a function of step in forward stepwise entry of predictors can be used as a guide for cutting off entry of predictors into the model. The step at which the root mean squared error of validation ($RMSE_v$) is minimized (or approximately so) can be set as the final step for the model"[5].

In order to assess the statistical quality and validity/predictive capacity of each reconstruction model, the MATLAB script runs and produces results for a series of goodness-of-fit tests, as described below[6]:

a) Coefficient of determination (R^2) and Adjusted R^2: The R^2 value expresses the explanatory power of the regression, indicating the proportion of variance being accounted for or explained by the regression model. Quite often the R^2 value can become inflated, or arbitrarily high as more predictors are added to the model. The adjusted R^2 (R^2_{adj}) statistic compensates for the artificial increase in accuracy. The addition of more predictors will increase the gap between the R^2 and R^2_{adj} values, and therefore the latter will depend on both the sample size and number of predictors in the model (Fritts 1976).

[5] Meko, D. 2005: GEOS 595 University of Arizona, course notes.
[6] Meko, D. 2005: GEOS 595 University of Arizona, course notes (Chapters 11 and 12)

b) Standard error of the estimate (SE) and the root mean squared error of validation ($RMSE_v$): The SE is the sample estimate of the variance of the regression residuals, where the $RMSE_v$ is a measure of the average size of the prediction error for the validation period. The difference between the SE and $RMSE_v$ is a practical measure of the accuracy of the model. If the difference is small, the model is said to be validated.

c) Reduction of Error (RE): The RE measures the *skill* or predictive capacity of a regression model based on "no-knowledge". In other words, with no other knowledge about the predictand other than its calibration-period data, it makes sense simply to substitute the calibration-period mean of the predictand as the predicted value for any year outside the calibration period. RE has a possible range of $-\infty$ to +1. As a rule of thumb, any positive RE is accepted as evidence of some skill of prediction, where a value of +1 would indicate a theoretically perfect prediction and validation (Fritts 1976; Fritts *et al.* 1990). Similarities between the values for R^2 and RE are considered evidence of validation.

d) Durbin Watson (D-W) and Portmanteau (Q) tests: These tests are run, respectively, to test for autocorrelation of residuals, specifically lag-1 autocorrelations, and as well, to determine whether the regression residuals are purely random, or white noise (Ostrom 1990). The D-W test is designed to test the null hypothesis that no first-order autocorrelation exists in the residuals. The advantage of including the Q test is that residuals are tested for 'any' level of autocorrelation and are not just restricted to first-order. If the residuals are random, the autocorrelation functions (acf) should be zero at all nonzero lags

(Ostrom 1990). In addition to running these two tests, the MATLAB function also builds plots of the residuals as a time series, scatterplot against predicted values and individual predictors, histogram, acf's and a lag-1 scatterplot, for visual interpretation.

e) Variance Inflation Factor (VIF): The VIF is used to detect multicollinearity in the models, by how much the explained variance is increased or inflated with the addition of predictors that are correlated with one another. Multicollinearity is said to be an issue when the VIF of one or more predictors becomes large. As interpretation of 'large' can be subjective, Haan (2002) suggests a VIF threshold of 5 to 10, before the null hypothesis can be rejected indicating that multicollinearity is an issue among the predictors, and that the validity of the model should be interpreted with caution.

4.2 Post reconstruction analyses:

In order to assess the hydroclimatic variability within the Souris Basin, reconstructed flows were ranked to characterize the timing and magnitude of moderate and extreme hydrological drought. The main oscillatory modes of variability were identified via the use of the multitaper method (MTM) (Mann and Lees 1996) of singular spectrum analyses and by continuous wavelet analysis (CWT; Grinsted *et al.* 2004). In an attempt to identify significant oscillatory frequencies corresponding to possible atmospheric and sea-surface temperature (SST) forcings of hydroclimatic variability, extracted frequencies were investigated using wavelet transform and coherency analyses. A brief description of each method is provided below.

4.2.1 Ranking system - single and multi-year 'Mega' droughts:

To assess the timing and duration of prolonged high and severe low flows, wet and dry intervals were defined as flows in the 75th and 25th percentiles, respectively (Axelson *et al.* 2009). Each reconstruction was plotted and periods of low flows were identified and compared amongst all reconstructed gauge records to determine if significant drought events were spatially isolated or occurred on a regional scale for the entire Souris Basin. This is a simple comparative method of drought identification that allows the magnitude of historic droughts to be placed within a long term context (Meko and Graybill 1995). In addition to the identification of sustained low flows, severe hydrological droughts, defined as flows in the lowest 10th percentile, were identified and the top ten worst droughts were compiled and compared amongst all reconstructions (Axelson *et al.* 2009).

4.2.2 Singular spectrum analysis - Multi-taper Method (SSA-MTM):

Singular spectrum analyses (SSA) is essentially a principal components analysis in the time domain that extracts information from short and noisy time series without prior knowledge of the dynamics affecting the time series (Vautard and Ghil 1989; Dettinger *et al.* 1995; Shoellhamer 2001). The multi-taper method (MTM) is a powerful and widely used nonparametric method of spectral analysis with high resolution and the ability to minimize spectral leakage while also reducing the variance of spectral estimates by using orthogonal tapers rather than the unique data taper or spectral window used by the classical methods (Thomson 1982; Percival and Walden 1993; Ghil *et al.* 2002; Axelson *et al.* 2009). The data are premultiplied by orthogonal tapers constructed to minimize the spectral leakage due to the finite length of the time series, and a set of

independent estimates of the power spectrum is computed (Ghil *et al.* 2002). The optimal tapers or 'eigentapers' belong to a family of functions defined as the eigenvectors that are the discrete set of eigenfunctions that solve the variational problem of minimizing leakage outside particular frequency bands (Ghil *et al.* 2002). Detailed algorithms for the calculation of the eigentapers are readily available from Thomson (1982) and Percival and Walden (1993). Averaging over the (small) ensemble of spectra obtained by this procedure yields better and more stable estimates (with lower variance) than do single-taper methods (Thomson 1990a). Once the tapers are computed for a chosen frequency bandwidth, the total power spectrum can be estimated by averaging the individual spectra given by each tapered version of the data set, and oscillatory components are shown as peaks of bumps within the spectra. All peaks, whether purely harmonic or narrowband, are tested for significance relative to the null hypothesis of a red-noise background (Mann and Lees 1996). Discrimination against a red-noise background is particularly important in climate studies, where the system under investigation always contains longer time-scales than those of immediate interest, which leads to greater power at lower frequencies and greater likelihood of prominent peaks in the spectrum there (Thomson 1990a; Ghil *et al.* 2002).

Once significant peaks have been isolated in the spectrum, associated signals can be reconstructed in the time domain using information from the multi-taper decomposition. Reconstructions of oscillatory signals are analogous to SSA reconstructed components, however, the information from a frequency-domain decomposition, rather than a lag-domain composition, is used to reconstruct the partial signal of interest (Ghil *et al.* 2002).

To identify dominant oscillations within each of the time series and their corresponding frequencies at which they occur, Multi-taper method spectral analyses of each streamflow reconstruction at each gauge was implemented using the SSA-MTM Toolkit, available for download at http://www.atmos.ucla.edu/tcd/ssa/.

4.2.3 Continuous wavelet analysis (CWT):

Time series are often generated by complex systems of which all driving factors are not known. Predictable behavior in such systems, such as trends and periodicities, is therefore of great interest. Most traditional mathematical methods that examine periodicities in the frequency domain, such as Fourier analysis, have implicitly assumed that the underlying processes are stationary in time, however, wavelet transforms expand time series into time-frequency-space (Grinsted *et al.* 2004). Decomposing a time series into time-frequency-space determines both the dominant modes of variability and how those modes vary in time (Torrence and Compo 1998).

Continuous wavelet analyses (CWT; Torrence and Compo 1998; Grinsted *et al.* 2004) were implemented via a user written MATLAB package, provided by Torrence and Compo (1998) available http://atoc.colorado.edu/research/wavelets/, to identify the dominant oscillation modes of variability within each streamflow reconstruction. Statistical significance of the wavelet is estimated against a red noise background at 95%. Because the data are bounded in time, the wavelet transform is affected by edge effects, and errors will occur at the beginning and end of the wavelet power spectrum (Torrence and Compo 1998; Jevrejeva *et al.* 2003). A solution to this has been to pad the ends of the time series with zeros, before doing the wavelet transform and removing them afterward. Because of the edge effect, the MATLAB function creates a cone of influence

(COI) that delimits a region of the wavelet spectrum in which edge effects become important and the power could be suppressed (Torrence and Compo 1998; Jevrejeva *et al.* 2003; Grinsted *et al.* 2004; Gobena and Gan 2009). The spectral power outside the cone of influence should be interpreted with caution.

4.2.4 Links to oscillatory indices:

Monthly climate indices of atmospheric teleconnections and sea-surface temperatures [the Pacific Decadal Oscillation (PDO, 1900 – 2009; Mantua *et al.* 1997), North Atlantic Oscillation (NAO, 1865 – 2009; Jones *et al.*1997), , El Niño Southern Oscillation (ENSO 3.4, 1856 – 2009; Kaplan *et al.* 1998), sunspot data (1700 - 2010, SIDC 2010), were obtained from the KNMI Climate Explorer available at http://climexp.knmi.nl.

Significant oscillatory frequencies were extracted from the reconstructed WY and summer flows and correlated with the respective frequencies of known oscillation modes of atmospheric and sea-surface temperature (SST) forcings thought to be primary drivers of hydroclimatic variability in the Souris River Basin (PDO ~25-30 years; NAO ~9-11 years; sunspot data ~7-11 years, and ENSO ~2-6 years). Significant correlations between particular frequencies in the streamflow data and atmospheric/sea surface temperature oscillation modes known to occur at those frequencies were further investigated via cross-wavelet transform (XWT) and wavelet coherency analysis. Areas in the time-frequency plane where two time series exhibit common power or consistent phase behaviour indicate a relationship between the signals. The following paragraphs provide brief descriptions of both techniques.

4.2.4.1 Cross-wavelet transform (XWT):

Cross-wavelet transform (XWT) method, an extension of the wavelet analysis (Torrence and Compo 1998), gives a measure of correlation between two waveforms in time-frequency domain (Dey *et al.* 2010). Cross-wavelet spectrum finds regions in the time-frequency plane where two waveforms possess high common power. The cross wavelet transform was used for analysis of the common power of two time series - significant periodicities/spectral peaks found within each of the streamflow reconstructions, and a plausible forcing (atmospheric-sea-surface temperature oscillation) described to occur at those frequencies. Given two time series X and Y, with wavelet transforms W_X and W_Y, the cross wavelet spectrum is defined as:

$$W_{XY}(s,t) = W_X(s,t)W^*_Y(s,t) \tag{4.8}$$

where the asterisk denotes complex conjugation, defining the cross-wavelet power as $|W_{XY}(s,t)|$ (Torrence and Compo 1998; Jevrejeva *et al.* 2003; Grinsted *et al.* 2004). Significant periodicities of covariance are delineated by contours in areas that meet and exceed values within the 95% confidence limits, and within the COI suggesting that during these points in time, waveforms of both time series possess high common power.

4.2.4.2 Wavelet coherence (WTC):

Another useful tool is the wavelet coherence analysis. Coherence is a measure of the intensity of the covariance of the two series in time-frequency space, unlike the cross-wavelet power which is a measure of the common power (Jevrejeva *et al.* 2003). Wavelet coherence analysis greatly facilitates the detection of the quasi-periodic component indicative of a system anomaly (MathWorks 2011). Following Torrence and Webster (1999) coherence is defined as:

$$R_n^2(s) = \frac{\left|S\left(s^{-1}W_n^{XY}(s)\right)\right|^2}{S\left(s^{-1}\left|W_n^X(s)\right|^2\right) * S\left(s^{-1}\left|W_n^Y(s)\right|^2\right)} \quad (4.9)$$

where S is a smoothing operator. $R_n^2(s)$ gives a quantity between 0 and 1, and measures the cross-correlation between two time series as a function of frequency. Equation (4.9) represents the normalized covariance between two time series because the wavelet transform conserves variance (Gobena and Gan 2009). The statistical significance level ($p < 0.05$) of the wavelet coherence is estimated using Monte Carlo methods with red noise background resulting in significant periodicities of coherence again being delineated by significance contours. As before, regions outside of the COI should be interpreted with caution.

5. RESULTS AND DISCUSSION

5.1 Streamflow reconstructions:

Average water year (October through September) and summer (June through August) streamflow were modeled for the Souris River Basin at four streamflow gauges (LCnN, PCnP, SRnS, SRnWa), by using proxies of annual, earlywood, latewood ringwidths, as well as a combination of the three types of chronologies, to capture the hydroclimatic variability at annual and sub-annual resolutions. Reconstructions were created for two stations along the Souris River itself, as well as for two of the major contributing tributaries, in order to try to represent and investigate streamflow variability for the entire basin, and not at a single location where localized anomalies may occur, spatially misrepresenting the basin as a whole. Both water year and summer flow reconstructions allow for the expansion of instrumental record data for more than 280 years for the Souris Basin, aiding in a better understanding of the historical variability affecting streamflow throughout the area. In the process of finding the optimal and best reconstruction models of streamflow at each gauge, numerous models were created (not reported), consisting of different predictors, number of predictors, as well as positive and negative lags of up to two years, accounting for tree growth responses to streamflow in the growth year and up to two years prior and following.

5.1.1. Calibration and full reconstructions:

Examining the relationships between estimated and observed streamflow data over the instrumental period allows for the evaluation of statistical validity or accuracy of a tree-ring model of historical streamflow. Calibration and verification statistics for the

regression models indicate skillful reconstructions for both WY and JJA flow at all gauges (Table 5.1) and the Durbin-Watson test

Table 5.1 Water year reconstructions - calibration and verification statistics.

Gauge	Model	Nest	Period	Predictors*	R^2	R^2_{adj}	RE	DW	VIF
Water year (October - September)									
SRnWa	RW	1	1907-2004	HIL, $CRR_{-1,+1,}$ NCH_{+2}, WLL_{+2}	0.521	0.477	0.33	H_0	1.43
		2	1832-2006	$WLL_{0,-1}$, $CRR_{+1,-1}$, NCH_{-1}	0.491	0.447	0.33	H_0	1.51
		3	1808-2006	$CRR_{0,-1,+1,+2}$, NCH	0.381	0.329	0.22	H_0	1.29
		4	1770-2007	$CRR_{0,-1,+1}$	0.250	0.221	0.08	H_0	1.10
	EW	1	1961-2004	$HIL_{0,-1}$, $CRR_{0,-2}$, GRI_{+2}	0.391	0.324	0.24	H_0	1.70
		2	1941-2007	$CRR_{0,+1}$, $GRI_{0,-1}$	0.189	0.140	0.05	H_0	1.34
	LW	1	1908-2002	WLL, $HIL_{-1,+2}$, $NCH_{0,+2}$	0.516	0.472	0.25	H_0	1.40
		2	1893-2006	WLL, $NCH_{-1,+2}$, $VDV_{0,-2}$	0.521	0.479	0.35	H_0	1.30
		3	1831-2004	$WLL_{0,+2}$, $NCH_{0,-1,+2}$	0.497	0.453	0.30	H_0	1.40
		4	1809-2006	$NCH_{0,-1,+2}$	0.324	0.297	0.16	H_0	1.00
	MULTI	1	1942-2004	WLL_L, CRR_L, HIL_{L-1}, DEV_{L+1}, GRI_{L-2}	0.540	0.498	0.35	H_0	1.12
		2	1908-2002	WLL_L, $HIL_{L-1,+2}$, $NCH_{L0,+2}$	0.516	0.472	0.25	H_0	1.40
		3	1831-2006	WLL_L, $NCH_{L-1,+2}$	0.443	0.420	0.32	H_0	1.00
		4	1809-2006	$NCH_{L0,-1,+2}$	0.324	0.297	0.16	H_0	1.00
PCnP	RW	1	1931-2004	DEV, GRI, $JCT_{0,+2}$, WLL_{+2}	0.550	0.494	0.08	H_0	2.41
		2	1909-2004	$HIL_{0,-1,-2}$, $WLL_{0,-1}$	0.511	0.450	0.04	H_0	2.27
		3	1843-2006	$WLL_{0,-1}$, CRR, $GRI_{-1,+1}$	0.492	0.428	0.07	H_0	1.18
		4	1770-2007	$CRR_{0,+1,-1}$	0.177	0.129	0.22	H_0	1.03
	EW	1	1960-2004	HIL, $CRR_{0,+2}$	0.392	0.350	0.02	H_0	1.24
		2	1940-2006	$CRR_{0,+2}$, KIL_{+1}	0.174	0.125	0.16	H_0	1.22
		3	1901-2008	$KIL_{0,-2}$	0.157	0.133	0.06	H_0	1.02
	LW	1	1932-2005	WLL, $HIL_{-1,-2}$, GRI, DEV_{-2}	0.680	0.640	0.28	H_0	2.20
		2	1909-2005	$WLL_{0,-1}$, $HIL_{-1,-2}$, GRI	0.641	0.596	0.23	H_0	2.07
		3	1841-2006	$WLL_{0,-1,-2}$, $GRI_{0,+1}$	0.599	0.549	0.21	H_0	1.12
		4	1833-2006	$WLL_{0,-1,-2}$	0.507	0.478	0.19	H_0	1.02
	MULTI	1	1932-2005	$WLL_{L0,-2}$, GRI_R, JCT_{R+2}, DEV_{L-2}	0.764	0.729	0.24	H_0	3.25
		2	1842-2006	$WLL_{L0,-1}$, CRR_R, $GRI_{R-1,+1}$	0.597	0.546	0.19	H_0	1.16
		3	1769-2007	$CRR_{R0,+1}$	0.168	0.144	0.16	H_0	1.00

DW: Durbin-Watson statistic: H_0 - no first order autocorrelation in residuals
*subscripts indicate forward (+) and negative (-) lags, and annual (R) and latewood (L) chronologies

Table 5.1 Water year reconstructions - calibration and verification statistics (continued).

Gauge	Model	Nest	Period	Predictors*	R^2	R^2_{adj}	RE	DW	VIF
Water year (October - September)									
LCnN	RW	1	1909-2006	$NCH_{0,-1,-2}$, VDV_{-2}, HIL_{-2}	0.542	0.494	0.33	H_0	1.50
		2	1889-2006	$NVH_{0,-1,+1,+2}$, SLF_{-2}	0.436	0.382	0.18	H_0	1.06
		3	1809-2007	$NCH_{0,-1,+1}$	0.403	0.376	0.21	H_0	1.02
	EW	1	1961-2004	$CRR_{+1,-1,-2}$, $HIL_{0,-1}$	0.324	0.249	0.03	H_0	1.47
		2	1941-2007	$CRR_{0,-1,+1}$	0.253	0.219	0.04	H_0	1.34
	LW	1	1898-2006	$NCH_{0,-1,+1}$, HIL_{+1}, VDV_{+2}	0.594	0.552	0.36	H_0	1.66
		2	1833-2006	$NCH_{0,-1,-2,+2}$, WLL_{-2}	0.522	0.475	0.29	H_0	1.47
		3	1809-2007	$NCH_{0,-1,+1}$	0.443	0.418	0.27	H_0	1.02
	MULTI	1	1898-2006	$NCH_{L0,-1}$, $SLF_{L+1,+2}$, KIL_{L+1}	0.571	0.523	0.29	H_0	1.72
		2	1833-2006	$NCH_{L0,-1,-2,+2}$, WLL_{L-2}	0.522	0.475	0.29	H_0	1.47
		3	1809-2007	$NCH_{L0,-1,+1}$	0.443	0.418	0.27	H_0	1.02
SRnS	RW	1	1931-2005	$GRI_{0,+1}$, VDV_{+2}, SLF_{+1}, DEV	0.396	0.359	0.14	H_0	1.23
		2	1889-2006	$GRI_{0,+1}$, VDV_{+2}, SLF_{+1}, NCH	0.388	0.353	0.16	H_0	1.28
		3	1841-2006	$GRI_{0,+1}$, $NCH_{-1,+2}$, CGT_{-1}	0.345	0.308	0.14	H_0	1.26
		4	1809-2006	$CGT_{0,+1,-1}$, $NCH_{-1,+2}$	0.317	0.279	0.12	H_0	1.31
		5	1726-2007	$CGT_{0,+1,-1}$	0.246	0.225	0.08	H_0	1.05
	EW	1	1961-2006	$HIL_{0,-1}$, CRR_{-2}	0.264	0.226	0.03	H_0	1.03
		2	1940-2006	$CRR_{0,+1}$, $KIL_{0,-2,+2}$	0.206	0.153	0.00	H_0	1.25
		3	1901-2008	$KIL_{0,-2}$	0.128	0.117	0.00	H_0	1.08
	LW	1	1930-2005	GRI_{+1}, WLL_{-1}, KIL, DEV, NCH_{+2}	0.406	0.370	0.19	H_0	1.27
		2	1840-2006	GRI_{+1}, $WLL_{0,-1}$, CGT, NCH_{+2}	0.405	0.370	0.18	H_0	1.22
		3	1809-2006	$NCH_{0,-1,+2}$, $CGT_{0,+1}$	0.361	0.325	0.17	H_0	1.38
		4	1726-2007	$CGT_{0,-1,+1}$	0.249	0.228	0.10	H_0	1.03
	MULTI	1	1940-2006	WLL_L, CGT_{R+2}, DEV_L, KIL_{L-1}, NCH_L	0.659	0.621	0.38	H_0	1.22
		2	1891-2006	$VDV_{L0,+2}$, CGT_{R+2}, NCH_L, GRI_{R+2}	0.415	0.375	0.02	H_0	3.49
		3	1841-2006	$GRI_{R0,+1}$, $NCH_{L0,-1,+2}$	0.382	0.346	0.20	H_0	1.34
		4	1809-2006	$NCH_{L0,-1,+2}$, $CGT_{R0,+1}$	0.348	0.312	0.16	H_0	1.40
		5	1726-2007	$CGT_{R0,-1,+1}$	0.246	0.225	0.08	H_0	1.05

DW: Durbin-Watson statistic: H_0 - no first order autocorrelation in residuals

*subscripts indicate forward (+) and negative (-) lags and annual (R) and latewood (L) chronologies

Table 5.1 Summer flow reconstructions - calibration and verification statistics (continued).

Gauge	Model	Nest	Period	Predictors*	R^2	R^2_{adj}	RE	DW	VIF
Summer (June - August)									
SRnWa	RW	1	1908-2007	$HIL_{0,-1}$, CRR_{+1}, WLL, CGT_{+2}	0.553	0.512	0.38	H_0	2.20
		2	1875-2007	CRR_{+1}, GRI, $WLL_{0,-1}$, BES_{-2}	0.527	0.486	0.36	H_0	1.16
		3	1841-2007	$CRR_{+1,-1}$, GRI, $WLL_{0,-1}$	0.511	0.468	0.32	H_0	1.15
		4	1806-2007	$CRR_{+1,-1}$, CGT, NCH_{+2}	0.393	0.342	0.15	H_0	2.36
		5	1770-2006	$CRR_{+1,-1}$, $CGT_{0,-2}$	0.381	0.329	0.17	H_0	2.48
		6	1726-2007	$CGT_{0,+1,-1}$	0.343	0.317	0.2	H_0	1.19
	EW	1	1961-2007	$HIL_{0,-1,+1,+2}$, CRR	0.368	0.298	0.14	H_0	1.17
		2	1940-2007	$GRI_{0,+1}$, CRR	0.176	0.144	0.07	H_0	1.26
	LW	1	1907-2007	HIL, $CRR_{+1,-2}$, VDV_{+2}, CGT	0.58	0.542	0.33	H_0	1.13
		2	1840-2007	WLL, $CRR_{0,+1}$, NCH_{-1}, CGT	0.56	0.521	0.35	H_0	2.18
		3	1809-2007	$CGT_{0,+1}$, $NCH_{0,-1,+2}$	0.393	0.342	0.15	H_0	1.57
		4	1726-2008	$CGT_{0,-1,+1}$	0.312	0.284	0.15	H_0	1.13
	MULTI	1	1907-2007	HIL_L, CRR_{L+1}, BES_{R+2}, VDV_{L-2}, WLL_{L+2}	0.584	0.546	0.32	H_0	1.30
		2	1840-2007	SLL_L, $CRR_{L0,+1}$, $NCH_{L-1,}$ CGT_L	0.56	0.521	0.35	H_0	2.18
		3	1809-2007	$CGT_{L0,+1}$, $NCH_{L0,-1,+2}$	0.393	0.342	0.15	H_0	1.57
		4	1726-2007	$CGT_{L0,-1,+1}$	0.312	0.284	0.15	H_0	1.13
PCnP	RW	1	1930-2007	DEV, CGT_{+2}, JCT_{+2}, WLL_{+2}, GRI	0.604	0.554	0.15	H_0	1.67
		2	1839-2007	$WLL_{0,-1}$, CGT_{+2}, GRI_{+2}	0.447	0.397	0.02	H_0	3.69
		3	1771-2007	$CRR_{0,-2}$, CGT_{+1}	0.166	0.117	0.02	H_0	1.08
		4	1725-2007	$CGT_{0,+2}$	0.125	0.1	0.01	H_0	1.02
	EW	1	1962-2004	$HIL_{0,-2}$	0.326	0.304	0.08	H_0	1.00
	LW	1	1909-2008	WLL, HIL_{-1-2}, GRI, SLF_{+2}	0.634	0.588	0.17	H_0	1.11
		2	1841-2008	$WLL_{0,-1}$, GRI, CGT_{+2}, NCH_{+2}	0.57	0.516	0.06	H_0	1.21
		3	1808-2007	CGT, NCH	0.163	0.139	0.06	H_0	1.00
		4	1725-2007	$CGT_{0,+1}$	0.136	0.111	0.02	H_0	1.01
	MULTI	1	1898-2007	$WLL_{L0.-1}$, CGT_{L+2}, GRI_{R-1}, KIL_{L+1}	0.674	0.626	0.02	H_0	1.16
		2	1832-2007	$WLL_{L0,-1}$, CGT_{L+2}	0.508	0.479	0.1	H_0	1.00
		3	1809-2007	CRR_R, $NCH_{L0,+2}$, CGT_{L+2}, NCH_{L-1}	0.268	0.176	0.02	H_0	1.39
		4	1769-2007	CRR_R, CGT_{L+1}	0.139	0.115	0.02	H_0	1.01
		5	1725-2007	$CGT_{L0,+1}$	0.136	0.111	0.02	H_0	1.01

DW: Durbin-Watson statistic: H_0 - no first order autocorrelation in residuals

*subscripts indicate forward (+) and negative (-) lags and annual (R) and latewood (L) chronologies

Table 5.1 Summer flow reconstructions - calibration and verification statistics (continued).

Gauge	Model	Nest	Period	Predictors*	R^2	R^2_{adj}	RE	DW	VIF
Summer (June - August)									
LCnN	RW	1	1898-2007	KIL_{+1}, BES, LMG_{-1}, CGT_{+2}	0.335	0.285	0.2	H_0	1.41
		2	1808-2007	$CRR_{+1,-1,-2}$, NCH, LMG_{-2}	0.206	0.13	0.02	H_0	1.24
		3	1771-2007	$CRR_{+1,-1,-2}$, LMG_{-2}, CGT_{-2}	0.207	0.131	0.07	H_0	2.10
		4	1725-2007	CGT_{+1}	0.08	0.08	0.02	H_0	1.00
	EW	1	1930-2008	BES	0.084	0.084	0.02	H_0	1.00
	LW	1	1932-2007	KIL_{+1}, $BES_{0,+1}$, CRR_{-2}, DEV_{-2}	0.366	0.301	0.2	H_0	1.25
		2	1898-2007	KIL_{+1}, $BES_{0,-1}$, VDV_{-2}	0.296	0.247	0.15	H_0	1.29
		3	1841-2007	$NCH_{0,-2}$, $CRR_{+1,-1}$	0.156	0.098	0.03	H_0	1.24
		4	1725-2008	CGT_{+1}	0.078	0.078	0.01	H_0	1.00
	MULTI	1	1898-2007	KIL_{L+1}, BES_R, LMG_{R-1}, CGT_{R+2}, VDV_{R-1}	0.375	0.311	0.21	H_0	1.42
		2	1808-2007	$CRR_{R+1,-1,-2}$, NCH_L, LMG_{R-2}	0.204	0.129	0.01	H_0	1.24
		3	1771-2007	$CRR_{R+1,-1,-2}$, LMG_{R-2}, CGT_{R-2}	0.207	0.131	0.07	H_0	2.10
		4	1725-2007	CGT_{R+1}	0.08	0.08	0.02	H_0	1.00
SRnS	RW	1	1929-2006	VDV, JCT_{+1}, BES_{+2}, CGT_{+1}, SLF_{+1}	0.452	0.418	0.24	H_0	1.52
		2	1840-2007	GRI_{+1}, $WLL_{-1,-2}$, CRR_{+2}, NCH	0.381	0.345	0.24	H_0	1.30
		3	1809-2007	CGT_{+1}, $CRR_{-1,+2}$, $NCH_{0,-1}$	0.279	0.239	0.11	H_0	1.32
		4	1770-2007	$CGT_{0,+1}$, $CRR_{-1,+2}$	0.224	0.191	0.1	H_0	1.12
		5	1725-2007	$CGT_{0,+1,+2}$	0.177	0.154	0.05	H_0	1.05
	EW	1	1960-2006	$WLL_{-1,+2}$, HIL, CGT_{+2}, KIL_{+2}	0.48	0.423	0.04	H_0	1.44
		2	1822-2007	$WLL_{0,-1,-2,}$ CGT_{+1}	0.254	0.221	0.01	H_0	1.30
		3	1899-2007	$CGT_{+1,+2}$, KIL	0.149	0.156	0.02	H_0	1.08
		4	1859-2007	$CGT_{+1,+2}$	0.113	0.101	0.01	H_0	1.01
	LW	1	1940-2007	GRI_{+1}, DEV, WLL_{-1}, SLF, VDV	0.446	0.413	0.29	H_0	2.10
		2	1891-2007	GRI_{+1}, WLL_{-1}, VDV, $BES_{+1,+2}$	0.425	0.392	0.25	H_0	1.52
		3	1840-2007	GRI_{+1}, $WLL_{0,-1,-2}$, CRR_{+2}	0.374	0.337	0.15	H_0	1.14
		4	1808-2007	$CGT_{0,+1}$, $NCH_{0,+2}$	0.217	0.185	0.07	H_0	1.36
		5	1725-2007	$CGT_{0,+1}$	0.162	0.151	0.07	H_0	1.02
	MULTI	1	1930-2007	VDV_R, JCT_{R+1}, DEV_L, SLF_{R+1}, HIL_{R-1}	0.505	0.47	0.33	H_0	1.53
		2	1891-2007	GRI_{L+1}, VDV_R, $BES_{R+1,+2}$, SLF_{R+1}	0.475	0.446	0.32	H_0	1.94
		3	1841-2007	$GRI_{L0,+1}$, $NCH_{L0,+2}$	0.27	0.239	0.14	H_0	1.31
		4	1808-2007	$CGT_{R0,+1}$, $NCH_{L0,+2}$	0.219	0.186	0.08	H_0	1.39
		5	1725-2007	$CGT_{R0,+1}$	0.164	0.152	0.07	H_0	1.02

DW: Durbin-Watson statistic: H_0 - no first order autocorrelation in residuals

*subscripts indicate forward (+) and negative (-) lags and annual (R) latewood (L) chronologies

statistic show that residuals from the models were uncorrelated (Draper and Smith 1981). In the verification period, reconstructions were significant and the positive values for the reduction of error (RE) statistic indicate that the models have significant predictive capabilities (Fritts 1976). All types of reconstructions were able to accurately model streamflow at each of the gauges, however in all cases, except for summer flow at SRnS, reconstructions comprised of earlywood chronologies as predictors, yielded significantly lower amounts of explained variance, when compared to models using ringwidth, latewood, or a combination of proxies. Reconstructions using earlywood as predictors also exhibited much lower RE values, indicating that their predictive capacity is much less suitable for such models of streamflow. In most cases (excluding water year flow at SRnWa and summer flow at SRnS), reconstructions comprised only of latewood chronologies were able to account for more explained variance than models using annual ringwidths as predictors. These results, in conjunction with chronology statistics listed previously in Table 3.2, indicate that latewood chronologies are quite comparable to annual ringwidths, and suggest that the amount of annual tree growth per year, is more a function of what is occurring later on in the growing season, without necessarily a dependence on early season growth promoting factors. Thus, when building models comprised of a combination of the best predictors (primarily annual, and latewood chronologies) at each station, the amount of explained variance increases substantially, as the models incorporate particularly optimal temporal response times of tree growth reflecting the same temporal events in streamflow variability.

The four types of reconstructions at each gauge (RW, EW, LW, and an optimal combination of proxies) are plotted over the calibration period for both water year and

summer streamflow (Figures 5.1 - 5.2). Calibration models capture well the interannual variability in streamflow, however, were generally better at capturing the magnitude of the low flows, and underestimated the high flows throughout the calibration periods (Vanstone and Sauchyn 2010). Underestimation of peak flows is a common feature of tree-ring reconstructions and, to some extent, occurs because there is a biological limit to the response of tree growth to high precipitation/low evapotranspiration during wet years (Fritts 1976); thus accounting for much of the unexplained variance.

5.1.2 Multi-proxy comparison:

All regressions were successful in reconstructing both WY and JJA flows, however models incorporating multiple proxies (combinations of annual, early- and or latewood widths), were able to account for more (~54% - 76% and ~38% - 67%) of the instrumental variance than annual ringwidth alone (~40% - 55% and ~34% - 60%; WY and JJA respectively), and had significant skill when subjected to cross validation (Axelson *et al.* 2009; Table 5.1). Based on these findings, reconstructions comprised of multi proxy predictors are thus used for the subsequent entirety of the analyses and discussion. The mean variance inflation factor (VIF) is below the critical threshold for reconstruction purposes (Haan 2002), suggesting that with the addition of each predictor into the regression models, multicollinearity is not an issue, and the models are considered valid. Models comprised of a combination of proxies were likely able to account for more variance because they incorporate periods of growth that were limited to specific durations throughout the year when moisture most influences growth (primarily late growing season), and did not just incorporate the cumulative annual growth that integrates moisture conditions throughout the year.

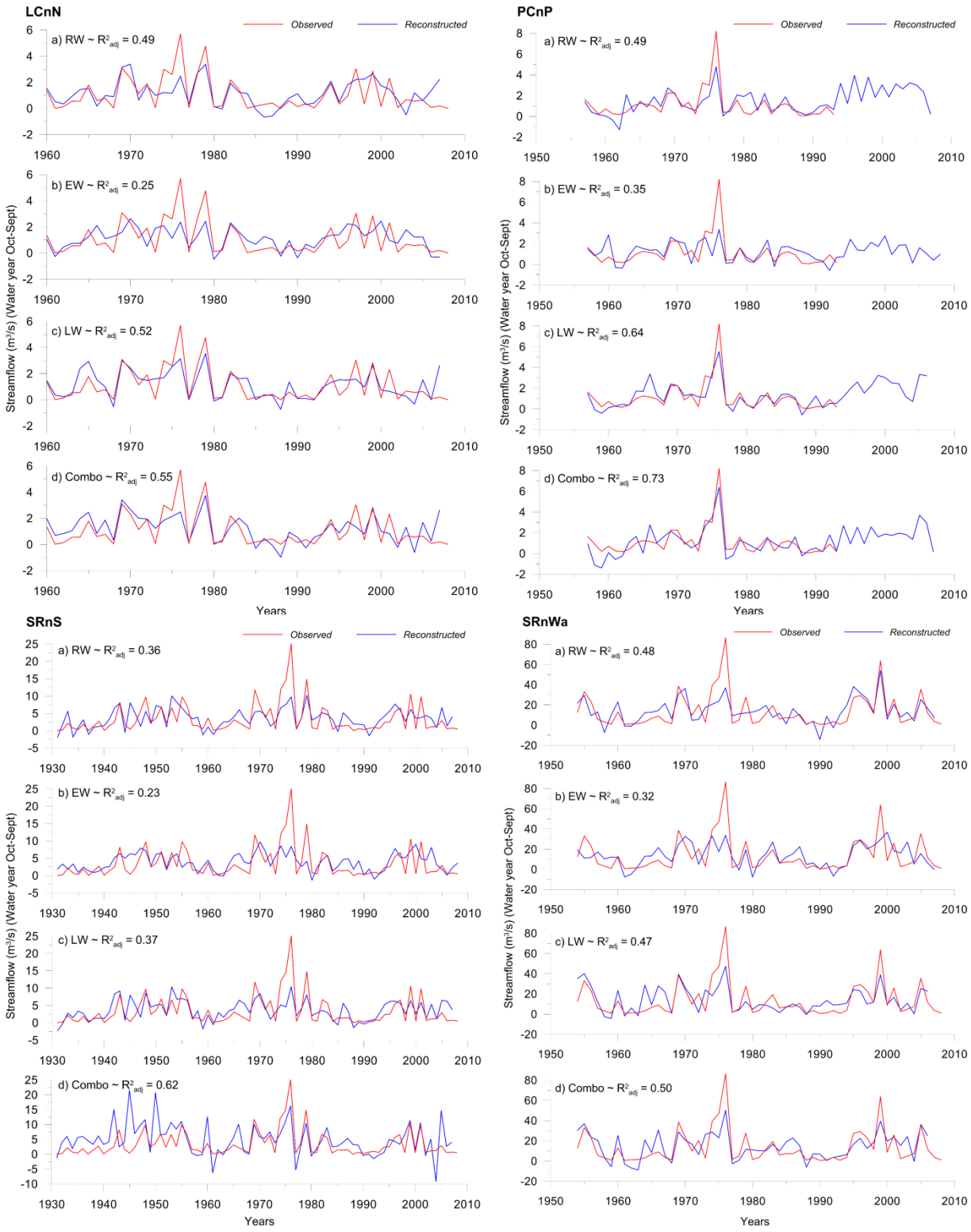

Figure 5.1 Observed and reconstructed water-year (October to September) streamflow for the calibration periods: LCnN 1960-2008; PCnP 1957-1993; SRnS 1931-2008; SRnWa 1954-2008.

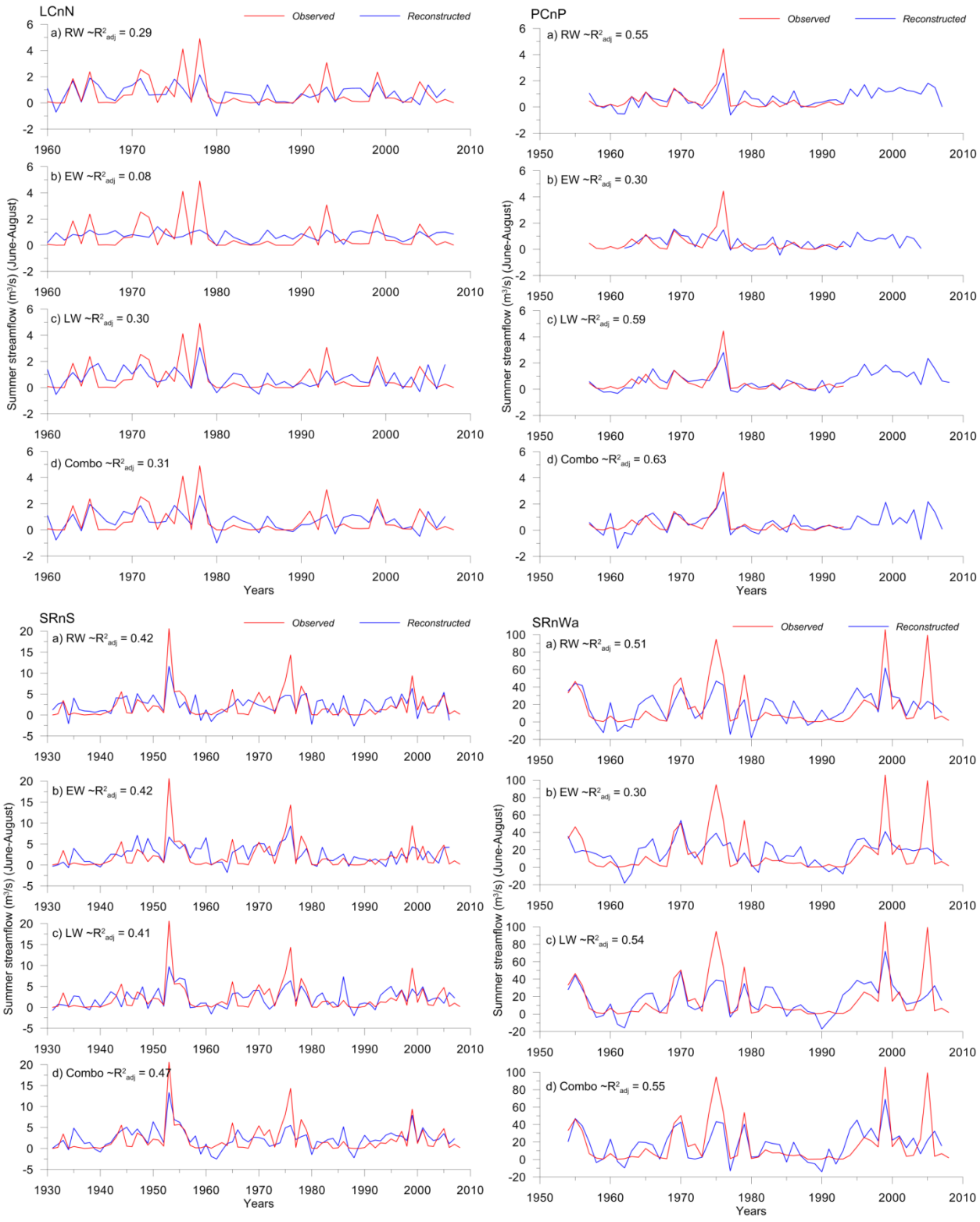

Figure 5.2 Observed and reconstructed summer (June to August) streamflow for the calibration periods: LCnN 1960-2008; PCnP 1957-1993; SRnS 1931-2008; SRnWa 1954-2008.

Comparative statistics between instrumental gauge flows and the full length reconstructions at each station are listed in Table 5.2. In all models, except reconstructed

Table 5.2 Comparison between reconstructed and instrumental descriptive statistics.

Site	Type[1]	Mean	Standard deviation	Minimum	Maximum	Range	N
LCnN	wy	1.100	1.305	0.000	5.698	5.698	49
	wy_rec	1.131	1.257	-3.026	4.672	7.698	199
	JJA	0.702	1.128	0.000	4.903	4.903	49
	JJA_rec	0.732	0.775	-1.367	2.840	4.207	283
PCnP	wy	1.103	1.432	0.049	8.183	8.134	37
	wy_rec	1.470	1.475	-2.004	7.691	9.695	239
	JJA	0.477	0.791	0.002	4.445	4.443	37
	JJA_rec	0.613	0.783	-1.724	3.578	5.301	283
SRnS	wy	3.444	4.375	0.018	25.062	25.044	78
	wy_rec	3.802	4.063	-9.207	21.548	30.755	282
	JJA	2.214	3.329	0.002	20.587	20.585	78
	JJA_rec	2.193	2.228	-4.034	13.325	17.359	283
SRnWa	wy	13.846	17.049	0.649	56.532	55.883	55
	wy_rec	14.935	15.848	-17.206	74.910	92.116	198
	JJA	17.605	25.352	0.226	105.730	105.504	55
	JJA_rec	17.008	20.082	-27.809	95.035	122.844	282

[1]: wy = water year flows (October - September); JJA = summer flows (June - August)

summer flows at SRnS and SRnWa, the mean is slightly higher than the period of observed flows, and for all instances, except reconstructed water year at PCnP, the standard deviations are lower than reported for the instrumental period. Reconstructions for both water year and summer streamflow exhibited lower minimum and maximum flows for the reconstructed flows (pre-instrumental) than the instrumental data, which reflects the conservative tendencies of regressions models (*i.e.* there is limited variance about the mean). Lower flows found during pre-instrumental times suggest more

extreme dry climate events, causing lower flows than experienced recently and recorded instrumentally.

Average water year and summer flow models are plotted for the full reconstruction periods as departures from the reconstructed mean, for each of the four streamflow gauges (Figures 5.3 - 5.4). Reconstruction lengths differ for each gauge, as well as for between average water year and summer flows, due to the predictors used in each reconstruction. Each gauge's potential predictors varied, based on correlation significance, which restricted the pool to specific index chronologies with a strong statistical relationship to the record of hydrologic variability, which were further limited in length via EPS cutoff dates for each chronology. Average water year reconstructions were able to extend streamflow records for a total of 197 years at gauges LCnN and SRnWa, 237 years at PCnP, and 280 years at SRnS. Reconstruction lengths for all average summer flow models cover a period of 280 years.

Reconstructions at all gauges show a clear inter-decadal variability in streamflow events amongst all gauges, while departures from mean flows further exemplify the models' abilities to accurately capture persistent flows above and below the mean, synchronously on a basin-wide scale.

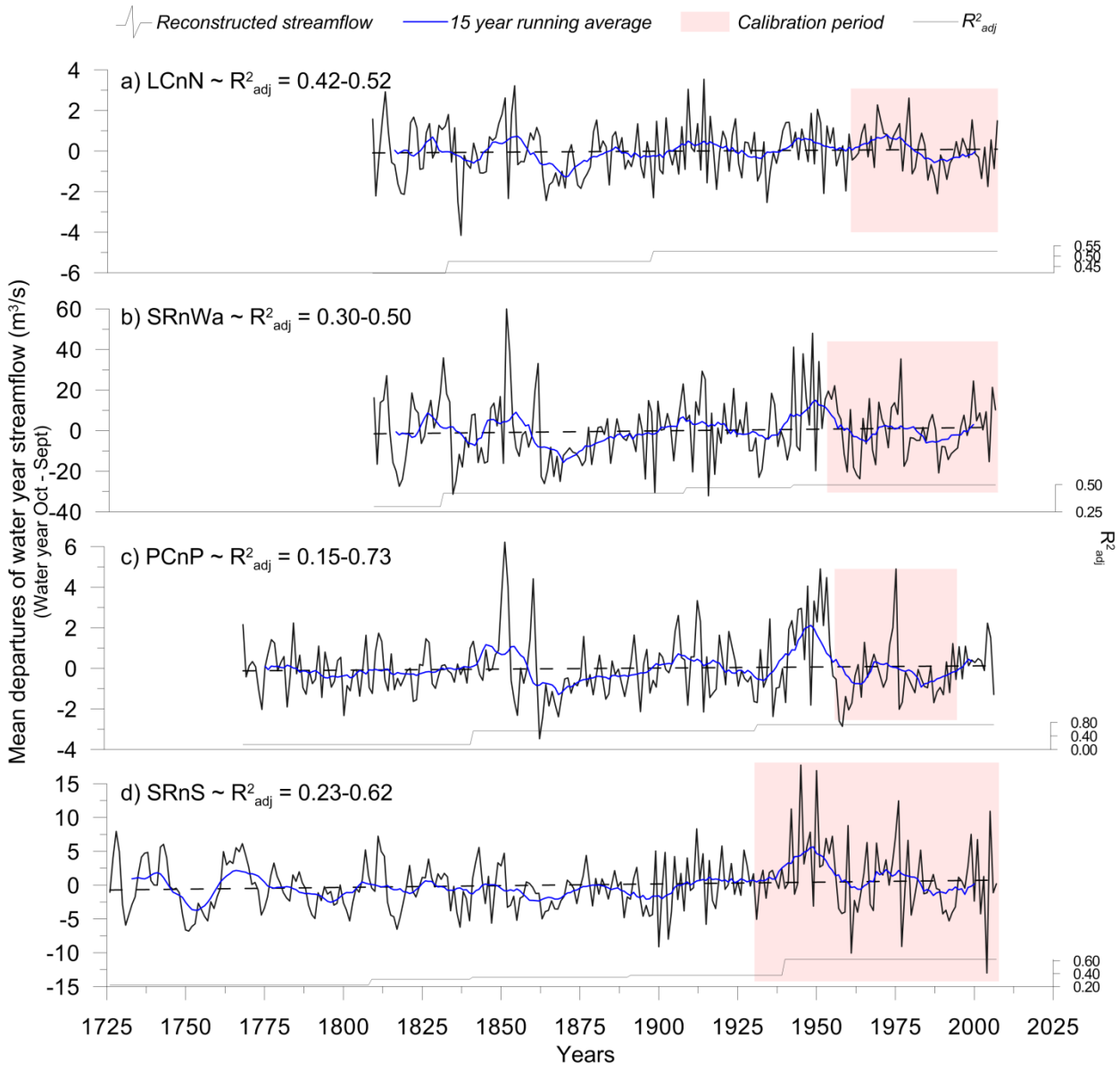

Figure 5.3 Full length multi-proxy reconstructions of water-year (October to September) flows of LCnN (1809-2007), SRnWa (1809-2006), PCnP (1769-2007), SRnS (1726-2007); the adjusted R^2 values for the entire length of the reconstruction are shown along the bottom of the plots, and 15 year running averages for each reconstruction is shown in blue.

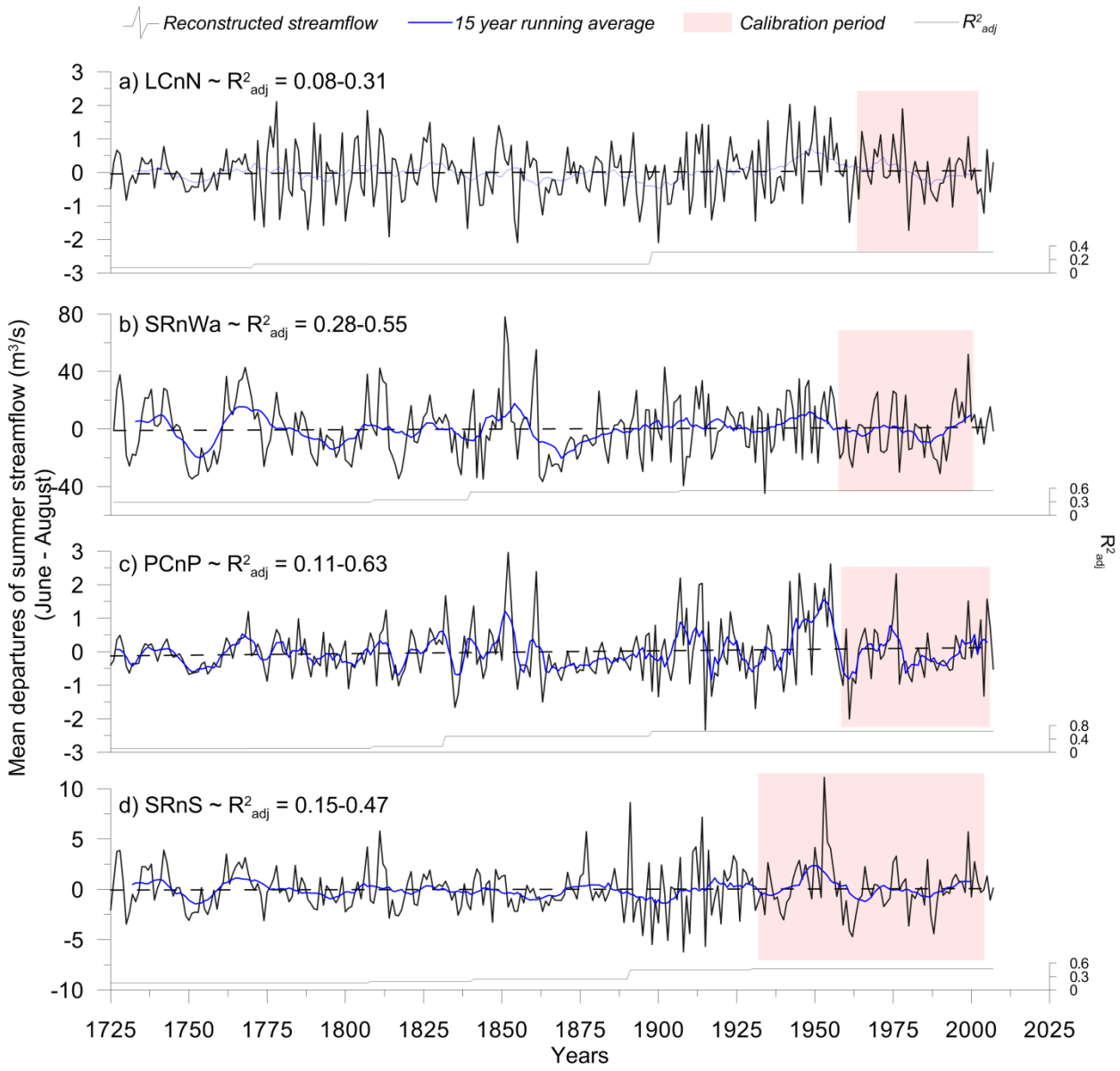

Figure 5.4 Full length multi-proxy reconstructions of summer (June to August) flows of LCnN (1725-2007), SRnWa (1726-2007), PCnP (1725-2007), SRnS (1725-2007); the adjusted R^2 values for the entire length of the reconstruction are shown along the bottom of the plots, and 15 year running averages for each reconstruction is shown in blue.

5.2 Post reconstruction analyses:

5.2.1 Sustained wet and dry years:

In order to examine the variability, magnitude and coherency of high and low flows throughout the Souris River Basin, hydrological extremes were quantified, and classified as above normal (wet) years in the 75th percentile, dry years in the lowest 25th percentile and severe drought in the lowest 10th percentile. This classification allowed for the identification of single, multi (more than two and less than five), and 'mega' (five or more consecutive years) droughts at each station for both water year and summer flow for the full length of each reconstruction (Tables 5.3 - 5.10). Low flow/drought events occurred in each century, with a majority in the 19th century. Figures 5.5 - 5.6 and Tables 5.3 - 5.10 indicate that reconstructions at each of the four gauges show similar agreement (±1 or 2 years) in the occurrence of the most extreme single year droughts, indicating a common coherent signal in timing of events throughout the basin. The top ten most severe droughts in each reconstruction were compared and similarities among gauges were identified. Figure 5.5 represents the synchrony of the most severe single year drought events at each gauge for average water year flows, showing that the late 1810s and mid 1830s experienced significant single year drought episodes, followed by a more sustained period of severe low flows in the 1860s, late 1890s to early 1900s, and again in the mid 1950s. Reconstructed summer flows yield similar results in the timing of severe drought events throughout the basin, however, Figure 5.6 shows that the most sustained period of reoccurring severe single year droughts was throughout a 24-year period from 1894 to 1917, common amongst all stations investigated within the Souris Basin.

Table 5.3 Hydrological droughts (<25th percentile) with severe droughts (<10th percentile) indicated in bold, for water-year flows at LCnN (1809-2007).

Single year	More than 2 and less than 5 years	5 or more consecutive years
1810, 1840, **1852**, 1884,	1817, 1818, **1819**, 1820	1863, **1864**, 1865, 1866, 1867
1889, 1891, **1898**	1824, 1825	1868, 1869, 1870
	1836, 1837	
	1843, 1844, 1845	1874, 1875, 1876, 1877, 1878
	1894, 1895	
1906, 1908, 1913, 1915,	1900, 1901	
1918, 1922, 1926, **1952**,	1931, 1932	
1956, 1959, 1968, 1977,	**1934**, 1935	
1985, 1991,	1987, **1988**	
2002, 2004, 2006		

Table 5.4 Hydrological droughts (<25th percentile) with severe droughts (<10th percentile) indicated in bold, for water-year flows at PCnP (1769-2007).

Single year	More than 2 and less than 5 years	5 or more consecutive years
1783, 1794, 1997,	1774, 1775	
	1788, 1789	
1806, 1815, 1817, 1819,	**1801**, 1802, 1803	1866, 1867, 1868, **1869**, 1870
1830, 1873, 1875, 1878,	1809, 1810	
1880, 1890, **1895**, 1898	1823, 1824	
	1855, **1856**	
	1863, 1864	
	1884, 1885	
1900, 1910, **1915**, 1922,	1917, 1918, 1919	**1958**, **1959**, 1960, 1961, 1962
1926, 1934, 1941, 1949,	1931, 1932	
1965, 1972, 1993,	**1937**, 1938, 1939	
	1977, 1978	
	1981, 1982	
	1985, 1986	
	1988, 1989, 1990, 1991	
2003		

Table 5.5 Hydrological droughts (<25th percentile) with severe droughts (<10th percentile) indicated in bold, for water-year flows at SRnS (1726-2007).

Single year	**More than 2 and less than 5 years**	**5 or more consecutive years**
1783, 1792,	1730, 1731, 1732, 1733 1774, 1775 1789, 1790, 1791 1797, 1798	1749, **1750, 1751, 1752**, 1753, 1754, 1755, 1756, 1757, 1758, 1759
1834, 1840, 1845, 1847, 1855, 1874, 1879, 1889,	1800, 1801, 1802, 1803 1836, **1837** 1852, 1853 1895, 1896, 1897, 1898	1814, 1815, 1816, **1817**, 1818, 1819 1863, 1864, 1865, 1866, 1867, 1868, 1869
1900, 1906, 1908, 1915, 1931, 1949, **1977**, 1980,	**1903**, 1904 1917, 1918 1957, 1958, 1959 **1961**, 1962, 1963 1967, 1968	1990, 1991, 1992, 1993, 1994
2000, 2002, **2004**		

Table 5.6 Hydrological droughts (<25th percentile) with severe droughts (<10th percentile) indicated in bold, for water-year flows at SRnWa (1809-2006).

Single year	**More than 2 and less than 5 years**	**5 or more consecutive years**
1810, 1842, 1850, 1855, 1878, 1884, 1892, **1895**, **1898,**	**1834, 1835**, 1836, 1837 1844, 1845 1862, **1863**, 1864	1815, 1816, **1817, 1818**, 1819 1866, 1867, **1868**, 1869, 1870, 1871, 1872, 1873, 1874, 1875, 1876
1904, 1910, **1915**, 1917, 1940, 1943, 1949, 1988,	1928, 1929 1931, 1932 1958, 1959 1961, 1962, **1963** 1967, 1968 1977, 1978 1991, 1992, 1993, 1994	
2004		

Table 5.7 Hydrological droughts (<25th percentile) with severe droughts (<10th percentile) indicated in bold, for summer flows at LCnN (1725-2007).

Single year	**More than 2 and less than 5 years**	**5 or more consecutive years**
1725, 1730, 1739, 1759, **1793**, 1797	1755, 1756 1773, **1774** 1779, 1780 1782, 1783 1786, 1787, **1788**, 1789	1749, 1750, 1751, 1752, 1753
1809, **1814, 1839,** 1847, 1883	1800, 1801 1805, 1806 1818, 1819 1828, 1829 1843, 1844 1854, **1855** 1862, 1863, 1864, 1865 1868, 1869 1877, 1878 1889, 1890 1893, **1894**, 1895	
1908, 1915, 1921, 1931, 1934, 1940, 1946, 1952, 1964, **1980**, 1985, 1994,	**1900**, 1901 1903, 1904 1910, 1911 1917, 1918 1936, 1937 **1961**, 1962 1987, 1988, 1989	
2006	2002, 2003, 2004	

Table 5.8 Hydrological droughts (<25th percentile) with severe droughts (<10th percentile) indicated in bold, for summer flows at PCnP (1725-2007).

Single year	**More than 2 and less than 5 years**	**5 or more consecutive years**
1725, 1783, 1789, 1792, 1794, 1797,	1730, 1731 1756, 1757 1759, 1760 1774, 1775	1749, 1750, 1751, 1752, 1753
1801, 1803, 1810, 1815, 1824, 1866, 1872, 1891, 1895, 1898	1817, 1818, 1819 1834, **1835**, **1836** 1844, 1845 1855, 1856 1858, 1859 **1863**, 1864 1868, 1869, 1870 1874, 1875, 1876 1878, 1879, 1880 1884, 1885	
1900, 1915, 1926, 1928, **1931**, 1937, 1944, 1949, 1968, 1978, 1985, 1989,	1903, 1904 **1917**, 1918, 1919 **1940**, 1941 1958, 1960 **1961**, 1962, 1963 1980, 1981 1993, 1994	
2004, 2007		

Table 5.9 Hydrological droughts (<25th percentile) with severe droughts (<10th percentile) indicated in bold, for summer flows at SRnS (1725-2007).

Single year	**More than 2 and less than 5 years**	**5 or more consecutive years**
1725, 1733, 1739, 1759, 1774, 1782, 1793, 1797	1730, 1731 1755, 1756 ,1757 1789, 1790, 1791	1749, 1750, 1751, 1752 ,1753
1834, 1844, 1847, 1852, 1857, 1879, 1883, 1889, **1898**,	1800, 1801, 1802 1808, 1809 1822, 1823 1836, 1837 1839, 1840 1854, 1855 1863, 1864, 1865 1867, 1868, 1869 1892, 1893 **1895**, 1896	1814, 1815, 1816, 1817, 1818
1900, **1903, 1908, 1910, 1915**, 1917, 1920, 1926, 1934, **1980**, 1986,	1931, 1932 1939, 1940, 1941 1972, 1973 1987, **1988**, 1989	1959, 1960, **1961, 1962**, 1963
2006		

Table 5.10 Hydrological droughts (<25th percentile) with severe droughts (<10th percentile) indicated in bold, for summer flows at SRnWa (1726-2007).

Single year	**More than 2 and less than 5 years**	**5 or more consecutive years**
1783, 1793	1730, 1731, 1732, 1733 1774, 1775 1789, 1790, 1791 1797, 1798	1749, **1750, 1751, 1752**, 1753 1755, 1756, 1757, 1758, 1759, 1760
1805, 1834, **1842, 1844,** 1855, 1884, 1890, 1898,	1800, 1801, 1802 1836, 1837 1874, 1875 1894, 1895	1814, 1815, 1816, **1817**, 1818, 1819
1904, 1931, **1934**, 1936, 1944, 1946, 1949, 1951, 1967, 1977, 1985, 1992	**1908**, 1909, 1910 1917, 1918 1958, 1959 1961, 1962 1971, 1972, 1973 1980, 1981 1988, 1989, 1990	**1862, 1863**, 1864, 1865, 1866, 1867, 1868, 1869, 1870

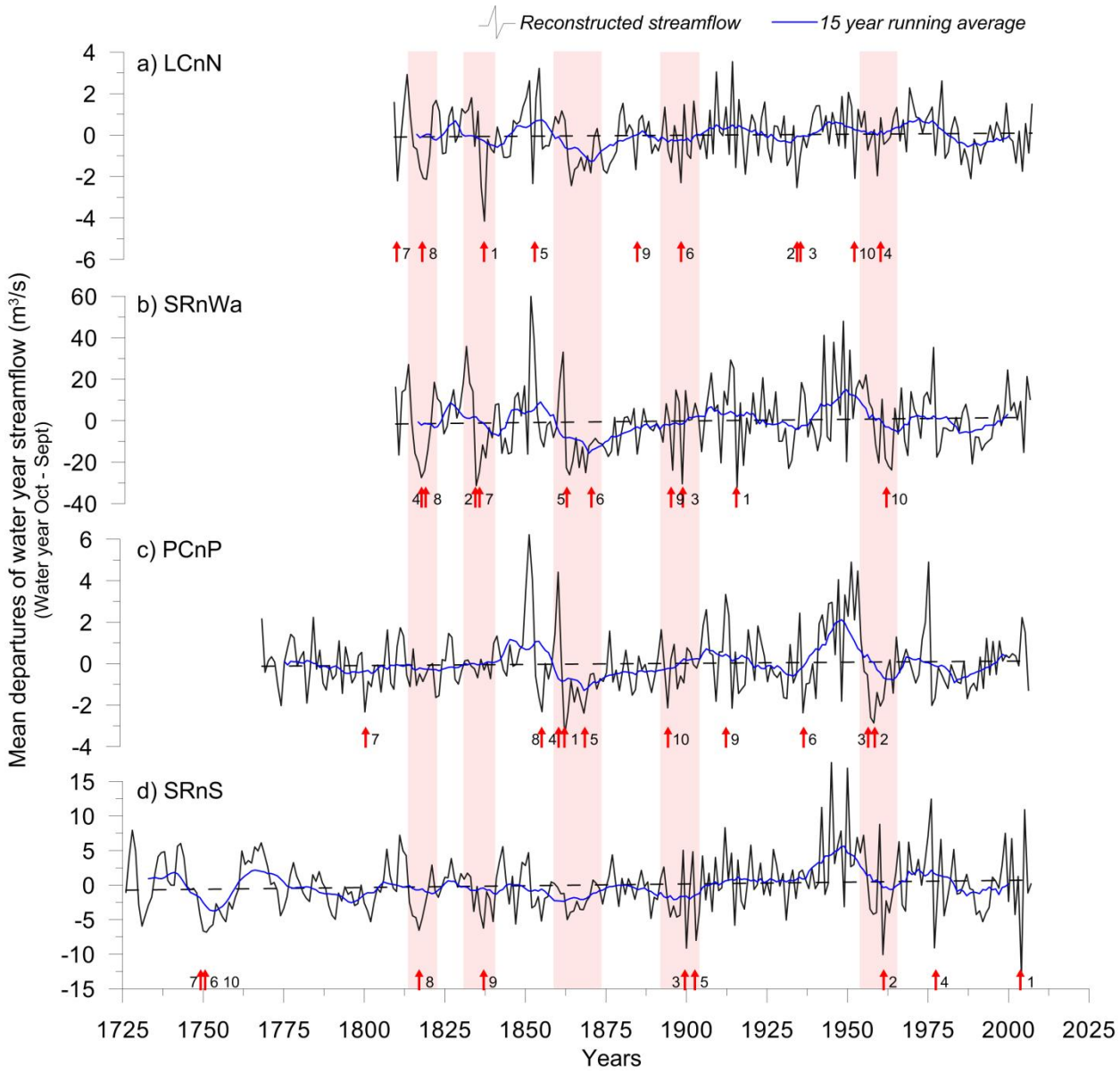

Figure 5.5 Top 10 most severe drought years identified for water-year streamflow reconstructions. Red bars indicate periods of commonality between gauges. Arrows and numbers depict severe single year droughts and their respective ranking.

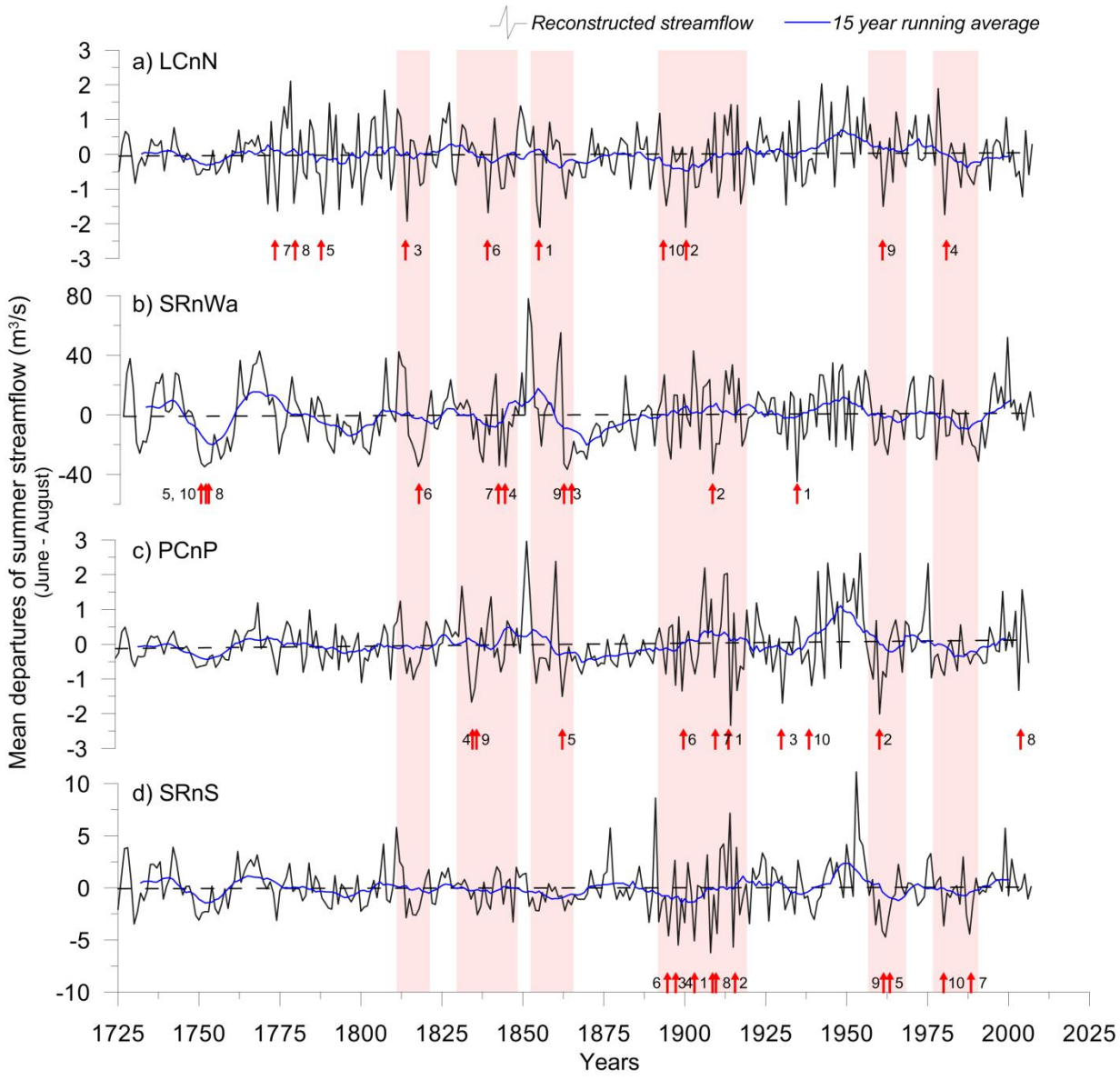

Figure 5.6 Top 10 most severe drought years identified for summer streamflow reconstructions. Red bars indicate periods of commonality between gauges. Arrows and numbers depict severe single year droughts and their respective ranking.

Drought synchrony across large geographical areas is interesting, not only in terms of hydroclimatic variability, but it also serves to validate droughts identified for particular locales, as well as for providing periods or markers in time that can be linked to large atmospheric scale forcings of abnormal or significantly above/below normal

deviations from average conditions (*i.e.* streamflow, precipitation, temperature, etc.). When compared to other paleoproxy records of past climate variability, intervals of persistent low flows identified in streamflow reconstructions, generally correspond to independently specified periods of prolonged drought (Gedalof *et al.* 2004). Figures 5.7 - 5.8 visually depict reconstructions for average water year and summer flows, respectively, highlighting significantly wet or dry years (75^{th} and 25^{th} percentiles).

The reconstructions indicate that the mid 20^{th} century was a time of prolonged wet conditions, with some of the most sustained high flows on record (Figures 5.7 - 5.8). Also apparent is the 'dirty 30s', one of the worst drought periods in memory in western North America. During the most recent part of the records, in the late 1950s to early 1960s, and the late 1970s to the 1990s, streamflow fluctuated from above and below normal flows, staying primarily below normals, including the major droughts of 1961 and 1988, as well as the early 2000s. "During 1961 (the worst single year drought on the Prairies, with approximately 50% of normal growing season precipitation), total net farm income dropped by 48% ($300 million) from the previous year" (Bonsal *et al.* 1999, 191). The drought of 1988 had many impacts on the agricultural sectors of Canada "(with emphasis on Manitoba and Saskatchewan), including wind erosion, production, grain quality, inventories, marketing, livestock, incomes, farm management, global production and prices" (Wheaton *et al.* 1992, 192). The sparse snow cover and high spring temperatures resulted in little or no spring runoff from prairie watersheds in 1988, such that the mean volume was 60 to 70% of normal volume. The lack of precipitation caused an agricultural output decrease of 12% resulting in a direct production loss of $1.8 billion in 1981 dollars (Wheaton *et al.,* 1992). The drought of 2001 "resulted in an economic

shortfall of $4 billion or more and required supportive measures from various governments. Grain yield data reveal a similar shortfall in total yields during 1961 and 1977, both also being severe drought years" (Khandekar 2004, 12).

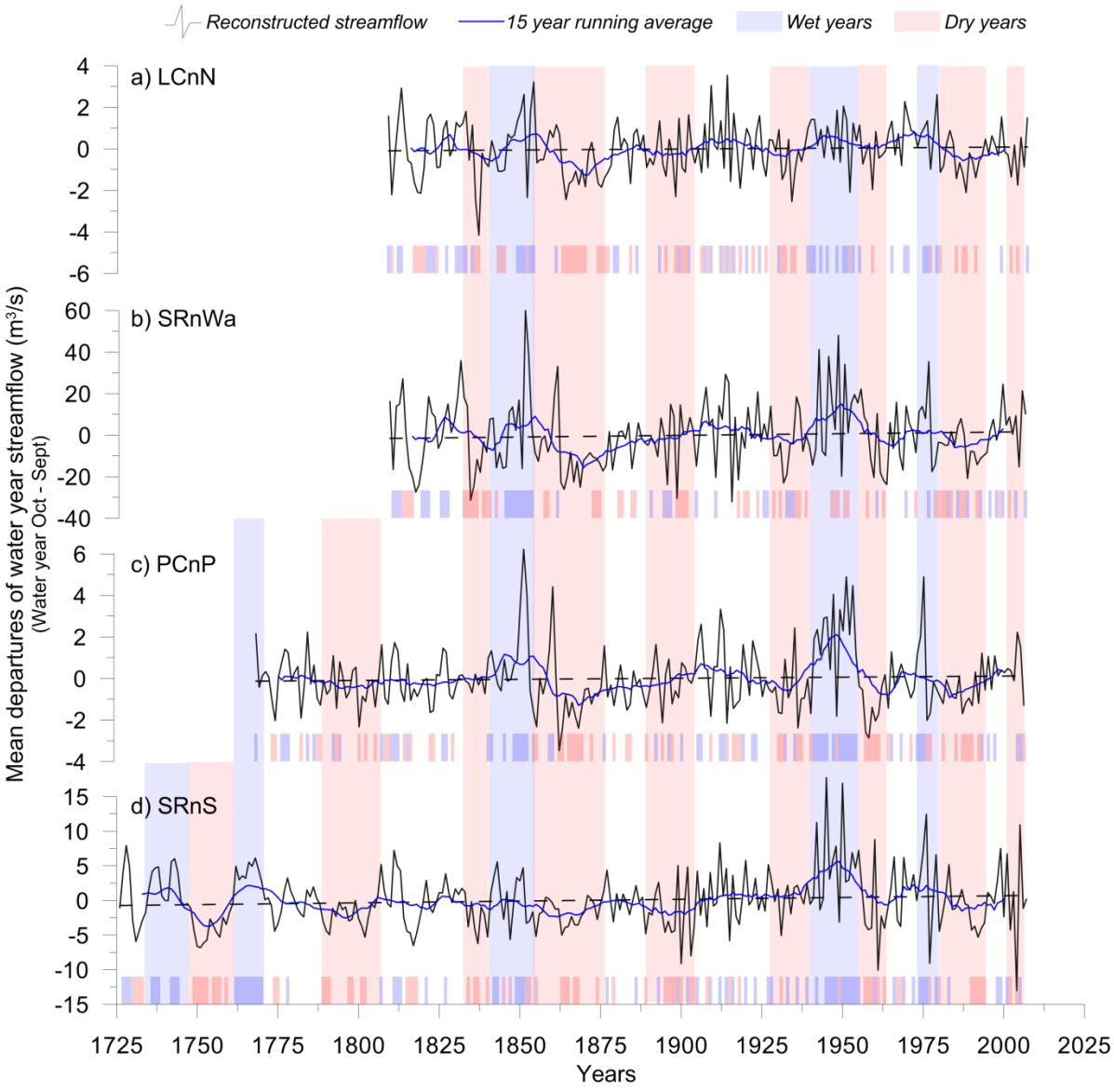

Figure 5.7 Sustained wet and dry intervals for the water-year streamflow reconstructions for the Souris River Basin. Red bars and shading represent low flows in the 25th percentile, while blue bars and shading represent high flows (75th percentile). Reconstructions are smoothed with a 15-year running average (blue line).

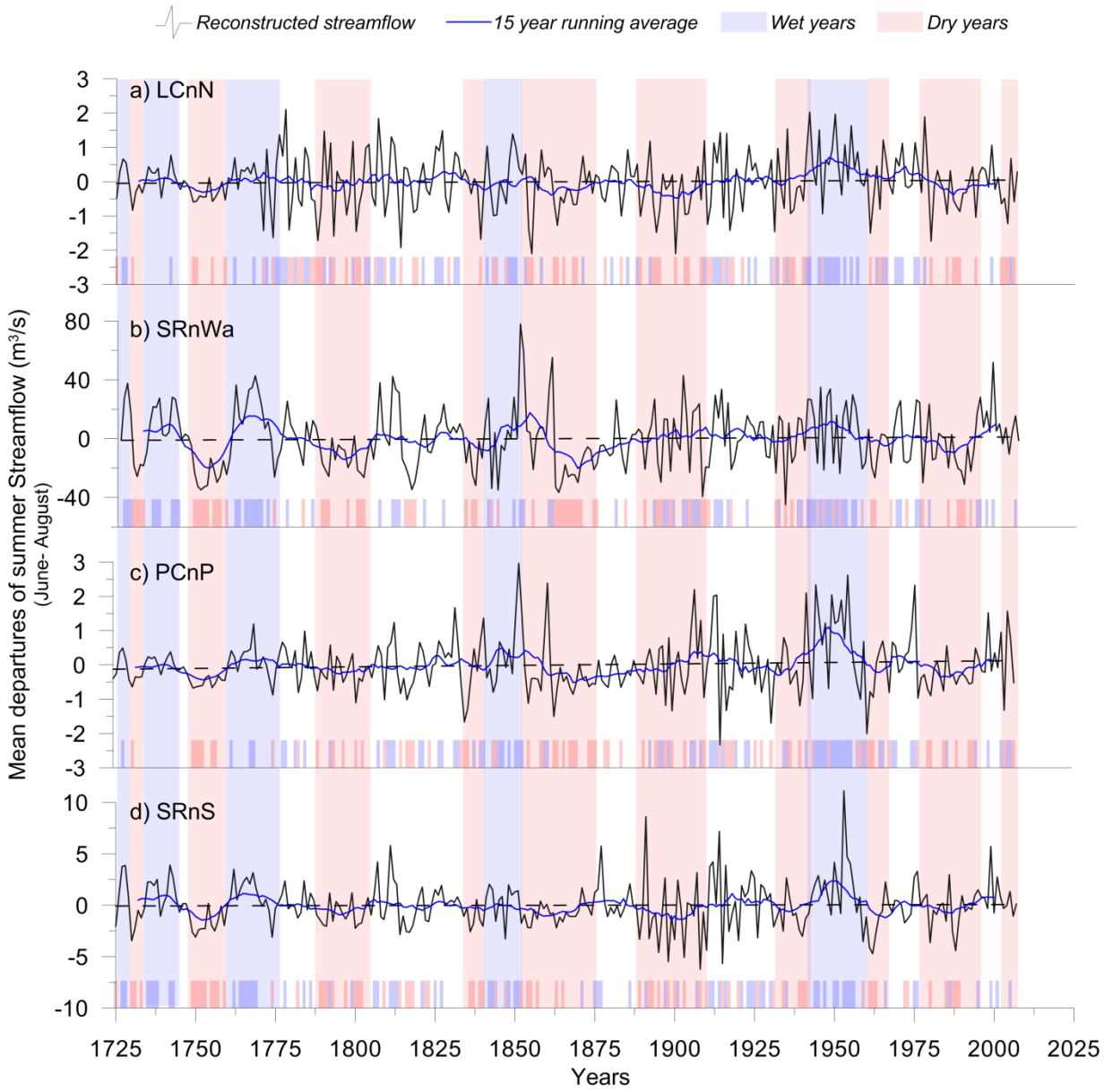

Figure 5.8 Sustained wet and dry intervals for the summer streamflow reconstructions for the Souris River Basin. Red bars and shading represent low flows in the 25th percentile, while blue bars and shading represent high flows (75th percentile). Reconstructions are smoothed with a 15-year running average (blue line).

Droughts of the last century were of lesser magnitude and were shorter in duration as compared to some of the multi or 'mega-droughts' earlier in the record. Stahle and Dean (2011) state that compared to the past 500 years, dendroclimatically speaking, the twentieth century was unusually wet, regardless of the devastating episodes like those of

the 'Dust Bowl' (1930s and 1940s) and the late 1950s to 60s (Figures 5.7 - 5.8), also noted in tree-ring drought investigations by Stahle and Cleaveland (1988) and Meko *et al.* (1995), and by D'Arrigo and Jacoby (1991) when examining winter precipitation abnormalities in northwestern New Mexico. The nineteenth century was drier, and was punctuated by several prolonged droughts that were known to have significant socioeconomic and environmental impacts, magnified in part by human activities (Stahle and Dean 2011). Figures 5.7 - 5.8 depict a number of significant and sustained periods of low flows, while multiple sources of proxy data, including tree-ring reconstructions and historical records and accounts, work together to confirm the occurrence of several nineteenth-century droughts (Woodhouse and Overpeck 1998).

Just prior to the twentieth century, the Souris Basin appears to have experienced significant low flows during the late 1880s through the 1890s. During this time, widespread drought was occurring throughout much of the central and northern Great Plains, and was thought to have been most severe over the Dakotas and the Canadian Prairies (Stahle and Dean 2011). Although not as apparent in reconstructed water year flows, reconstructed summer flows depict a period of extreme low flows year after year, with some of the most extreme years on record (Figures 5.7 - 5.8). "The drought, which began in 1886, 'was a slow starvation for water, and it lasted through 1887, 1888, 1889, into the eighteen-nineties. What began in 1886 was a full decade of drouth, the cyclic drying-out that [John Wesley] Powell had warned of in 1878' (Stegner 1954, p. 296)" (Stahle and Dean 2011, p. 309). Amplifying the effects of this significant dry period were the extreme blizzards of 1886, which resulted in the 'Great Die-Up' of range cattle across the Great Plains. The drought of the 1880s and 1890s was part of a recurring

pattern of surplus and deficit moisture on the Great Plains that contributed to the waxing and waning of non-irrigated farms in the uplands (Stahle and Dean 2011).

One of the most sustained periods of drought is depicted in both reconstructed water year and summer streamflow for the Souris Basin (Figures 5.7 - 5.8) during the mid 19th century, and is documented as being the most intense and long-lasting tree-ring reconstructed drought that occurred with very little relief from 1841 through 1865 (Hardman and Reil 1936; Fritts 1965, 1983; Stockton and Meko 1975, 1983; Stahle *et al.* 1985; Stahle and Cleaveland 1988; Haston and Michaelsen 1997; Stahle and Dean 2011). "The centre and intensity of the mid-nineteenth-century drought shifted over time and was interrupted by a few wet years (e.g. Woodhouse *et al.* 2002), but the western United States, Canada, and the borderlands of northern Mexico are estimated to have averaged incipient drought or worse for the entire 25-year period. This multidecadal drought appears to have been most extreme over the central Great Plains, where an 'environmental crisis' described by West (1995) afflicted the Arapaho and Cheyenne Indians and interacted with their newly adopted horse culture and with the stock animals of the Euroamerican overlanders to degrade critical riparian habitat and lead to the extirpation of the bison from the central High Plains" (Stahle and Dean 2011, p. 309).

During the late 18th and early into the 19th century, the Souris Basin again experienced below normal flows over a period of approximately 20 years. Although interspersed with a few years of increased flows, two significant periods of low flows were identified during this twenty-year span: 1) during the late 1790s into the early 1800s, with 1797 and 1800-1803 being the driest years, and 2) around 1787, lasting for approximately three to four years. Tree ring reconstructions of precipitation in the Great

Plains (Stockton and Meko 1983) and June PDSI for the state of Texas (Stahle and Cleaveland 1988) also describe coincident drought episodes for the early 1800s and 1790s, as well as for the late 1780s. Fritts' extensive tree-ring chronology investigation of climatic change in western North America (1965) also indicates below average dry conditions during 1786 - 1805 in the Pacific Northwest, including the northern Rocky Mountains. "'El Año del Hambre', the year of hunger, was identified by Stahle and Dean (2011) and described by Gibson (1964) as the 'most disastrous single event in colonial maize agriculture' in Mexico; it occurred in 1786 after the August frost of 1785 in highland Mexico during the severe 3-year drought of 1785-1787 (Therrell 2005). Gridded PDSI reconstructions indicate moderate drought (or worse) for this 3-year average extended from central Mexico into Texas. [During this time] some 300,000 people are reported to have perished in the famine and epidemic disease that followed the frost, drought, and crop failures (Florescano 1980; Garcia Acosta 1995)" (p.311).

For the Souris Basin, the 1750s was also a period of prolonged and widespread drought documented for Western North America, by many other sources of climatic investigations (Woodhouse and Overpeck 1998). During the early 1750s dry conditions began to develop for southern California, and the northern Rockies, and by 1756, through to 1765, the entire Pacific Coast was deemed as having very dry conditions with limited moisture and warm temperatures (Fritts 1965). Reconstructed PDSI (Cook *et al.* 1999) representing variability within the Columbia River Basin also specify the late 1750s as a period of dry conditions stated to exist along western North America. These conditions extended into central North America, also affecting the Great Plains region (Fritts 1965), as can be seen in Figures 5.7 - 5.8, where severe low flows are exhibited for a period of

almost 12 successive years beginning in the early 1750s to early 1760s. Comparisons to the study by Stockton and Meko (1983) independently verify this period of drought in the USA Great Plains. Severe droughts were clustered around the late 1750s (Laird *et al.* 1998) extending as far south as southern Oklahoma and southwestern Arkansas. Therrell (2005) also documented the impact of drought during this time period, in the severe and sustained decrease in maize yield in central Mexico. Although the absolute severity of drought in the 1750s varies from location to location, much of North America was drought stricken, resulting in decrease or lack of precipitation, streamflow discharge, economic yields and increased temperatures.

5.2.2 Spectral analyses:

Possible cause and duration of droughts at interdecadal to multidecadal time scales may be associated with modes of variability in the ocean-atmospheric climate system. Several external and internal forcings influence temperature, precipitation, and/or streamflow over regions of North America (Fye *et al.* 2006), including the Pacific Decadal Oscillation (Mantau *et al.* 1997), the North Atlantic Oscillation (Hurrel 1995; Jones 1999), and the El Niño/Southern Oscillation (Trenberth 1997). If an ocean-atmospheric mode of variability can be associated with patterns of drought and wetness, it may be the basis for modeling drought/pluvial episodes and their duration over North America (Fye *et al.* 2006).

Spectral analyses (SSA-MTM and wavelet) were applied to the reconstructed average water-year and summer flows for the Souris River Basin. Results of the MTM analyses (Figure 5.9) show highly significant components of variability at interannual (2-6 years), interdecadal (7-11 years), and multidecadal (20-30 years) time scales. Singular

spectrum analysis was used to separate the significant oscillation modes detected by the MTM analysis and to quantify the explained variance for each oscillation and for each reconstruction: ~30% - ~58% and ~38% - ~59% of the total variance for average water year and summer streamflow reconstructions, respectively (Table 5.11). SSA results for both reconstructions indicate that average water-year flow in the Souris Basin is influenced by both low (~25 year) and high (~2-6 year) frequency oscillations. Lower frequencies account for 19.6% while the sums of the high frequency modes account for up to 31.9% of the variance. When examining summer streamflow, discharge in the Souris Basin is dominated by the high frequency 2-6 year mode oscillation, explaining 19.0% to 44.1% of the variance. Unlike average water-year flows, the second most influential oscillation mode is not found in the multidecadal frequency band, but is within the ~7-11 year interdecadal mode, accounting for 8.6 - 16.4% of the variance in summer flows within the basin.

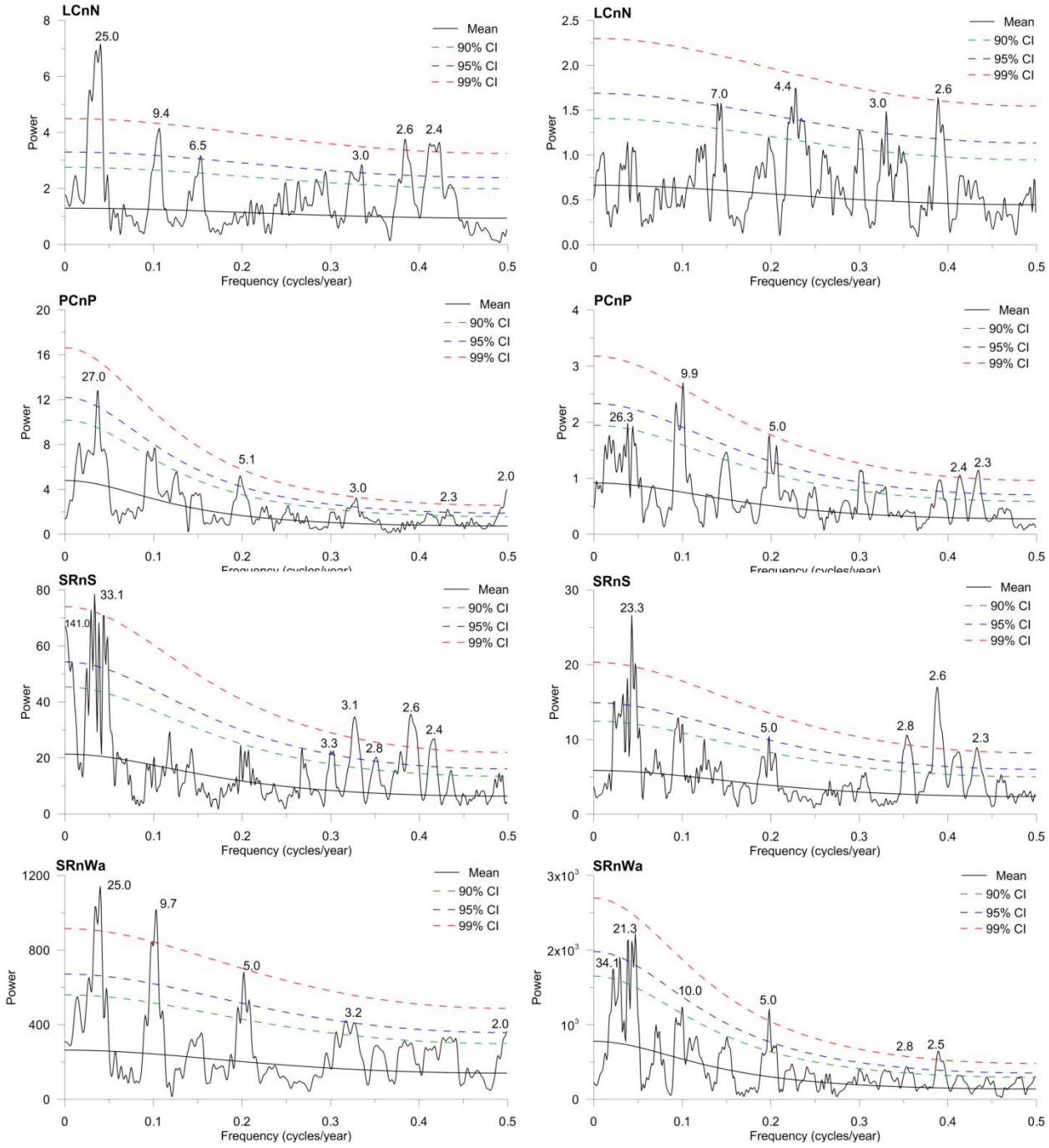

Figure 5.9 Results of the single-spectrum MTM analyses for both reconstructions of water-year (left) and summer (right) flows. Significant spectral peaks and the years they occur, are labeled.

Table 5.11 Amount of variance explained by significant spectral peaks in both water-year (top) and summer (bottom) streamflow reconstructions.

		100+	~30	~25	~9	~5	~4-2	Total explained
LCnN	WY			25.0	9.4	6.5	3.0 - 2.4	
	% variance			**15.9**	**10.6**	**31.9**		**58.35**
PCnP	WY			27.0		5.1	3.0 - 2.0	
	% variance			**19.6**		**11.2**		**30.75**
SRnS	WY	141.0	33.1				3.3 - 2.4	
	% variance	**7.3**	**18.3**				**14.1**	**39.76**
SRnWa	WY			25.0	9.7	5.0	3.2 - 2.0	
	% variance			**19.4**	**13.9**	**20.1**		**53.42**

		100+	~30	~25	~9	~5	~4-2	Total explained
LCnN	JJA				7.0		4.4 - 2.6	
	% variance				**8.6**		**44.1**	**52.77**
PCnP	JJA			26.3	9.9	5.0	2.4 - 2.3	
	% variance			**6.4**	**12.3**	**19.5**		**38.20**
SRnS	JJA			23.3		5.0	2.8 - 2.3	
	% variance			**16.4**		**27.6**		**43.94**
SRnWa	JJA		34.1	21.3	10.0	5.0	2.8 - 2.5	
	% variance		**10.9**	**11.6**	**17.5**	**19.0**		**58.96**

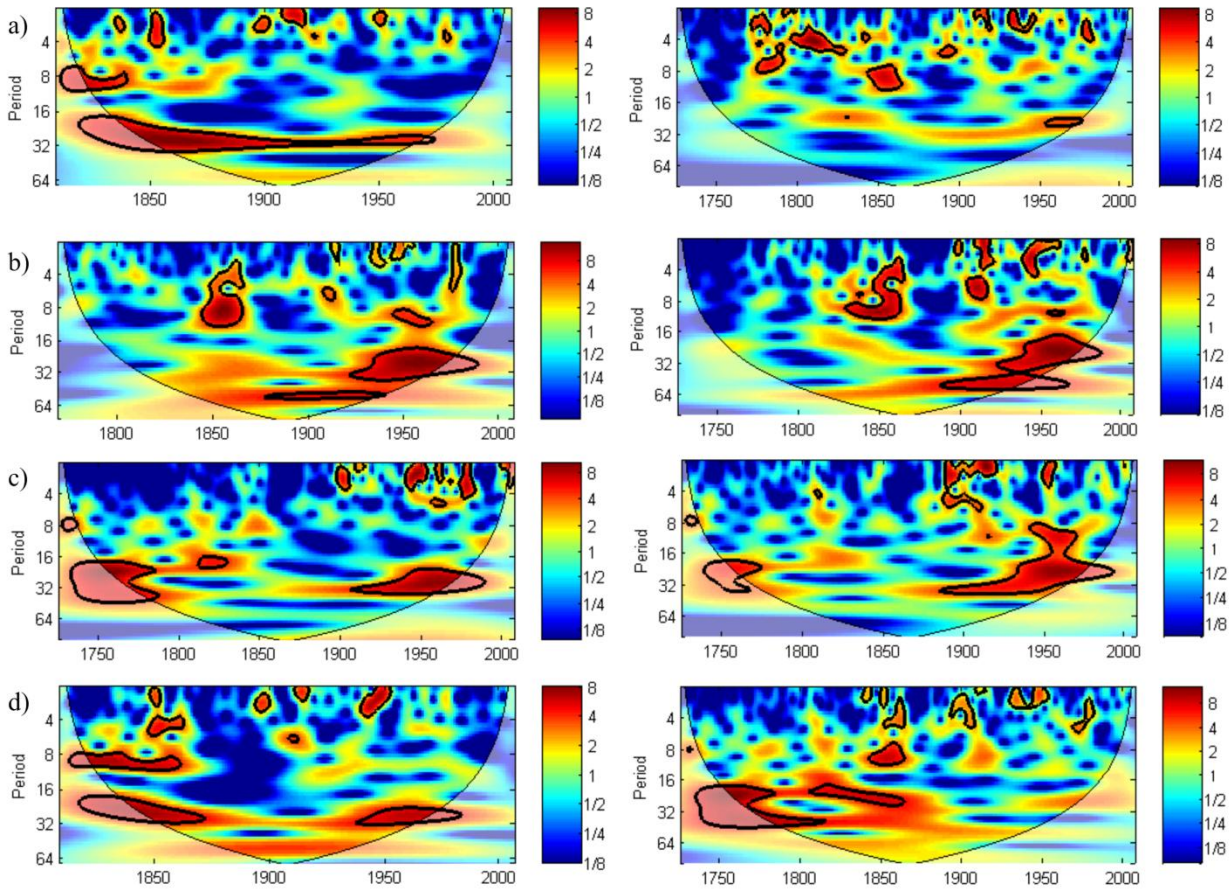

Figure 5.10 Wavelet power spectrums for water-year (left) and summer (right) flow reconstructions. Gauges are noted as: a) LcnN, b)PCnP, c)SRnS, and d) SRnWa. The thick black contour in the wavelet spectrum indicates significance at the 95% level.

The wavelet power spectrum mirrors the results of the MTM analysis, but includes the additional context of the time and frequency domain (Figure 5.10; Axelson *et al.* 2009). Spectral analyses show that when annual ring widths are the only predictors, much of the lower frequency oscillations are masked and not significant (results not shown). Therefore, the ability of the multi-proxy reconstructions, for both water-year and summer streamflow, to fully capture both the high and low frequency forcings, demonstrates the importance of incorporating responses of tree growth to climatic variability at sub-annual time scales, such as that recorded in both the EW and LW

widths, suggesting that there is a temporal dependence in response to different drivers at different frequencies of occurrence.

In multi-proxy reconstructions of both average water year and summer streamflow, a strong multidecadal (~20 - ~30 years) component is evident in the wavelet spectrum during much of the mid to late 18th, and 20th centuries, corresponding to periods of sustained drought identified in the present reconstructions, as well as by others noted previously. The 20 - 30 year frequency band has been associated with sea surface temperature (SST) forcing, such as the PDO (Mantua *et al.* 1997; Minobe 1997), where shifts in oscillation patterns, 'warm' or 'cool' phases (defined by ocean temperature anomalies in the northeast and tropical Pacific Ocean), are marked by widespread variations in Pacific Basin and North American climate. There is above average temperatures and below average precipitation in the interior Pacific Northwest and Great Lakes regions during positive or 'warm' phases, with reversed climate anomaly patterns during a negative or 'cool' phase. PDO-related temperature and precipitation patterns have been strongly linked to regional snow pack and stream flow anomalies, especially in western North America (Cayan 1995; Mantua *et al*. 1997; Bitz and Battisti 1999; Nigam *et al.*1999).

Interdecadal oscillations (~7 - ~11 years) are also found in both average water year and summer streamflow reconstructions most notably during the mid to late 1850s and sporadically around the early 1900s and late 1950s to 1970s. Connections between solar activity and climate are based on the regular eleven-year Schwabe cycle (Lean 1991; Lean *et al.* 1995; Lean and Rind 1996; Waple 1999; Oh *et al*. 2003). Maxima and minima in solar activity approximately every 11 years (Lean 1991) has been linked to

temperature variations (Struiver *et al.*1997), atmospheric dust loading (Ram *et al.* 1997) and possible bidecadal drought rhythms in the southwest USA (Cook *et al.* 1997). Similar spectral signatures have been documented by Jones *et al.* (1997) when investigating patterns of the NAO from Gibraltar and south-west Iceland. Fye *et al.* (2006) noted that the winter NAO index (1781 - 2002) has significant spectral properties at this same 7 - 8 year decadal frequency and is coherent with summer PDSI across a broad sector of the central U.S. with drought prevailing during negative extremes, and wetness during positive extremes of the NAO. Hurrell (1995) documented significant interdecadal variability in the winter NAO index, showing a positive trend from around 1900 - 1916 and again from 1919 until the 1930s, and shifts to negative phases dominating the circulation from the late 1930s to the winter of 1978-79 (Perry 2000).

Significant interannual climate variability found within the 2-6 year band, usually related to the El Niño-Southern Oscillation (ENSO; Shabbar and Skinner 2004; Gobena and Gan 2006) band, is evident throughout much of the entire length of both water-year and summer streamflow reconstructions, however, is concentrated most heavily from the early 1900s to the present date.

Discrepancies in the occurrence of low-frequency oscillations and their lack of occurrence in *all* stations may be an indication of the limitation that are due to short instrumental records on which the reconstructions are based on, or the possibility that atmospheric oscillations may have a spatially localized effect within the basin. In order to determine if drivers of hydroclimatic variability are spatially localized, affecting regions of the basin differently, both spatially and temporally, further investigation is required.

5.2.3 Linking streamflow and oscillatory indices

To associate plausible drivers of streamflow variability, modes at significant frequencies were extracted from both water-year and summer streamflow reconstructions and correlated with oscillations associated with sea surface temperature forcings, specifically ENSO, NAO, PDO, and also with solar irradiance variation related to sunspot cycles (Tables 5.12 - 5.13). Significant correlations ($p \leq 0.05$) suggest that much of the high frequency (2-6 year band) can be associated with ENSO forcings, causing much of the interannual variability, seen in both average water-year and summer streamflow reconstructions (Shabbar and Skinner 2004; Gobena and Gan 2006). While both reconstructions showed significant correlations between low frequency oscillations (20-30 year band) and the PDO index; it is strongest for summer (JJA) flow, perhaps indicating the influence of the PDO on the amount of seasonal precipitation affecting peak summer flows within the basin (Gedalof and Smith 2001; Gray *et al.* 2003; Axelson *et al.* 2009). As seen from the SSA analyses, a significant interdecadal (7-11 year band) variability also exists with summer flows, however, unlike previously thought, this relationship was not significantly correlated with the NAO index, but rather with solar sunspot cycles (Lean 1991; Lean *et al.* 1995).

Links between climate indices and the Souris River Basin's hydroclimatology were further examined by computing cross-wavelet transforms (XWT) and wavelet transform coherence (WTC) between extracted significant frequencies from both water-year and summer streamflow reconstructions at each gauge, and the climate indices (ENSO, sunspot data, and PDO).

The XWT of reconstructed water-year and summer flows with ENSO is shown in Figure 5.11. Common spectral features that were noted from the individual wavelet transforms within the ~2-6 year band (Figure 5.10) stand out as being significant at the 5% level (Grinsted *et al.* 2004). Cross-wavelet transforms of water-year flows and ENSO show significant, but sporadic, common power in the ~2-6 year band predominantly during the 1870s - 80s, and again from 1950 to the early 2000s. Analyses of summer flows, however, show more sustained periods of common power within the ~2-6 year band, for much of the entire timeframe delimited by the cone of influence

Table 5.12 Results of correlation analyses between significant spectral peaks in water-year flows and atmospheric teleconnections. Significant correlations ($p<0.05$) are indicated in red.

WY	LCnN			PCnP		SRnS			SRnWa		
Oscillation	24yr	9yr	6,2yr	24yr	6,4yr	141yr	27yr	3,2yr	24yr	9yr	4-2yr
Sunspot	-0.082	-0.022	-0.046	0.003	-0.014	0.222	0.009	0.026	-0.032	-0.169	0.009
ENSO	-0.047	-0.084	-0.149	-0.070	-0.104	-0.033	-0.141	0.026	-0.066	-0.178	-0.151
NAO	-0.027	-0.016	-0.002	0.047	-0.120	0.144	0.008	-0.087	0.050	-0.162	-0.068
PDO	-0.254	-0.074	-0.051	-0.259	-0.167	-0.218	-0.268	-0.086	-0.243	0.066	-0.099

Table 5.13 Results of correlation analyses between significant spectral peaks in summer flows and atmospheric teleconnections. Significant correlations ($p<0.05$) are indicated in red.

JJA	LCnN		PCnP			SRnS			SRnWa			
Oscillation	7yr	6-2yr	26yr	9yr	5,3,2yr	23yr	10yr	5,2yr	34yr	21yr	10yr	5,2yr
Sunspot	-0.047	-0.017	-0.014	-0.209	-0.001	0.018	-0.282	-0.029	0.000	-0.030	-0.206	0.041
ENSO	0.016	0.029	-0.100	-0.215	-0.169	-0.128	-0.011	-0.164	-0.040	-0.040	-0.029	-0.150
NAO	0.036	-0.100	0.041	0.028	-0.003	0.029	0.025	0.022	0.040	-0.038	-0.024	-0.034
PDO	-0.051	-0.085	-0.306	0.011	-0.117	-0.336	0.068	-0.135	-0.244	-0.215	0.129	0.019

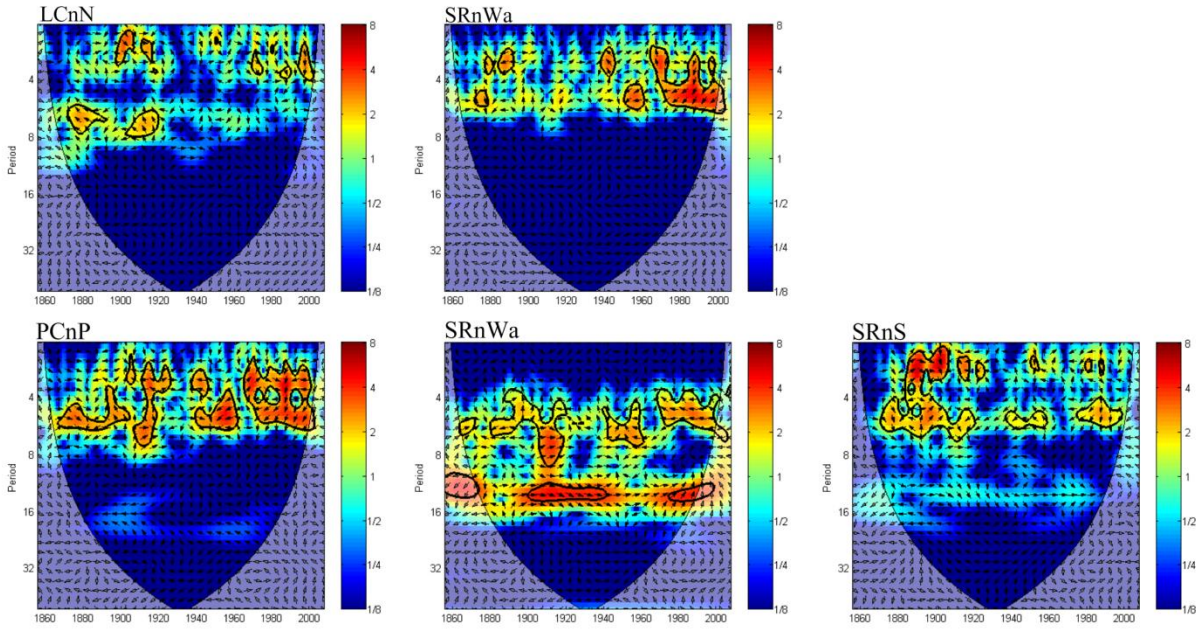

Figure 5.11 Cross-wavelet transform of water-year (top) and summer (bottom) streamflow and ENSO time series. The 5% significance level against red noise is shown as a thick contour. The relative phase relationship is shown as arrows.

(COI), most notably during the 1870s to 1920s, 1940 to 1960, and as well as from the late 1960s to the early 2000s.

Investigations at the interdecadal timescale indicate a distinct zone of common power between summer flows and sunspot data, along the ~7-11 year band throughout much of the entire COI (Figure 5.12). Periods where common power is most significant, where spectral bands appear to be thicker, cover more of the entire ~7-11 year mode (~1825-1875, early 1900s, and ~1940s to late 1990s), and are distinguishable from periods where the banding narrows, and common power is not as strong (early 1800s, late 1800s to early 1900s).

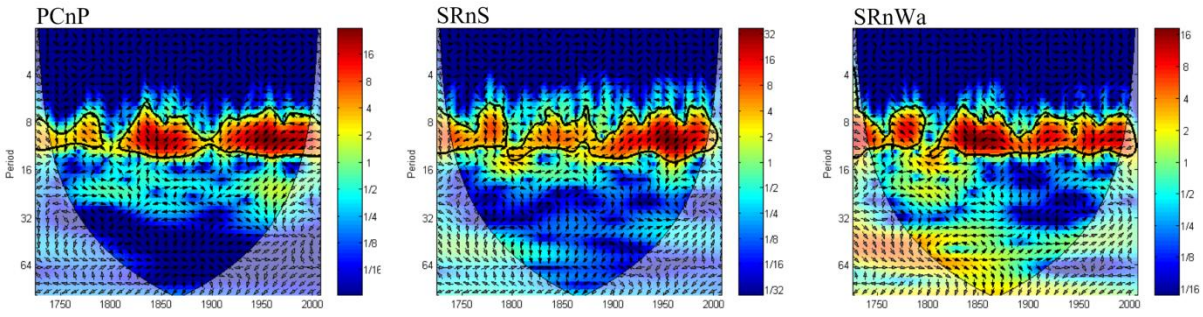

Figure 5.12 Cross-wavelet transform of summer streamflow and sunspot time series. The 5% significance level against red noise is shown as a thick contour. The relative phase relationship is shown as arrows.

Cross-wavelet transform analyses of reconstructions with the PDO indices indicate that for all significantly correlated gauges, high common power exists at the low frequency oscillation mode (~20-30 year band; Figure 5.13) from the 1930s to the early 1980s. Although correlation analyses signified a stronger relationship between summer flows and the PDO indices, it is difficult to ascertain whether water-year or summer flows exhibit higher significant power with PDO oscillations, strictly based on XWT alone, therefore the need for WTC analyses.

WTC was used to identify both frequency bands and time intervals within which streamflow reconstructions and climate indices are covarying (Torrence and Webster 1999). Significant coherence is shown in each run of the WTC analysis, where contours enclose statistically significant periods ($p \leq 0.05$), based on a red-noise process as determined by a Monte Carlo experiment (Jevrejeva *et al.* 2003).

Water year and summer flows show common coherence with the ENSO index (Figure 5.14) in the 2 and 4-6 year bands, most predominantly in the late 1970s to very early 2000s. While water-year reconstructions seem to be most coherent with ENSO in the 2-4 year band, summer flows show significance more so in the 4-6 year band, with

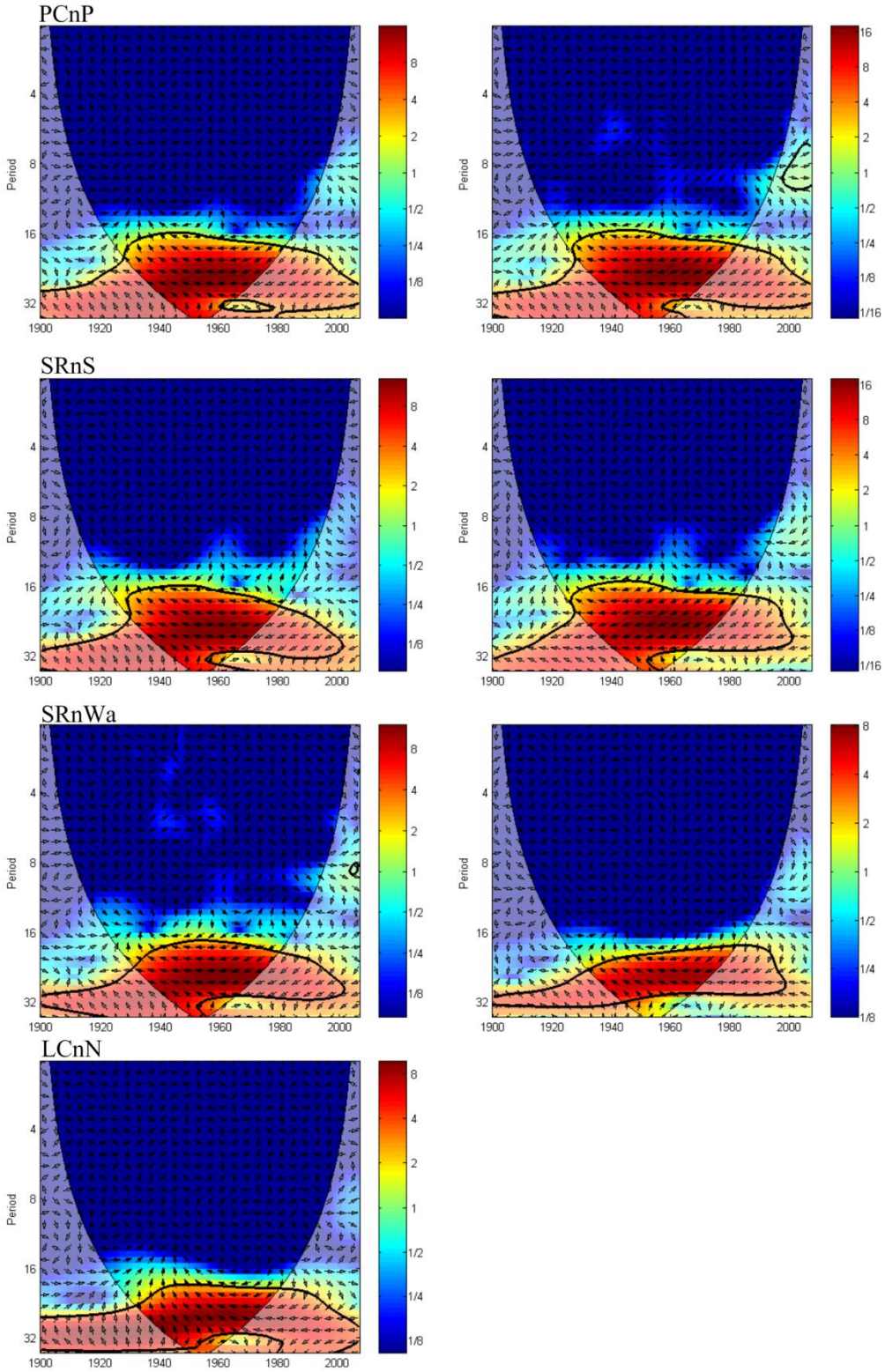

Figure 5.13 Cross-wavelet transform of water-year (left) and summer (right) streamflow and PDO time series. The 5% significance level against red noise is shown as a thick contour. The relative phase relationship is shown as arrows.

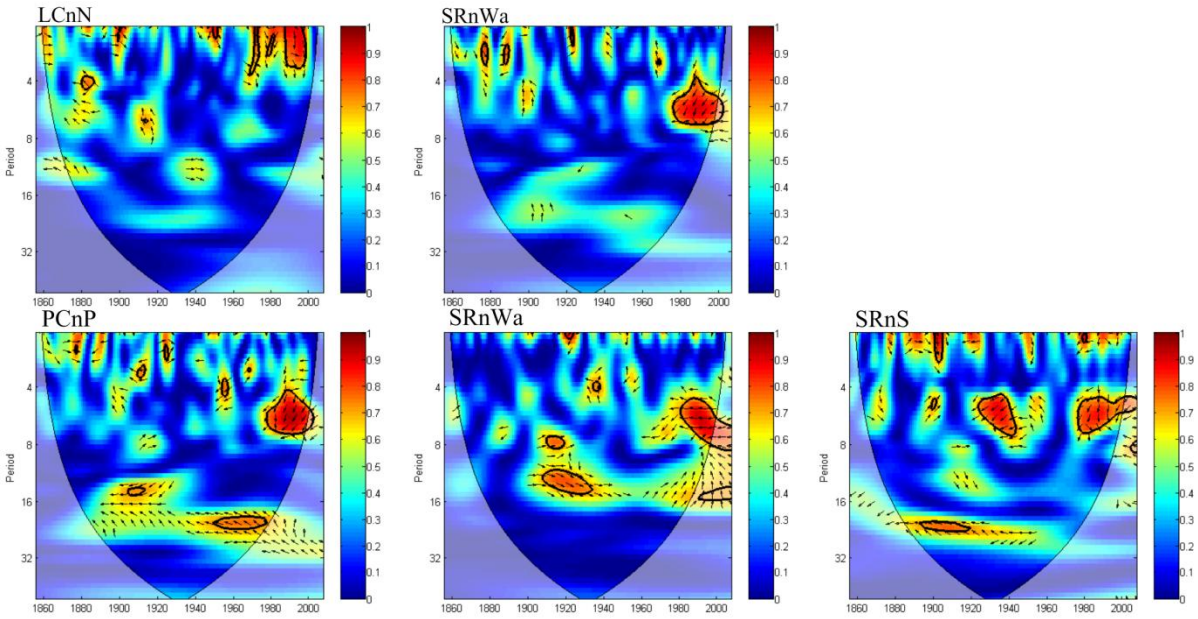

Figure 5.14 Wavelet coherence between water-year (top) and summer (bottom) streamflow and ENSO. The contours indicate a 95% confidence level. The vectors show the phase difference between the two signals where phase difference is shown for coherence greater than 0.5.

additional periods of covariance during the 1890s and the 1930s to 1940s, similar to results of high common power found with the XWT analyses, and also with investigations of streamflow and the Niño-3 index in Southern Alberta (Gobena and Gan 2009).

Much like XWT analyses at interdecadal timescales, WTC results in significant coherence between reconstructed summer flows and solar sunspot data in the 7-11 year band (Figure 5.15). As suggested by the XWT, the WTC analyses show a strong coherence between reconstructed summer flows and sunspot data in the late 1770s to 1790s, 1825 to 1875, and from the early 1900s to the late 1990s. Oh *et al*. (2003) had similar findings during these time periods (specifically 1825-1875 and the mid to late 1900s), for temperature reconstructions (Jones *et al.* 1998; Mann *et al.* 1998; Briffa *et al.*

2001) thought to be influenced by solar variability, whereby increased amplitudes in solar variability were congruent with increased surface temperatures.

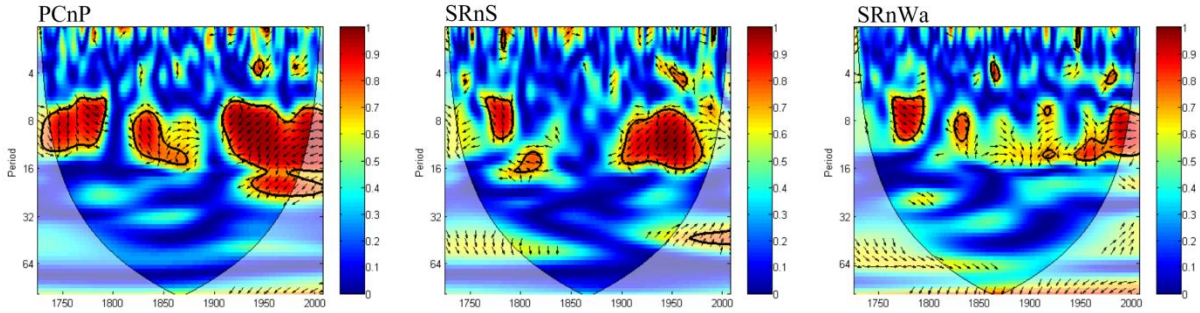

Figure 5.15 Wavelet coherence between streamflow and Sunspot data. The contours indicate a 95% confidence level. The vectors show the phase difference between the two signals where phase difference is shown for coherence greater than 0.5.

The strongest and most consistent covariance between streamflow and PDO (Figure 5.16) occurs at low frequencies (greater than about 20 years), and is very pronounced during the 1930s to the 1980s. Wavelet coherency also depicts significance at the interannual scale, for example during the 1920s and 1940s, within the 2-4 year band, which coincides with covariance established for ENSO events. "McCabe and Dettinger (2002) state that the unfiltered PDO index reflects important ENSO episodes in addition to the interdecadal variability of the North Pacific climate" (Gobena and Gan 2009, p.1472); this additional covariance is outside the common oscillatory mode dominated at the ~20-30 year scale.

Comparisons between water-year and summer streamflow coherence with the PDO index suggest that summer flows exhibit stronger covariance with PDO oscillations, as the contours enclosing areas of significance cover a larger area, and include higher values of coherence (Figure 5.16). On average, values of water-year coherence range from ~0.7 - ~0.8, whereas, summer flows exhibit coherence of ~0.85 - ~0.95, indicating a

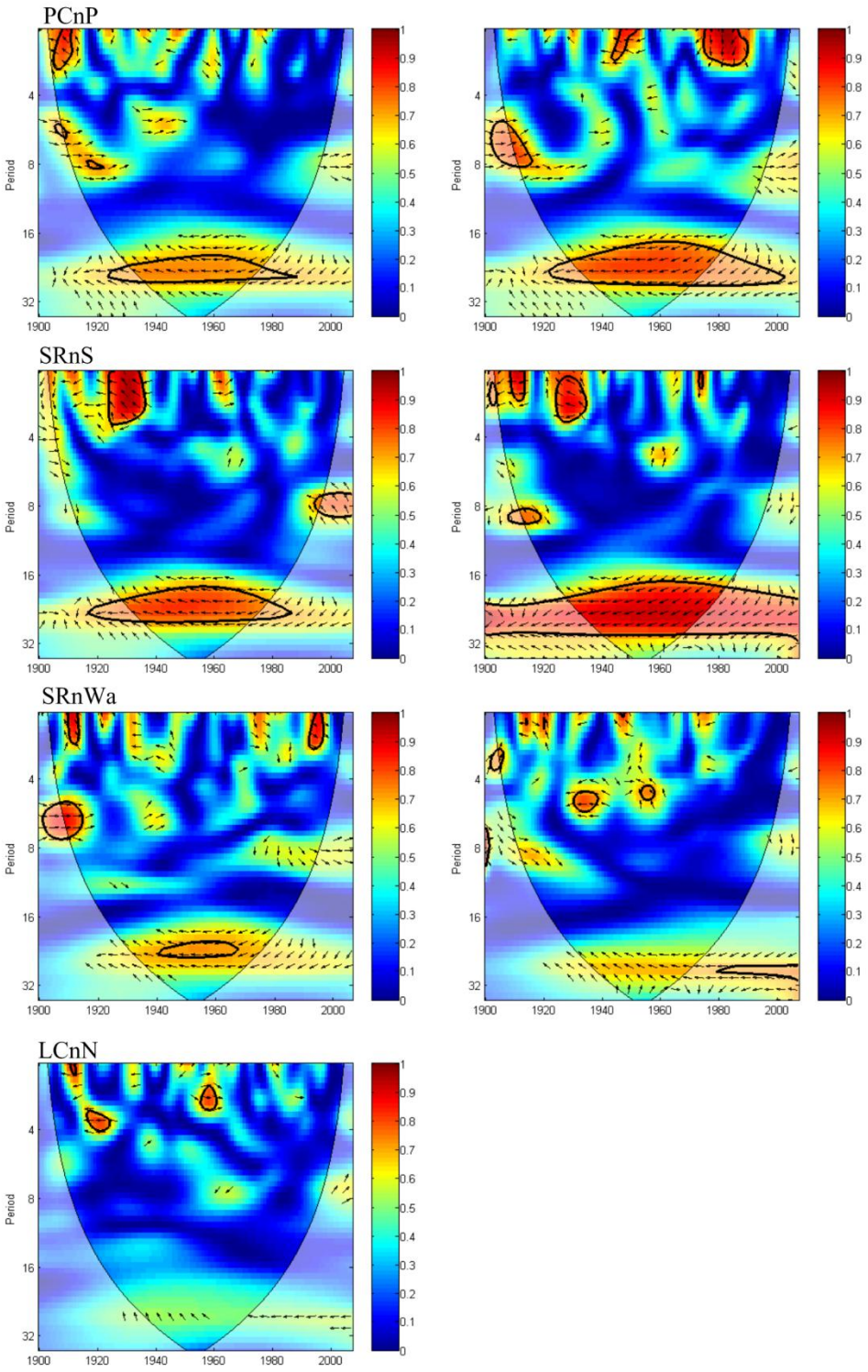

Figure 5.16 Wavelet coherence between water-year (left) and summer (right) streamflow and PDO data. The contours indicate a 95% confidence level. The vectors show the phase difference between the two signals where phase difference is shown for coherence greater than 0.5.

stronger relationship between the two indices in time frequency space (Grinsted *et al.* 2004).

Another important feature of both the XWT and WTC analyses is the ability to investigate the phase difference between the components of the two time series during periods of high common power and significant coherence. The vectors plotted in Figures 5.11 - 5.16 indicate the phase differences between significant spectral oscillations identified for the streamflow reconstructions and the climate indices at each respective frequency, and at each time and period. For clarity, only one vector is plotted every 2 years, and every other vector is plotted in the period direction (because of the timescale averaging no information is lost) (Torrence and Webster 1999). Vectors pointing to the right indicate that the two signals are in phase, whereas a left-pointing arrow indicates an anti-phase relationship. Arrows deviating from the horizontal are indicative of lead-lag relationships between the two signals (Gobena and Gan 2009). If a link exists between two time series, a consistent or slowly varying phase lag would be expected, and the phenomena would be considered to be phase-locked (*i.e.* phase-arrows point only in one direction for a given wavelength; Grinsted *et al.* 2004). If the vector direction varies between in-phase and anti-phase, it indicates that the signal may not be solely a cause and effect/'mirrored' relationship, but rather one that still has statistical properties of and is affected by other outside forcings. Because the lead/(lag) relationships can be difficult to interpret, (*i.e.* a lead of 90° can also be interpreted as a lag of 270° or a lag of 90° relative to the anti-phase – opposite sign; Grinsted *et al.* 2004), for this study, phase angle associations were noted strictly as either being in-phase/anti-phase locked, or if a lead/lag relationship exists.

Figures 5.11 and 5.14 portray a somewhat inconsistent relationship between streamflow and ENSO as is evident from the phase distribution at the interannual scale (2-6 year band). Primarily it appears as though throughout much of the 1970s to 2000s, the signals are not phase-locked, and alternate in vector direction, indicating that a lead/lag relationship exists between the two time series. When comparing phase differences between annual water year and summer flows, the latter seems to show more of a consistent pattern, with vectors either facing, or tending towards facing, the same direction, indicating a possible stronger link in relationship between ENSO and summer flow variability.

Similar results are displayed in interdecadal analyses of summer streamflow and solar sunspot data (Figures 5.12 - 5.15). Phase angles are inconsistent in the 7-11 year band; however, analyses at each of the gauges show similar directionalities of phase angles during periods of common power and coherence. Much of the entire 1900s to late 1990s primarily display an anti-phase distribution of phase angles, with the influence of a lead/lag relationship between streamflow and sunspot data, as the vectors tend to slightly deviate from the horizontal. Significant relationships between 1825 and 1875, show very distinct vertical phase arrows, indicating a very prominent lead-lag relationship between streamflow and sunspot data. Throughout the 1750s to 1790s vector angles are out of phase, however, it is not nearly as distinct as during the 50 year period previously described. The phase arrows during the 1750s to 1790s tend to represent more of an in-phase relationship as the vector angles are closer to horizontal than vertical.

XWT and WTC analyses between water-year and summer flows and the PDO indicate a very strong and coherent relationship between the two time series, for roughly

a 50 year period from 1930 to 1980. The vector angles in Figures 5.13 - 5.15 are constant, in an anti-phase locked orientation, across all significant scales, supporting a physical mechanism of signal propagation from the PDO to streamflow variability (Grinsted *et al.* 2004).

Relationships between streamflow and significant climate oscillations were further investigated using either a high- or low-pass filtered time series. To emphasize the interannual, interdecadal and multidecadal components, the streamflow and ENSO, Sunspot and PDO time series were filtered using a high-/low-pass cutoff scale of 5, 11, and 25 years, respectively (Gobena and Gan 2009). Reconstructions plotted with the oscillation indices gives a visual representation of when these cycles were in their respective negative or positive phases (Figures 5.17 - 5.18). Strong agreements exist between the indices and reconstructed streamflows, with an increase in ENSO, solar irradiance associated with sunspot number, and PDO, with a decrease in streamflow. Significant periods of below mean flow during the mid 1750s and early 1860s appears to be during a time of increased solar irradiance associated with increased sunspot data (Lean *et al*. 1995), and also during positive ENSO phases. Most noticeable are the phase changes in the PDO. Historical periods of drought, such as during the 'dirty thirties' (1927 - 1940), and again during the late 1970s and 80s, occurred when the PDO was in its extreme warm phase. Above average flows, on the other hand, during the late 1940s to early 50s, and again in mid 1970s, coincide with years when the PDO was in its extreme cool phase. Low streamflow during the early 1960s, corresponding to the historical drought of 1961 was associated with a temporary spike in the PDO signal in the midst of the cool PDO phase of 1947 - 76 (Goben and Gan 2006; 2009).

Major drought years throughout the early to mid 20th century coincide with positive phases of ENSO, Sunspot data, and PDO. El Niño (La Niña), and increased amounts of solar irradiance, coinciding with extreme positive (negative) values of the PDO seem to have an enhanced negative (positive) effect on the streamflow

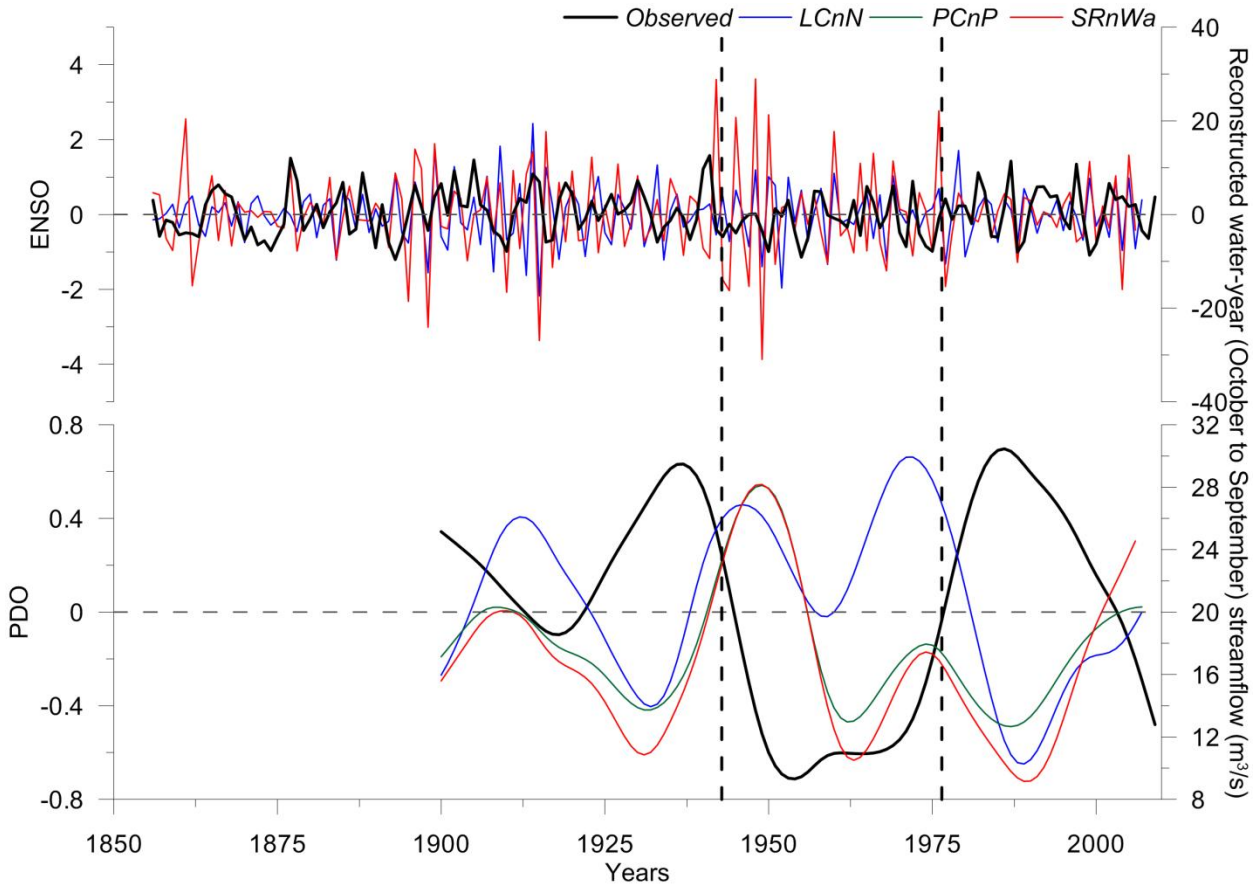

Figure 5.17 High- and low frequency components of water-year streamflow, ENSO and PDO. High- and low-pass filters with a cutoff scale of 5, and 25 years were used to reconstruct the signals, respectively.

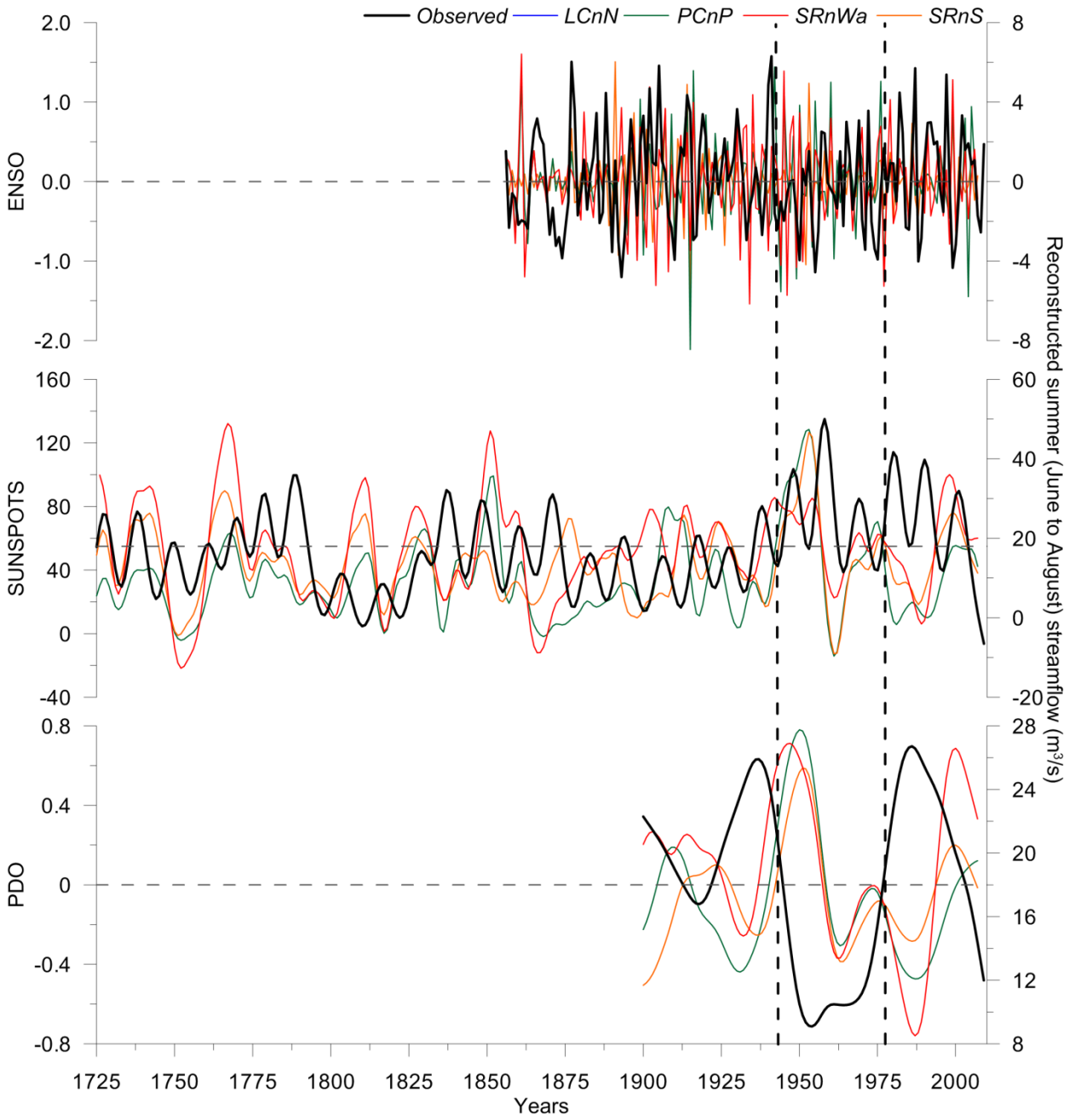

Figure 5.18 Interannual, interdecadal, and multidecadal frequency components of summer streamflow, ENSO, sunspot data and PDO. High- and low-pass filters with a cutoff scale of 5, 11, and 25 years were used to reconstruct the signals, respectively.

of the Souris River Basin (Figures 5.17 - 5.18). Goben and Gan (2009) found similar results between principle components of streamflow in the South Saskatchewan River

Basin and the PDO index, when investigating the role of Pacific climate on low-frequency hydroclimatic variability in southern Alberta. Conversely "the effects of mature El Niño (La Niña) years that occurred during a cool (warm) PDO phase appear to be either muted or are in opposition to the expected response" (Gobena and Gan 2009, 1473).

When any of these teleconnections are in their positive phase, interior Canada and the US experience warmer and drier winters. When these sea-surface temperatures and atmospheric oscillations are coupled (in-phase), this may lead to more prolonged, and possibly higher magnitude, extremes; the teleconnections have less influence on the hydrologic variability on their own, or when they are out of phase, with relatively modest effects.

6. CONCLUSIONS

6.1 Summary of research findings:

The objective of this study was to examine the hydroclimatic variability of the Souris River Basin by creating robust dendroclimatic reconstructions of streamflow for the Souris River and its main contributing tributaries. The inclusion of early- and latewood chronologies were incorporated to test the hypothesis that seasonal growth responses of *Q. macrocarpa* can serve as multi-proxies of streamflow providing more reliable information at annual and sub-annual (seasonal) times scales than flow reconstructions derived from chronologies of annual ring width alone. In addition, relationships with atmospheric and sea-surface temperature forcings were analyzed with aims to identify plausible drivers of annual and sub-annual streamflow variability within the Souris River Basin.

Development of a network of new moisture sensitive tree-ring chronologies throughout the Souris River Basin, allowed for the production of robust, multi-proxy reconstructions of water-year and summer streamflow for four gauges within the basin. Reconstruction models incorporating multiple proxies (combinations of annual, early- and or latewood widths), were able to account for ~54% - 76% and ~38% - 67% of the instrumental variance for water-year and summer flows, respectively, extending the historical record up to 280 years. Because much of the unexplained variance in the calibration period can attributed to the underestimation of high flows, more confidence can be applied in the interpretation of the low flows, which consistently correspond to narrow tree rings, capturing the timing and duration of drought. Results indicate that the use of early- and latewood widths as multi-proxies proves more useful than using annual

widths as the only proxies of streamflow at annual and sub-annual resolutions, as the models incorporate particularly optimal temporal response times of tree growth reflecting the same temporal happenings in streamflow variability.

Hydrological extremes were quantified and classified as abnormally wet years being in the 75th percentile, while discharge in the lowest 25th percentile were considered as drought years, with the most severe episodes indicated by flows in the lowest 10th percentile. Reconstructions at each of the four gauges show similar agreement (±1 or 2 years) in the occurrence of the most extreme single year droughts, indicating a common coherent signal in timing of events throughout the basin. Low flow/drought events were found to occur in each century, (1750s-60s, late 1780 to early 1800s, 1830s, 1850s-1875, late 1920s to early 40s, and again from late 1950s to mid 1960s), however the majority of critical drought years occurred within the 19th century. Water year flows indicate that the most severe low flow events took place in the late 1810s, mid 1830s, 1860s, late 1890s to early 1900s, and again in the mid 1950s. Summer flows yielded similar results, however the most sustained period of recurring severe single year droughts was experienced throughout at 24 year period from 1894 to 1917, common amongst all stations investigated within the Souris Basin.

Not only were the reconstructions successful in capturing severe single year droughts, but they also are able to capture the timing and magnitude of persistent low flow events also documented by other sources of proxy data, including tree-ring reconstructions and historical records and accounts. Examining periods prior to the 20th century indicates that droughts of the last century were of less magnitude and were short lived in comparison to some of the multi or 'mega-droughts' earlier in the record.

Streamflow reconstructions for the Souris Basin capture the low flow events occurring during the late 1880s through the 1890s (the 'Great Die-Up', Stahle and Dean 2011), another event known as one of the most severe and long lasting reconstructed droughts from 1841 through 1865 (Hardman and Reil 1936; Fritts 1965, 1983; Stockton and Meko 1975, 1983; Stahle *et al.* 1985; Stahle and Cleaveland 1988; Haston and Michaelsen 1997; Stahle and Dean 2011), the drought of the late 1790s through the early 1800s, and the occurrence of 'El Año del Hambre' – the year of hunger, during the late 1780s (Gibson 1964; Fritts 1965; Stahle and Dean 2011), as well as during the 12 year period from the 1750s to early 1760s (Stockton and Meko 1983; Laird *et al.* 1998; Cook *et al.* 1999; Therrell 2005).

Spectral analyses provide evidence that streamflow variability in the Souris River Basin is driven by a combination of interannual (~2-6 year), interdecadal (~7-11 year), and multidecadal (~20-30 year) ocean-atmosphere oscillations, such as indices of ENSO, solar sunspot cycles, and PDO, respectively. Results indicate that when annual ring widths are the only predictors of streamflow, much of the lower frequency oscillations are masked and not significant. The ability of the multi-proxy reconstructions, in both water-year and summer streamflow, to fully capture both the high and low frequency forcing, demonstrates the importance of incorporating responses of tree growth to climatic variability at sub-annual time scales, such as that recorded in both the EW and LW widths, suggesting that there is a temporal dependence in response to different drivers at different frequencies of occurrence.

Correlation analyses, cross-wavelet transforms and wavelet transform coherence identify significant periods of high common power and coherence of high, interdecadal,

and low frequency oscillation relationships of streamflow with ENSO, solar sunspot cycles, and PDO indices, respectively. Plots of high- and low-pass filtering of streamflow, ENSO, sunspot data, and the PDO, visually represent when these cycles were in their respective negative or positive phases, and their respective influences on streamflow variability. When these sea-surface temperatures and atmospheric oscillations are coupled, and in-phase with each other, it may lead to more prolonged and possibly greater in magnitude extremes than when climate anomalies are out of phase, resulting in a relatively modest influence of streamflow variability.

6.2 Future research:

As a result of this study, a robust, new, moisture sensitive network of 14 tree-ring chronologies has been generated for the Souris River Basin in the Canadian Prairies and Great Plains region. This study is the first to generate water-year and summer streamflow reconstructions to investigate hydroclimatic variability within this region, and is an important step towards filling the 'Prairie-gap' in the North American dendroclimatic network.

These reconstructions of streamflow for the Souris River Basin provide an important context for water managers and policy makers, providing long-term records that reveal extended periods of low flows compared to those recorded in short instrumental records. This study has successfully identified large-scale atmospheric teleconnections that influence the amount of hydroclimatic variability both spatially and temporally on a basin wide level. A critical component to advancing our understanding of the consequences of climatic change to regional climate variability and extremes, is the communication between scientific and water management communities to span the

knowledge gap and apply this new knowledge to the design of improved adaptation strategies.

In an attempt to do so, this network of chronologies could be further used for: the reconstructions of rivers and or gauges not addressed in this study; the application of density and or anatomical feature analysis for better prediction of extremes, such as for major flood events; and also in the incorporation of larger scale spectral investigations of atmospheric and sea-surface temperature forcings, and how they vary in their spatial and temporal distributions, over multiple basins throughout the Prairie region.

7. REFERENCES

Akkemik, U., D'Arrigo, R., Cherubini, P., Kose, N., Jacoby, G.C. 2004. Tree-ring reconstructions of precipitation and streamflow for northwestern Turkey. International Journal of Climatology 28: 173-183.

Astrade, L., Begin, Y. 1997. Tree-ring response of *Populus tremula* L., and *Quercus robur* L., to recent spring floods of the Saone River, France. Ecoscience 4: 232-239.

Axelson, J.M., Sauchyn, D.J., and Barichivich, J. 2009. New reconstructions of streamflow variability in the South Saskatchewan River Basin from a network of tree ring chronologies, Alberta, Canada. Water Resources Research 35: W09422. doi:10.1029/2008WR0077639.

Baillie, M.G.L. 1982. *Tree-Ring Dating and Archaeology.* The University of Chicago Press, Chicago. pp. 274.

Barber, V.A., Juday, G.P., Finney, B.P., and Wilmking, M. 2004. Reconstruction of summer temperatures in interior Alaska from tree-ring proxies: evidence for changing synoptic climate regimes. Climatic Change 63(1-2): 91-120.

Barnston, A.G., and Livezey, R.E. 1987. Classification, seasonality and persistence of low-frequency atmospheric circulation patterns. Monthly Weather Review 115: 1083-1126.

Bergan, J. 1987. Effects of temperature on annual ring growth of different Norway spruce provenances planted at various altitudes at 69° N. Meddel. Nor. Inst. Skogforskn. 40(3):1-46.

Bitz, C.C., and Battisti, D.S. 1999. Interannual to decadal variability in climate and the glacier mass balance in Washington, Western Canada, and Alaska. Journal of Climate 12: 3181-3196.

Blasing, T.J., and Fritts, H.C. 1976. Reconstructing past climatic anomalies in the North Pacific and western North America from tree-ring data. Quaternary Research 6: 563-579.

Bonin, D.V., and Burn, D.H. 2005. Use of tree ring reconstructed streamflows to assess drought. Canadian Journal of Civil Engineering 32: 1114-1123. doi: 10.1139/L05-069.

Bonsal, B.R., Zhang, X. and Hogg, W.D. 1999. Canadian Prairie growing season precipitation variability and associated atmospheric circulation. Climate Research 11: 191-208.

Bradley, R.S. 1985. *Quaternary paleoclimatology: methods of paleoclimatic reconstruction.* Allen & Unwin Inc., Winchester, Massachusetts.

Briffa, K. 1984. Tree-Climate Relationships and Dendroclimatological Reconstruction in the British Isles. Ph.D. Dissertation, University of East Anglia, Norwish, England, UK.

Briffa, K. 1990. Interpreting high-resolution proxy climate date - The example of dendroclimatology. In Von Storch, H. and Navarra, A. (Eds.) *Analysis of Climate Variability: Applications of Statistical Techniques*. Springer-Verlag Berlin, Heidelberg, Germany:78-94.

Briffa, K., and Jones, P.D. 1990. Basic chronology statistics and assessment. In Cook, E.R. and Kairiukstis, L.A. (Eds.) *Methods of Dendrochronology: Applications in the Environmental Sciences*, Klumer Academic Plubishers, Dordrecht: 137-152.

Briffa, K.R., Bartholin, T.S., Eckstein, D., Jones, P.D., Karlen, W., Schweingruber, F.H., and Zetterber, P. 1990. A 1400-year tree-ring record of summer temperatures in Fennoscandia. Nature 346: 434-439.

Briffa, K.R., Jones., P.D., Schweingruber, F.H. 1988. Summer temperature patterns over Europe: a reconstruction from 1750 AD based on maximum latewood density indices of conifers. Quaternary Research 30: 36-52.

Briffa, K., Osborn, T.J., Scweingruber, F., Harris, I.C., Jones, P., Shiyatov, S.G., andVaganov, E.A. 2001. Low-frequency temperature variations from a northern tree ring density network. Journal of Geophysical Research 106(D3): 2929-2941.

Burns, R.M. and Honkala, B.H. 1990. *Silvics of North America: 2. Hardwoods.* Agriculture Handbook 654. U.S. Department of Agriculture, Forest Service, Washington, D.C. Volume 2. pp. 877.

Campbell, R., McCarroll, D., Loader, N., Grudd, H., Robertson, I., and Jalkanen, R. 2007. Blue intensity in Pinus sylvestris tree rings: developing a new palaeoclimate proxy. The Holocene 17:6, 821-828.

Campbell, R., McCarroll, D., Roberston I., Loader, N., Grudd, H, and Gunnarson, B. 2011. Applications manual blue intensity in *Pinus sylvestris* tree rings: A manual for a new palaeolcimate proxy. Tree-Ring Reseasrch 67(2): 127-134.

Campelo, F., Nabais, C., Gutiérrez, E., Freitas, H., and García-González, I. 2010. Vessel features of *Quercus ilex* L. growing under Mediterranean climate have a better climatic signal than tree-ring width. Trees 24: 463-470. doi: 10.1007/s00468-010-0414-0.

Case, R.A. 2000. *Dendrochronological investigations of precipitation and streamflow for the Canadian Prairies.* PhD dissertation. University of California, Los Angeles, CA.

Case, R., and MacDonald, G. 2003. Tree ting reconstructions of streamflow for three Canadian prairie rivers. Journal of the American Water Resources Association. 39, 703-716.

Cayan, D.R. 1996. INterannual climate variability and snowpack in the western United States. Journal of Climate 9: 928-948.

Cleaveland, M.K. and Duvick, D.N. 1992. Iowa climate reconstructed from tree rings, 1640- 1982. Water Resources Research 28(10): 2607-2615.

Cleaveland, M.K., and Stahle, D.W. 1989. Tree ring analysis of surplus and deficit runoff in the White River, Arkansas. Water Resources Research 25(6): 1391-1401.

Cleaveland, M.K., Hager, A., Hobbie, E., Jones, D., McKane, B., Orth, K., and Wimmer, R. 1993. Report: Earlywood-latewood project. Fourth Annual Dendroecological Fieldweek, 4-12 June. Mountain Lake Biological Station of the University of Virginia, Pembroke, Virginia.

Conover, W. 1980. *Practical Nonparametric Statistics*. 2nd Edition. John Wiley & Sons, New York. p. 357.

Cook, E.R. 1985. A time series approach to tree-ring standardization. Unpublished. PhD dissertation. The University of Arizona, Tuscon, AZ.

Cook, E. and Briffa, K. 1990. Data Analysis. In Cook, E.R. and Kairiukstis, L.A. (Eds.) *Methods of Dendrochronology: Applications in the EnvironmentalSciences*, Klumer Academic Plubishers, Dordrecht: 97-162.

Cook, E.R., D'Arrigo, R.D., and Briffa, K.R. 1998. A reconstruction of the North Atlantic Oscillation using tree-ring chronologies from North America and Europe. The Holocene 8(1): 9-17.

Cooke, E.R., Meko, D.M., and Stockton, C.W. 1997. A new assessment of possible solar and lunar forcing of the bidecadal drought rhythm in the western United States. Journal of Climate 10: 1343-1356.

Cook, E.R., Meko, D.M., Stahle, D.W., and Cleaveland, M.K. 1999. Drought reconstructions for the continental United States. Journal of Climate 12: 1145-1162.

Currie, R.G. 1990. Deterministic signals in precipitation records from the American corn-belt. International Journal of Climatology 10: 179-189.

Currie, R.G. 1991. Deterministic signals in tree-rings from North America. International Journal of Climatology 11: 861-876.

Currie, R.G., and O'Brien, D.P. 1990. Deterministic signals in precipitation records from the American corn belt. International Journal of Climatology 10(2): 179-189.

D'Arrigo, R.D., Abram, N., Ummenhofer, C., Palmer, J., Mudelsee, M. 2009. Reconstructed streamflow for Citarum River, Java, Indonesia: linkages to tropical climate dynamics. Climate Dynamics. doi: 10.1007/s00382-009-0717-2.

D'Arrigo, R.D., and Jacoby, G.C. 1991. A 1000-year record of winter precipitation from northwestern New Mexico, USA: a reconstruction from tree-rings and its relation to El Niño and the Southern Oscillation. The Holocene 1,2: 95-101. doi: 10.1177/095968369100100201.

D'Arrigo, R.D., Cook, E.R., Jacoby, G.C., and Briffa, K.R. 1993. NAO and sea surface temperature signatures in tree-ring records from the North Atlantic sector. Quaternary Science Reviews 12: 431-440.

Dettinger, M.D., Ghil, M., Strong, C.M., Weibel, W., and Yiou, P. 1995. Software expedites singular-spectrum analysis of noisy time series. Eos Transactions American Geophysical Union 76(2): 12-21.

Dey, D., Chatterjee, B., Chakravorti, S., and Munshi, S. 2010. Cross-wavelet transform as a new paradigm for feature extraction from noisy partial discharge pulses. IEEE Transactions on Dielectrics and Electrical Insulation 17(1): 157-166.

Douglass, A.E. 1919. *Climatic cycles and tree-growth. A study of the annual rings of trees in relation to climate and solar activity. Volume I.* Carnegie Institution of Washington Publication. pp. 289.

Domec, J., and Gartner, B. 2002. How do water transport and water storage differ in coniferous earlywood and latewood? Journal of Experimental Botany 53:379, 2369-2379.

Douglass, A.E. 1928. *Climatic cycles and tree-growth. A study of the annual rings of trees in relation to climate and solar activity. Volume II.* Carnegie Institution of Washington Publication. pp.289.

Douglass, A.E. 1936. *Climatic cycles and tree-growth. A study of cycles. Volume III.* Carnegie Institution of Washington Publication. pp. 289.

Draper, N.R., and Smith, H. 1981. *Applied Regression Analysis* 2nd Edition. New York. John Wiley.

Earth Gauge. 2009. Oscillations and Teleconnections. Available online: http://www.eartgauge.net. [Last updated: June 19, 2009].

Eckstein, D. 2004. Change in past environments - secrets of the tree hydrosystem. New Phytologist 163: 1-4.

Eilmann, B., Weber, P., Rigling, A., and Eckstein, D. 2006. Growth reactions of *Pinus sylvestris* L. and *Quercus pubescens* Willd. to drought years at a xeric site in Valais, Switzerland. Dendrochronologia 23:121-132.

Enfield, D.B., Mestas-Nuñez, A.M., and Trimble, P.J. 2001. The Atlantic Multidecadal Oscillation and its relation to rainfall and river flows in the continental U.S. Geophysical Research Letters 28: 2077-2080.

Farge, M. 1992. Wavelet transforms and their applications to turbulence. Annual Review of Fluid Mechanics 24: 395-457.

Fagre, D.B., Peterson, D.L., and Hessl, A.E. 2003. Taking the pulse of mountains: Ecosystem responses to climatic variability. Climatic Change. 59(1-2): 263-282.

Farrar, J.J., and Evert, R.F. 1997. Seasonal changes in the ultrastructure of the vascular cambium of *Robinia pseudoacacia.* Trees 11:191-202.

Florescano, E. 1980. Análisis Histórico de las Sequías en México. Comisión del Plan Nacional Hidráulico, México City.

Fonti, P., and García-González, I. 2004. Suitability of chestnut earlywood vessel chronologies for ecological studies. New Phytologist 163: 77-86.

Fonti, P., and García-González, I. 2008. Earlywood vessel size of oak as a potential proxy for spring precipitation in mesic sites. Journal of Biogeography 35, 2239-2257.

Fonti, P., Solomonoff, N., and García-González, I. 2007. Earlywood vessels of *Castanea sativa* record temperature before their formation. New Phytologist 173: 562-570.

Fonti, P., von Arx, G., García-González, I., Eilmann, B., Sass-Klassen, U., Gärtner, H., and Eckstein D. 2009b. Studying global change through investigation of the plastic responses of xylem anatomy in tree rings. New Phytologist 185: 42-53.

Fritts, H.C. 1965. Tree-ring evidence for climatic changes in Western North America. Monthly Weather Review 93: 421-443.

Fritts, H.C. 1976. Tree rings and climate. Academic Press, London.

Fritts, H.C. 1983. Tree-ring dating and reconstructed variations in central Plains climate. Transactions of the Nebraska Academy of Science and Affiliated Societies 11: 37-41.

Fritts, H.C. 1991. *Reconstruction Large-Scale Climatic Patterns from Tree-Ring Data*. The University of Arizona Press, Tuscon. 286.

Fritts, H.C., and Shao, X.M. 1992. Mapping climate using tree-rings from western North America. In: R.S. Bradley and P.D. Jones (Eds.) *Climate since AD 1500*. Routledge, London. pp. 269-295.

Fritts, H.C., Blasing, T.J., Hayden, B.P., and Kutzback, J.E. 1971. Multivariate techniques for specifying tree-growth and climate relationships and for reconstructing anomalies in paleoclimate. Journal of Applied Meteorology 10(5): 845-864.

Fritts, H.C., Guiot, J., and Gordon, G.A. 1990. Verification. In Cook, E.R., and Kairiukstis, L.A. Eds. *Methods of Dendrochronology, Applications in the Environmental Sciences*. Kluwer Academic Publishers. pp. 178-185.

Fye, F., Stahle, D., Cook, E., and Cleaveland, M. 2006. NAO influence on sub-decadal moisture variability over central North America. Geophysical Research Letters 33,L15707.

García-González, I., and Eckstein, D. 2003. Climatic signal of earlywood vessels of oak on a maritime site. Tree Physiology 23: 497-504.

García-González, I., and Fonti, P. 2006. Selecting earlywood vessels to maximize their environmental signal. Tree Physiology 26, 1289-1296.

García-González, I., and Fonti, P. 2008. Selecting earlywood vessels for dendroecological studies: an example from two ring-porous species. Trees - Structure and Function 22: 237-244.

Garcia Acosta V. 1995. *Los Precios de Alimentos y Manufacturas Novohispanos*. Comité Mexicano de Estudios Superiores, Instituto de Investigaciones Históricas, UNAM, Mexico City.

Gedalof, Z, and Smith, D. 2001. Interdecadal climate variability and regime scale shifts in Pacific North America. Geophysical Research Letters 28: 1515-1518.

Gedalof, Z., Peterson, D., and Mantua, N. 2004. Columbia River flow and drought since 1750. Journal of American Water Resources Association. 40, 1579-1592.

Ghil, M., Allen, M.R., Dettinger, M.D., Ide, K., Kondrashov, D., Mann, M.E., Robertson, A.W., Saunders, A., Tian, Y., Varadi, F., and Yiou, P. 2002. Advanced spectral methods for climatic time series. Reviews of Geophysics 40(1003): 41 pp. doi: 10.1029/2000RG000092.

Girardin, M.-P., Tardif, J.C., Flannigan, M.D., and Bergeron, Y. 2006a. Synoptic-scale atmospheric circulation and boreal Canada summer drought variability of the past three centuries. Journal of Climate 19:1922-1947.

Gobena, A.K. and Gan, T.Y. 2006. Low-frequency variability in southwestern Canadian stream flow: links with large-scale climate anomalies. International Journal of Climatology 26: 1843-1869. doi: 10.1002/joc.1336.

Gobena, A.K. and Gan, T.Y. 2009. The role of Pacific climate on low-frequency hydroclimatic variability and predictability in Southern Alberta, Canada. Journal of Hydrometeorology 10: 1467-1478. doi: 10.1175/2009JHM1119.1.

Gou, X., Chen, F., Cook, E., Jacoby, G., Yang, M., Li, J. 2007. Streamflow variations of the Yellow River over the past 593 years in western China reconstructed from tree rings. Water Resources Research 43: W06417. doi: 10.1029/2008WR005705.

Guiot, J. 1990. Tree-ring standardization and growth-trend estimation. In Cook, E.R. and Kairiukstis, L.A. (Eds). *Methods of Dendrochronology: Applications in the Environmental Sciences*. Klumer Academic Publishers, Dordrecht: 165-178.

Graumlich, L.J. 1987. Precipitation variation in the Pacific Northwest (1675-1975) as reconstructed from tree rings. Annals of the Association of American Geographers 77(1): 19-29.

Gray, S., Betancourt, J., Fastie, C., and Jackson, S. 2003. Patterns and sources of multidecadal oscillations in drought-sensitive tree-ring records from the central and southern Rocky Mountains. Geophysical Research Letters 30. doi: 10.1029/2002GL016154.

Gray, S.T., Graumlick, L.J., Betancourt, J.L., and Pederson, G.T. 2004. A tree-ring based reconstruction of the Atlantic Multidecadal Oscillation since 1567 A.D. Geophysical Research Letters 31(12): L12205. doi: 10.1029/2004GL019932.

Grinsted, A., Moore, J.C., and Jevrejeva, S. 2004. Application of the cross wavelet transform and wavelet coherence to gephysical time series. Nonlinear Processes and Geophysics 11: 561-566.

Grissino-Mayer, H. 2001. Research Report: Evaluating crossdating accuracy: a manual and tutorial for the computer program COFECHA. Tree-Ring Research 57(2):205-221.

Haan, C.T. 2002. *Statistical methods in Hydrology, Second Edition.* Iowa State University Press. Ames, Iowa.

Hardman, G. and Reil, O.E. 1936. The relationship between tree-growth and stream runoff in the Truckee River basin, California - Nevada. Agricultural Experiment Station, Bulletin no 141, January. University of Nevada, Reno, Nevada. pp. 38

Haston, L., and Michaelsen, J. 1997. Spatial and temporal variability of southern California precipitation over the last 400 years and relationships to atmospheric circulation patterns. Journal of Climate 10: 1836-1852.

Hawley, F.M. 1937. Relationship of southern cedar growth to precipitation and runoff. Ecology 18(3): 398-405.

Hendricks, E. L. 1962. Hydrology. Science 135(2505): 699:705.

Hirschboeck, K.K., Ni, F., Wood, M.L. and Woodhouse, C.A. 1996. Synoptic dendroclimatology: overview and outlook. In: J.S. Dean, D.M. Meko, and T.W. Swetnam, (Eds.) *Tree Rings, Environment, and Humanity: Proceedings of the International Conference*, Tucson, Arizona. May 17-21. Radiocarbon, Tucson. pp. 205-223.

Hoadley, B. 1990. *Identifiying wood; Accurate results with simple tools.* The Taunton Press: Newtown, CT.

Holmes, R.L. 1983. Computer-assisted quality control in tree-ring dating and measuring. TreeRing Bulletin 43:69-78.

Hughes, M.K., Kelly, P.M., Pilcher, J.R., and Lamarche Jr., V.C., Eds. 1982. *Climate from tree rings*. Cambridge, Cambridge University Press.

Hurrell, J.W. 1995. Decadal trends in the North Atlantic Oscillation: regional temperatures and precipitation. Science 269: 676-679.

International Joint Commission. 2011. International Souris River Board. Available online:http://www.ijc.org/conseil_board/souris_river/en/souris_home_accueil.htm [Last updated: January 11, 2011].

International Souris River Board of the International Joint Commission. 2009. Hydrology. No. ISRB-2009B. Available online: http://www.ijc.org.

Jeverjeva, S., Moore, J.C., and Grinsted, A. 2003. Influence of the Arctic Oscillation and El Niño-Southern Oscillation (ENSO) on ice conditions in the Baltic Sea:

The wavelet approach. Journal of Geophysical Research 108(D21): 4677. doi:10.1029/2003JD003417.

Jones, P.D., Briffa, K.R., Barnett, T.P., and Tett, S.F.B. 1998. High –resoultion paleoclimatic records for the last millennium: interpretation, integration and comparison with general circulation model control-run temperatures. The Holocene 8: 455-471.

Jones, P., Jonsson, T., and Wheeler, D. 1997. Extension to the North Atlantic Oscillation using early instrumental pressure observations from Gibraltar and South-West Iceland. International Journal of Climatology 17: 1433-1450.

Keen, F.P. 1937. Climate cycles in eastern Oregon as indicated by tree rings. Monthly Weather Review 98: 142-153.

Kennedy, R. 1961. Variation and periodicity of summerwood in some second-growth Douglas-fir. Tappi Journal 44, 161-165.

Khandekar, M.L. 2004. Canadian Prairie drought: a climatological assessment. Alberta Environment. pp. 37.

Kirdyanov, A.V., Vaganov, E.A., and Hughes, M.K. 2007. Separating the climatic signal from tree-ring width and maximum latewood density records. Trees 21: 37-44.

Knox, J.L., and Lawford, R.G. 1990. The relationship between Canadian Prairie dry and wet months and circulation anomalies in the mid-troposphere. Atmosphere-Ocean 28: 189-215.

Koubaa, A., Zhang, S.Y.T., and Makni, S. 2002. Defining the transition from earlywood to latewood in black spruce based on intra-ring wood density profiles from X-ray densitometry. Annals of Forest Science 59: 511-518. doi: 10.1051/forest:2002035.

Kozlowski, T., and Pallardy, S. 1997. *Physiology of woody plants* (2nd Edn.). Academic Press: San Diego.

Laird, K.R., Fritz, S.C., and Cumming, B.F. 1998. A diatom-based reconstruction of drought intensity, duration, and frequency from Moon Lake, North Dakota: a sub-decadal record of the last 2300 years. Journal of Paleolimnology 19: 161-179.

LaMarche, V.C. Jr. and Fritts, H.C. 1972. Tree-rings and sunspot numbers. 32: 19-33.

Lawson, M.P., Heim, R. Jr., Mangimeli, J.A., and Moles, G. 1980. Dendroclimatic analysis of bur oak in eastern Nebraska. Tree-Ring Bulletin 40: 1-11.

Lean, J. 1991. Variations in the sun's radiative output. Reviews of Geophysics 29(4): 505-535.

Lean, J., and Rind, D. 1996. The sun and climate. Consequences 2(1): 27-36.

Lean, J., and Rind, D. 1998. Climate forcing by changing solar radiation. Journal of Climate 11: 3069-3094.

Lean, J., Beer, J., and Bradley, R. 1995. Reconstruction of solar irradiance since 1610: Implications for climate change. Geophysical Research Letters 22: 3195-3198.

Leavitt, S.W., and Wright, W.E. 2002. Spatial expressions of ENSO, drought, and summer monsoon in seasonal Del^{13}C of ponderosa pine tree rings in southern Arizona and New Mexico. Journal of Geophysical Research 107(D18): 1-10.

Liu, Y., Sun, J., Song, H., Cai, W., Bao, B., Li, X. 2010. Tree-ring hydrologic reconstructions for the Heihe River watershed, western China since A.D. 1430. Water Resources Research 44: 2781-2792.

Loaiciga, H.A., Haston, L., and Michaelsen, J. 1993. Dendrohydrology and long-term hydrologic phenomena. Reviews of Geophysics 31(2): 151-171.

Loaiciga, H.A., Michaelsen, J., Garver, S., Haston, L., and Leipnik, R.B. 1992. Droughts in river basins of the western United States. Geophysical Research Letters 19(20): 2051- 2054.

Lowson, J.M. 1966. *Textbook of Botany*. London.

Lilliefors, H.W. 1967. On the Kolmogorov-Smirnov test for normality with mean and variance unknown. Journal of the American Statistical Association 62: 399-402.

MacDonald, G.M., and Case, R.A. 2005. Variations in the Pacific Decadal Oscillation over the past millenium. Geophysical Research LEtters 32(8): L08703. doi:10.1029/2005GL022478.

Manitoba Agro Woodlot Program. 2002. Woodlot Management Plan: Craig Bessant; The Manitoba Habitat Heritage Corporation, Private land program for the benefit of all Manitobans.

Manitoba Agro Woodlot Program. 2005. Woodlot Management Plan: Turtle Mountain Conservations District c/o Newcomb's Hollow; Manitoba Agriculture, Food and Rural Initiatives.

Manitoba Agro Woodlot Program. 2007. Woodlot Management Plan: Andrew Van der Velde; Manitoba Agriculture, Food and Rural Initiative.

Manitoba Water Commission. 1984. Souris River Study. The Manitoba Water Commission. Winnipeg, Manitoba. pp. 45.

Mann, M.E., and Lees, J.M. 1996. Robust estimation of background noise and signal detection in climatic time series. Climate Change 33: 409-445. doi:10.1007/BF00142586.

Mann, M.E., Bradley, R.S., and Hughes, M.K. 1998. Global-scale temperature patterns and climate forcing over the past six centuries. Nature 392: 779-787.

Mantua, N.J., Hare, S.R., Zhang, Y., Wallace, J.M., and Francis, R.C. 1997. A Pacific interdecadal climate oscillation with impacts on salmon production. Bulletin of the American Meteorological Society 78: 1069-1079.

MathWorks. 2011. Wavelet coherence. The MathWorks, Inc. http://www.mathworks.com.

McCabe, G., Palecki, M., and Betancourt, J.L. 2004. Pacific and ATlantic Ocean influences on multi-decadal drought frequency in the United States. Proceedings of the National Academy of Science 101: 4136-4141.

McKay, G., Godwin, R., and Maybank J. 1989. Drought and hydrological drought research in Canada: An evaluation of the state of the art. Canadian Water Resources Journal 14, 71- 84.

Meehl, G.A., Washington, W.M., Wigley, T.M.L., Arblaster, J.M., and Dai, A. 2003. Solar and greenhouse gas forcing and climate response in the twentieth century. Journal of Climate 16: 426-444.

Meko, D., and Baisan, C. 2001. Pilot study of latewood-width of conifers as an indicator of variability of summer rainfall in the North American Monsoon Region. International Journal of Climatology 21, 697-708.

Meko, D., and Graybill, D.A. 1995. Tree-ring reconstruction of Upper Gila River Discharge. Water Resources Bulletin 31: 605-615.

Meko, D., Stockton, C.W., and Boggess, W.R. 1995. The tree-ring record of severe sustained drought. Water resources bulletin. 31(5): 789-801.

Meko, D., and Woodhouse, C. 2011. Application of streamflow reconstruction to water resources management. In: Hughes, M.K., Swetnam, T.W., and Diaz, H.F. (Eds) *Dendroclimatology Progress and Prospects*. Developments in paleoenvironmental research. Volume 11. Springer Dordrecht Heidelberg London, New York. doi: 10.1007/978-1-4020-5725-0.

Meko, D.M., Woodhouse, C.A., and Morino, K. 2010. Dendrochronology and links to streamflow. Journal of Hydrology (*In Press)*. doi: 10.1016/j.jhydrol.2010.11.041.

Metcalfe, C.R., and Chalk, L. 1950. *The Anatomy of the Dicotyledons*. CLarendon Press, Oxford.

Michaelsen, J. 1989. Long-period fluctuations in El Nino amplitude and frequency reconstructed from tree rings. Geophysical Monograph 55, American Geophysical Union. 69-74.

Miina, J. 2000. Dependence of tree-ring, earlywood and latewood indices of Scots pine and Norway spruce on climatic factors in eastern Finland. Ecological Modelling 132: 259-273.

Minobe, S. 1997. A 50-70 year climatic oscillation over the North Pacific and North America. Geophysical Research Letters 24: 683-686.

Mitchell, T., and Jones, P. 2005. An improved method of constructing a database of monthly climate observations and associated high-resolution grids. International Journal of Climatology 25: 693-712.

Martin, F.R.J., and Godwin, R.B. 1977. Natural Flow Report: Prepared for the Souris River Basin Study Board. Department of Regional Economic Expansion, Prairie Farm Rehabilitation Administration, Engineering Service, Canada. May, 1977, Regina, Saskatchewan.

Meko, D., Hughes, M., and Stockton, C. 1991. Climate change and climate variability: The paleo record, in *Managing Water Resources Under conditions of Climate Uncertainty; Proceedings of a Colloguiium Scottsdale, Arizona,* edited by Commity on Climate Uncertainty and Water Resource Management. pp. 71-100. National Academic Press. Washington, D.C.

Meko, D. 1997. Dendroclimatic reconstruction with time varying predictor subsets of tree indices. Journal of Climate 10: 687-696.

Michaelsen, J.C., Haston, L., and Davis, F.W. 1987. 400 years of central California precipitation variability reconstructed from tree-rings. Water Resources Bulletin 23: 809-818.

Naimas, J. 1983. Some causes of United States drought. Journal of Climate and Applied Meteorology 22: 30-39.

National Research Council (NRC). 1998. *Decade-to-century-scale climate variability and change, A science strategy.* Panel on Climate Variability on Decade-to-Century Time Scales; Board on Atmospheric Sciences and Climate. Commission on Geosciences, Environment and Resources, Washington, D.C. pp. 141.

Nigam, S., Barlow, M., and Berbery, E.H. 1999. Analysis links Pacific decadal variability to drought and streamflow in the United States. EOS, Transactions, American Geophysical Union 80(51) December 21, 1999.

Oh, H.S., Ammann, C.M., Naveau, P., Nychka, D., Otto-Bliesner, B.L. 2003. Multi-resolution time series analysis applied to solar irradiance and climate reconstructions. Journal of Atmospheric and Solar-Terrestrial Physics 53: 191-201.

Ostrom, C.W., Jr. 1990. *Time Series Analyses, Regression Techniques. Second Edition: Quantitative Applications in the Social Sciences*. v.07-009. Newbury Park, Sage Publications.

Percival, D.B., and Walden A.T. *Spectral Analysis for Physical Applications*. Cambridge University Press., New York. 583 pp.

Perry, A. 2000. The North Atlantic Oscillation: an enigmatic see-saw. Progress in Physical Geography 24(2): 289-294. doi: 10.1177/030913330002400209.

Phipps, R.L. 1967. Annual growth of suppressed chestnut oak and red maple, a basis for hydrologic interference. United States Geological Survey Professional Paper 485 - C.

Phipps, R.L. 1982. Comments on the interpretation of climatic information from tree rings, Eastern North America. Tree-Ring Bulletin 42: 11-22.

Ram, M., Stolz, M., and Koenig, G. 1997. Eleven year cycle of dust concentration variability observed in the dust profile of the GISP2 ice core from central Greenland: possible solar cycle connection. Geophysical Research Letters 24: 2359-2362.

Rayner, N., Brohan, P., Parker, D., Folland, C., Kennedy, J., Vanicek, M., Ansell, T., and Tett, S. 2006. Improved analyses of changes and uncertainties in sea surface temperature measured in situ since the mid-nineteenth century: The HadSST2 dataset. Journal of Climate 19: 446-469.

Robertson, P.A. 1992. Factors affecting tree growth on three lowland sites in southern Illinois. American Midland Naturalist 128: 218-326.

Rogers, J.C., 1984. The association between the North Atlantic Oscillation and the Southern Oscillation in the Northern Hemisphere. Monthly Weather Review 112: 1999-2015.

Saskatchewan Watershed Authority. 2005. Background report Lower Souris River Watershed: Executive Summary. 127 pp.

Sauchyn, D., and Kulshreshtha, S. 2008. The Prairies, in *From Impacts to Adaptation: Canada in a Changing Climate 2007*, edited by D. S. Lemmen et al. Chapter 7, pp. 275-328. Government of Canada, Ottawa.

Sauchyn, D., Vanstone, J., and Perez-Valdivia, C. *Accepted*. Modes and forcing of hydroclimatic variability in the North Saskatchewan River Basin Since 1063. Canadian Water Resources Journal.

Schindler, D.W. and Donahue, W.F. 2006. An impending water crisis in Canada's western prairie provinces. Proceedings of the National Academy of Sciences 103: 7210-7216.

Schoellhamer, D.H. 2001. Singular spectrum analysis for time series with missing data. Geophysical Research Letters 28(26): 3187-3190. Doi:10.1029/2000GL012698.

Schulman, E. 1956. Dendroclimatic changes in semiarid America. University of Arizona Press, Tuscon.

Schweingruber, F.H. 1992. Trees and wood in dendrochronology. Springer-Verlag, Berlin, Germany.

Schweingruber, F.H. 1996. *Tree Rings and Environment: Dendroecology*. Haupt Press, Berne. pp. 609.

Schweingruber, F.H., Bartholin, T., Schär, E., and Briffa, K.B. 1988. Radiodensitometric- dendroclimatological conifer chronologies from Lapland (Scandinavian) and the Alps (Switzerland). Boreas 17: 559-566.

Schweingruber, F.H., Kairiukstis, L., and Shyatov, S. 1990. Sample Selection. In Cook, E.R. and Kairiukstis, L.A. (Eds.) *Methods of Dendrochronology: Applications in the Environmental Sciences*, Klumer Academic Plubishers, Dordrecht: 23-35.

SIDC team. 2010. World Data Center for the Sunspot Index, Royal Observatory of Belgium. *Monthly Report on the International Sunspot Number*. online catalogue of the sunspot index: http://www.sidc.be/sunspot-data/'1700-2010'.

Sieg, C.H., Meko, D., DeGaetano, A.T., and Ni, W. 1996. Dendroclimatic potential in the northern Great Plains. In *Tree Rings, Environment and Humanity*. Dean, J.S., Meko, D.M., and Swetman, T.W., Eds. Radiocarbon 1996: 295-302.

Sirén, G. 1963. Tree rings and climate forecasts. New Scientist 346: 18-20.

Souris River Basin Study Board (SRB Study Board). 1978. Souris River Basin Study Report. Canada – Manitoba – Saskatchewan. Regina, Saskatchewan. pp. 188.

Speer, J.H. 2010. *Fundamentals of tree-ring research.* The University of Arizona Press. pp. 333.

St. George, S., Nielsen, E., and Brooks, G. 1999. Tree rings into the next millennium! In: Report of Activities, 1999, Manitoba Industry, Trade and Mines, Geological Services. p. 126-129.

St. George, S., Nielse, E., Conciatori, F., and Tardif, J. 2002. Trends in *Quercus macrocarpa* vessel areas and their implications for tree-ring paleoflood studies. Tree-Ring Research 58(1/2): 3-10.

St. George and Nielsen, E. 2000. Signatures of high-magnitude 19th-century floods in *Quercus macrocarpa* tree rings along the Red River, Manitoba, Canada. Geology 28: 899-902.

St. George, S., Meko, D.M., Girardin, M.-P., MacDonal, G.M., Nielsen, E., Pederson, G.T., Sauchyn, D.J., Tardif, J.C., and Watson, E. 2009. The tree-ring record of drought on the Canadian Prairies. Journal of Climate 22(3):689-710.

Stahle, D.W., and Cleaveland, M.K. 1988. Texas drought history reconstructed and analyzed from 1698 to 1980. Journal of Climate 1:59-74.

Stahle, D.W., and Dean, J.S. 2011. North American tree rings, climatic extremes, and social disasters: Social impacts of climate extremes during the historic era. In: Hughes, M.K., Swetnam, T.W., and Diaz, H.F. (Eds) *Dendroclimatology Progress and Prospects*. Developments in paleoenvironmental research. Volume 11. Springer Dordrecht Heidelberg London, New York. doi: 10.1007/978-1-4020-5725-0_10.

Stahle, D.W., Cleaveland, M.K., and Heher, J.G. 1985. A 450-year drought reconstruction for Arkansas, United States. Nature 316: 530-532.

Stegner, W. 1954. *Beyond the hundredth meridian.* Penguin, New York.

Stockton, C.W. and Jackoby, G.C. 1976. Long-term surface-water supply and streamflow trends in the Upper Colorado River Basin. Lake Powell Research Project Bulletin 18, Institute of Geophysics and Planetary Physics, University of California, Los Angeles. 70 pp.

Stockton, C.W., and Meko, D.M. 1975. A long-term history of drought occurrence in western United States as inferred from tree rings. Weatherwise 28: 245-249.

Stockton, C.W., and Meko, D.M. 1983. Drought recurrence in the Great Plains as reconstructed from long-term tree-ring records. Journal of Climate and Applied Meteorology 22: 17- 29.

Stokes, M.A. and Smiley, T.L. 1968. *An introduction to tree-ring dating*. University of Chicago Press, Chicago.

Stuiver, M., Braziunas, T.F., Grootes, P.M., and Zielinski, G.A. 1997. Is there evidence for solar forcing of climate in the GISP2 oxygen isotope record? Quaternary Research 44: 341-354.

Tardif, J.C., and Conciatori, F. 2006. Influence of climate on tree rings and vessel features in red oak and white oak growing near their northern distribution limit, southwestern Quebec, Canada. Canadian Journal of Forest Research 36: 2317-2330. doi:10.1139/X06-133.

Therrell, M.D. 2005. Tree rings and 'El Año del Hambre' in Mexico. Dendrochronologia 22: 203-207.

Thomson, D. J. 1982. Spectrum estimation and harmonic analysis. Proceeding of the IEEE. 70: 1055-1096.

Thomson, D.J. 1990a. Quadratic-inverse spectrum estimates: Applications to palaeoclimatology. Philosophical Transactions of the Royal Society of London, Series A. 332: 539-597.

Torrence, C., and Compo, G.P. 1998. A practical guide to wavelet analysis. Bulletin of the American Meteorological Society 79(1): 61-78.

Torrence, C., and Webster, P. 1999. Interdecadal changes in the ENSO-Monsoon system. Journal of Climatology 12: 2679-2690.

Touchan, R., Anchukaitis, K.J., Meko, D., Attalah, S., Baisan, C., and Aloui, A. 2008. Long term context for recent drought in northwestern Africa. Geophysical Research Letters 35: L13705. DOI:10.1029/2008GL034264.

Touchan, R., Woodhouse, C., Meko, D., and Allen, C. 2010. Millennial precipitation reconstruction for the Jemez Mountains, New Mexico, reveals changing drought signal. International Journal of Climatology 31(6):896-906. DOI:10.1002/joc.2117.

Trenberth, K.E. 1997. The definition of El Niño. Bulletin of the American Meteorological Society 78(12): 2771-2777.

U.S. Environmental Protection Agency, Western Ecological Division. 2010. Ecological Regions of North America. Available online: http://www.epa.gov/wed/pages/ecoregions.htm. [Last updated August 6, 2010].

Vaganov, E.A. 1990. The tracheidogram method in tree-ring analysis and its application. In: Cook, E.R., and Kairiukstis, L.A. (Eds) *Methods of dendrochronology: applications in the environmental sciences*. Kluwer, London. pp. 63-76.

Vaganov, E.A., Hughes, M.K., Shashkin, A.V. 2006. *Growth dynamics of conifer tree rings: images of past and future environments.* Springer, New York.

Van Loon, H., and Rogers, J.C. 1978. The seesaw in winter temperatures between Greenland and northern Europe: Part 1: general description. Monthly Weather Review 106: 296- 310.

Van Oldenborgh, G.J., te Raa, L.A., Dijkstra, H.A., and Philip, S.Y. 2009. Frequency- or amplitude-dependent affects of the Atlantic meridional overturning on the tropical Pacific Ocean. Ocean Science 5:293-301.

Vanstone, J.R. and Sauchyn, D.J. 2010. *Quercus macrocarpa* annual, early- and latewood widths as hydroclimatic proxies, southeastern Saskatchewan, Canada. IOP Conference Series: Earth and environmental science 9(1). doi: 10.1088/1755-1315/1/012016.

Varley, G.C. and Gradwell, G.R. 1962. The effect of partial defoliation by caterpillars on the timber production of oak trees in England. *XI Internationaler Kongress fur Entomologic Wien 1960*, Sonderdruck aus den Verhandlungen, BdII. pp. 211-14.

Vautard, R., and Ghil, M. Singular spectrum analysis in nonlinear dynamics with applications to paleoclimatic time series. Physica D. 35: 395-424.

Waple, A.M. 1999. The sun-climate relationship in recent centuries: a review. Progress in Physical Geography 23: 309-328. doi: 10.1177/030913339902300301.

Ward, R. C. and Robinson, M. 2000. *Principles of hydrology*. McGraw-Hill Publishing Company, London.

Watson, E. and Luckman, B.H. 2005. Spatial patterns of preinstrumental moisture variability in the southern Canadian Cordillera. Journal of Climate 18:2847-2863.

Watson, E. and Luckman, B.H. 2006. Long hydroclimate records from tree-rings in western Canada: potential, problems and prospects. Canadian Water Resources Journal 31:205-228.

West, E. 1995. *The way to the West*. University of New Mexico Press, Alberquerque.

Wheaton, E.E., Arthur, L.M., Chorney, B., Shewchuk, S., Thorpe, J., Whiting, J., and Wittrock, V. 1992. The prairie drought of 1988. Climatological Bulletin. 26(3): 188-205

Wheaton, E., Kulshreshtha, S., Wittrock, V., and Koshida, G. 2008. Dry times: hard lessons from the Canadian drought of 2001 and 2002. Canadian Geographer 52: 241-262.

White, P.B., Van de Gevel, S.L., Grissino-Mayer, H.D., Laforest, L.B., and Deweese, G.G. 2011. Climatic response of oak species across an environmental gradient in the southern Appalachian Mountains, USA. Tree-Ring Research 67(1):27-37.

Wigley, T.M.L., Briffa, K.R., and Jones, P.D. 1984. On the Average Value of Correlated Time Series, with Applications in Dendroclimatology and Hydrometeorology. Journal of Climate and Applied Meteorology 23: 201-213.

Wilks, D.S. 1995. *Statistical methods in the atmospheric sciences.* Academic Press. pp.467.

Will, G.F. 1946. *Tree Ring Studies in North Dakota*. North Dakota Agricultural Experiment Station. Fargo, North Dakota. Bulletin 338.

Woodcock, D.W. 1987. Sensitivity of vessel diameter to climatic conditions in bur oak (*Quercus macrocarpa*). In: Cosgrove, D.J., and Knievels, D.P. (Editors) *Physiology of Annual Penn State Symposium in Plant Physiology. May 21-23.* Pennsylvannia State University, University Park, Pa. American Society of Plant Physiologists, Rockville, Md. pp. 245-248.

Woodcock, D.W. 1989. Climate sensitivity of wood-anatomical features in a ring-porous oak (*Quercus macrocarpa).* Canadian Journal of Forest Research 19(5): 639-644.

Woodhouse, C.A., and Overpeck, J.T. 1998. 2000 years of drought variability in the central United States. Bulletin of the American Meteorological Society 79(12):2693-2714.

Woodhouse, C.A., Lukas, J.J., and Brown, P.M. 2002. Mid-nineteenth-century Colorado drought. Bulletin of the American Meteorological Society 83: 1484-1493.

Zobel, B., and Van Buijtenen, J. 1989. Variation among and within trees. In: *Wood variation: its causes and control*. New York: Springer-Verlag.

8. APPENDIX

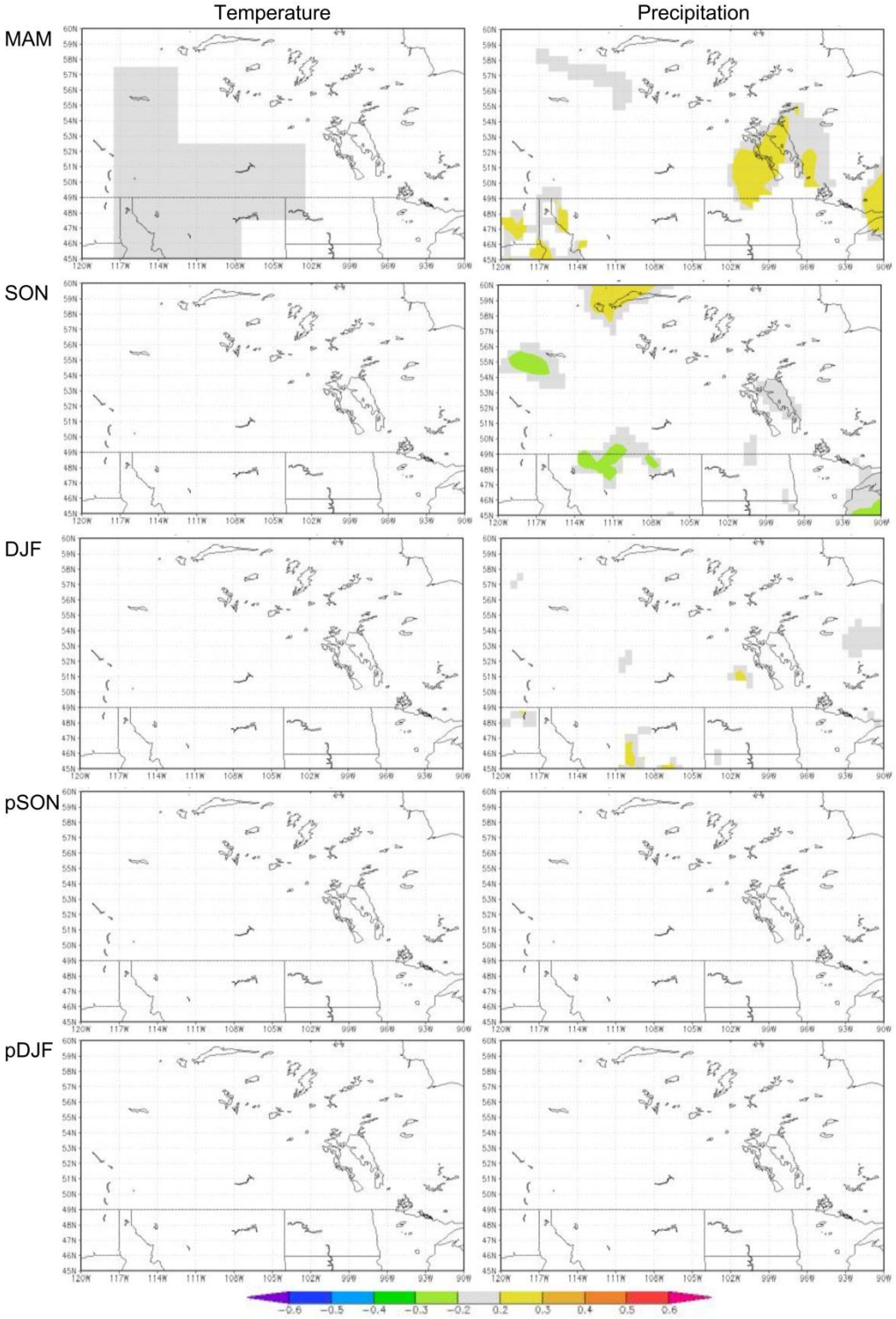

Figure 2.1 Seasonal correlation between annual (RW) ringwidth indices and temperature and precipitation ($p<0.05$). (MAM: March-May; SON: September-November; DJF: December-February; pSON: previous September-November; pDJF: previous December-February).

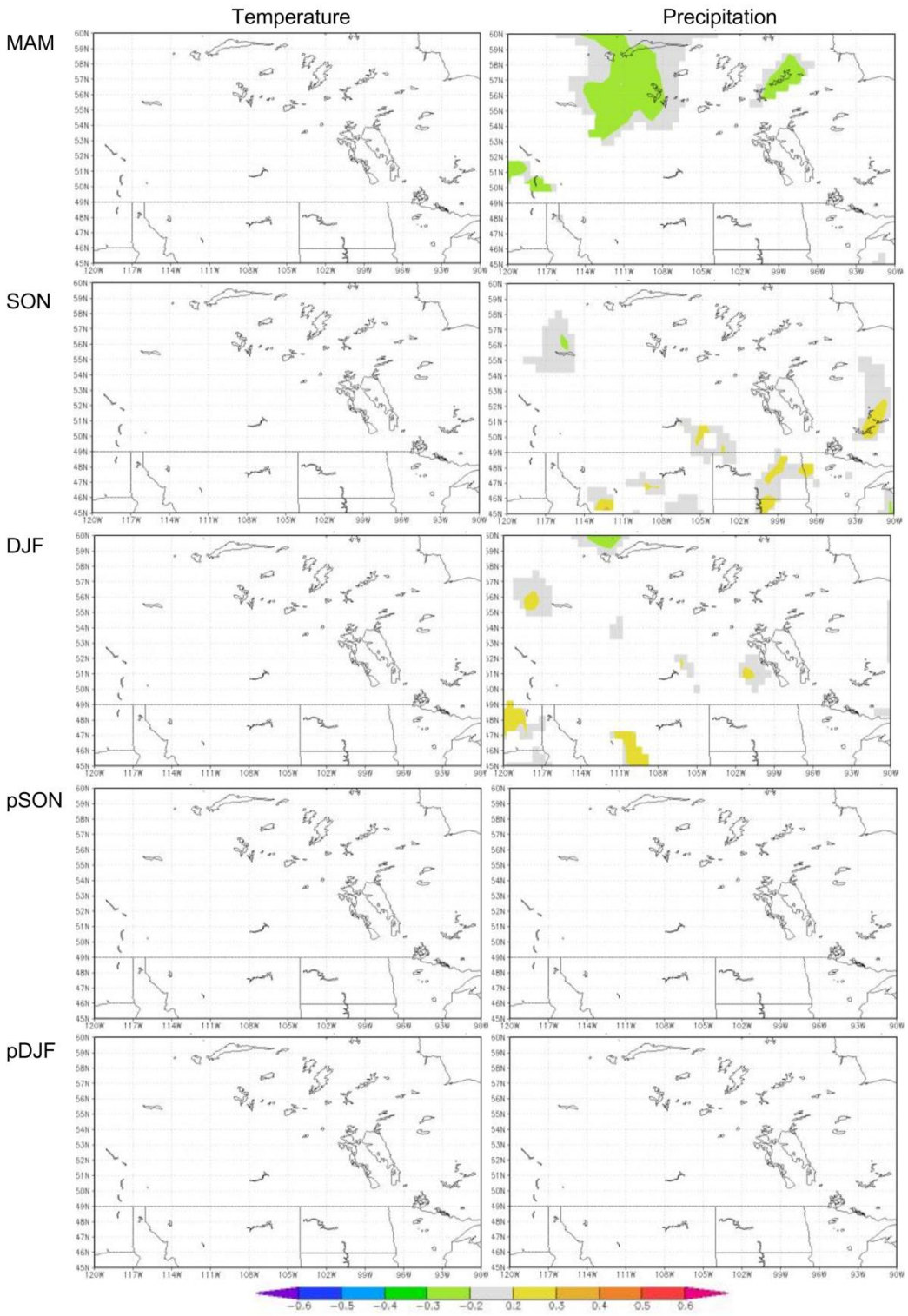

Figure 1.2 Seasonal correlation between EW ringwidth indices and temperature and precipitation ($p<0.05$). (MAM: March-May; SON: September-November; DJF: December-February; pSON: previous September-November; pDJF: previous December-February).

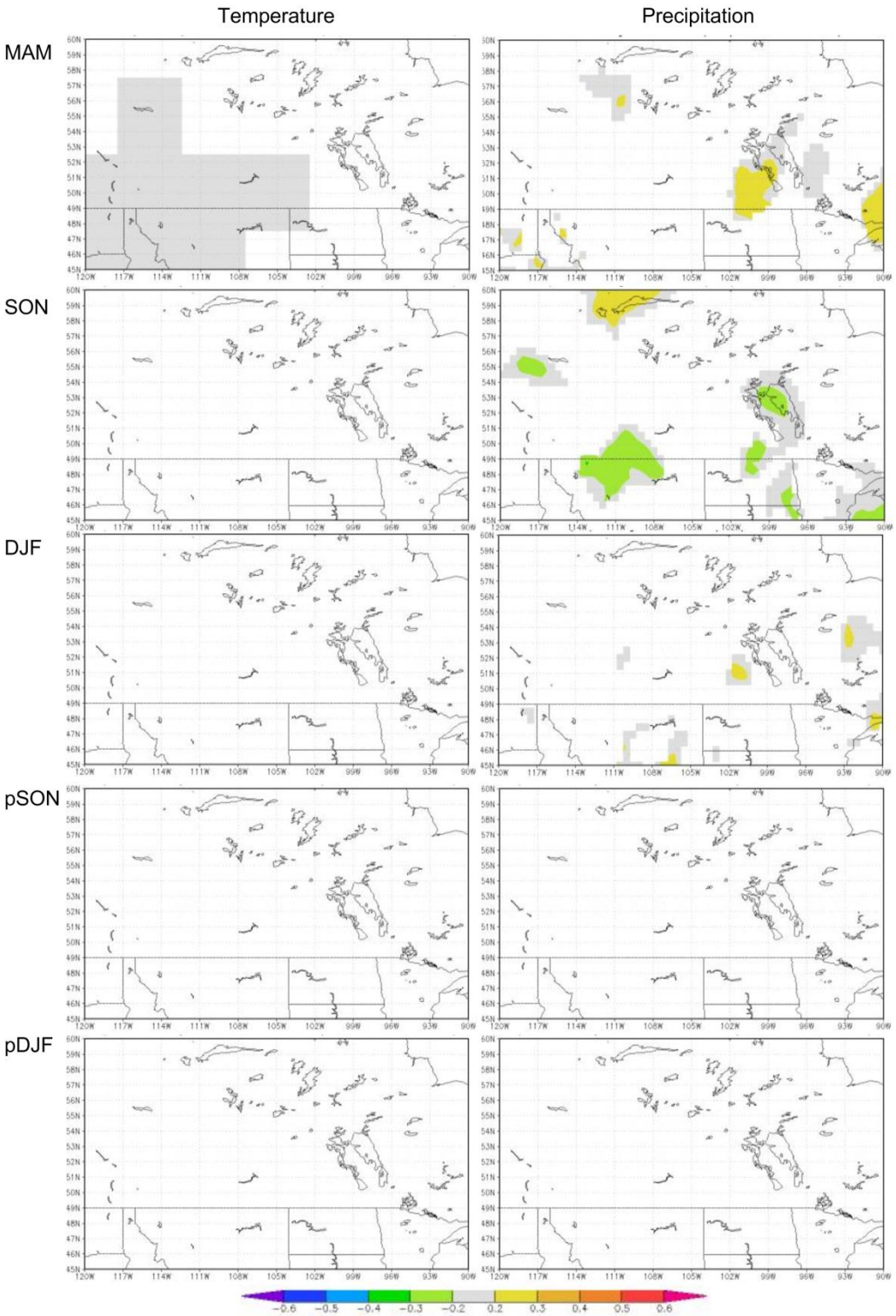

Figure 1.3 Seasonal correlation between LW ringwidth indices and temperature and precipitation ($p<0.05$). (MAM: March-May; SON: September-November; DJF: December-February; pSON: previous September-November; pDJF: previous December-February).